FROM BUD TO ORGAN: AN IN DEPTH ANALYSIS OF THE DEVELOPMENT OF THE PANCREAS.

APPROVED BY SUPERVISORY COMMITTEE

Ondine Cleaver, Ph.D.

Mark Henkemeyer, Ph.D.

Raymond MacDonald, Ph.D.

Eric N. Olson Ph.D.

DEDICATION

To my parents:

Luz María T. Aguilar and Pedro Villaseñor González

For their eternal love and support.

and to:

Cristina Tapia and Angel Tapia

For giving me the privilege of having a second family.

FROM BUD TO ORGAN: AN IN DEPTH ANALYSIS OF THE DEVELOPMENT OF THE PANCREAS.

by

ALETHIA VILLASEÑOR

DISSERTATION

Presented to the Faculty of the Graduate School of Biomedical Sciences

The University of Texas Southwestern Medical Center at Dallas

In Partial Fulfillment of the Requirements

For the Degree of

DOCTOR OF PHILOSOPHY

The University of Texas Southwestern Medical Center at Dallas

Dallas, Texas

June 2009

ACKNOWLEDGEMENTS

First, I would like to thank my mentor: Ondine Cleaver for four wonderful years of discoveries, learning, scientific/personal growth and for the AMAZING SCIENCE!! I am enormously in debt for all the guidance, encouragement, support, teaching and grilling!; for always being enthusiastic and willing to talk about science; for the famous "*prove it to me"* and the infamous "*but it has never happened to me*". Ondine you are both a scientific and personal inspiration! And it is my honor to have had you as my mentor.

To my committee members: Mark Henkemeyer, Ray MacDonald and Eric Olson. They have been incredible! I am thankful for their active participation in my research, for always showing genuine interest, for inviting me to give talks at their lab meetings, for their support, and for their great disposition to meet and discuss my projects. Specifically, I would like to thank: Mark for a great collaboration! and for letting me keep my mice in his mouse room; Ray for his wise insight in pancreatic development and for founding PIG meetings where I can share my love for pancreas and developmental biology; and Eric for putting music in the Molecular Biology department and giving me great dancing nights.

To my labmates and friends: Diana, Kristen, Ke Xu and Stryder for their continued enthusiasm, love for science, hard work and their enormous help and support;

for all the science and life discussions; for sharing my tears and frustrations as well as my clapping and joy. Coming to work is a pleasure! Thank you so much!!!

To Tom Carroll for his invaluable scientific input and constant interest in my research. To Courtney Karner for all the good scientific discussions and his dear friendship: Evolution rules mOOse! To the Henkemeyer and MacDonald Lab: For their help with techniques and reagents. Especially to Mike Hale, Tim Catchpole, and Chris Dravis. To my collaborators: Mike Dellinger and Tomas Wilkie for two beautiful stories. One that is not mentioned in this thesis. Thanks to JMST and the squirrel on the bench.

To my friends from all five continents that have shared with me this journey and have helped me not to miss my family so much. Thanks for all the laughs, joy, support and sometimes food. Especially I would like to thank: Diana Chong, Laura Motta-Mena, the boys: Andrei, Alex, Pop, and Temo; and the girls: Naoko, my lovely Tusa, and my unforgettable Claudia.

Exclusive thanks to Rabe for all magic! and Capparezza.

I am very thankful to my siblings, Zoe and Sebastian, for their constant love and support.

Finally, I thank my whole family for all the love and care that they have given me through all my life. For everything and anything... I am nomadic and move, but I am anchored to you through my heart and mind… always.

FROM BUD TO ORGAN: AN IN DEPTH ANALYSIS OF THE DEVELOPMENT OF THE PANCREAS.

Alethia Villaseñor, Ph.D.

The University of Texas Southwestern Medical Center at Dallas, 2009

Supervisor: Ondine Cleaver, Ph.D.

In this dissertation, a careful analysis of different aspects of pancreatic development was conducted in order to expand our understating of the biology of this organ. This thesis encompasses an in depth description of pancreas macro morphology throughout development as well as the analysis of the role of signaling molecules not previously studied in the pancreas. In brief, Chapter 2 presents a characterization of pancreatic branching and cellular polarization. It provides an anatomical model for branching of the pancreas and establishes the dynamics of cell polarity changes within the pancreatic epithelium throughout development. This chapter provides seminal work in an area that has received little attention in forwarding our understanding of how the epithelium reshapes itself to form a functional organ. Chapter 3 and Chapter 4 focus on the endocrine compartment of the pancreas. In Chapter 3, the expression of *Neourogenin3*, or *Ngn3*, a master gene regulator of endocrine fate was studied and a novel molecular correlation with the first and secondary transitions of pancreatic endocrine differentiation was demonstrated. In Chapter 4 it was shown that *Rgs* genes,

specifically *Rgs8* and *Rgs16*, are expressed in endocrine cells during pancreatic development and become quiescent during adulthood. Only under models of islet regeneration and pancreatic stress was a re-activation of *Rgs8* and *Rgs16* expression in endocrine cells observed. Our results suggest that *Rgs16* and *Rgs8* control aspects of islet progenitor cell activation, differentiation, and their actions might be required to compensate pancreatic metabolic stress. Finally, Chapter 5 analyzes the role *Eph/ephrinB* signaling in pancreatic development. Mice lacking signaling of *EphB2* and *EphB3* receptors showed fewer insulin-producing cells, abnormal islet distribution, anomalies in vasculogenesis and disrupted epithelial polarity and branching. In addition, they showed abnormal pancreatic function since the mutants are hypoglycemic after a glucose tolerance test. Studies in this chapter clearly reveal a role for *Eph/ephrinB* signaling during pancreatic morphogenesis, differentiation, and physiology. Moreover, since the ephrins (ligands) are expressed in the pancreatic mesoderm and blood vessels and the Eph (receptors) are expressed in the pancreatic endoderm; our results suggest that *Eph/ephrinB*-mediated tissue-cross-talk is required for proper pancreatic morphogenesis and islet formation. Overall, this thesis provides an in depth analysis of the biology of the developing pancreas.

TABLE OF CONTENTS

PRIOR PUBLICATIONS

Villasenor A, Chong D, Cleaver O. Biphasic *Ngn3* expression in the developing pancreas. *Dev Dyn. 2008 Nov;237(11):3270-9.*

Danesh SM, Villasenor A, Chong D, Soukup C, Cleaver O. BMP and BMP receptor expression during murine organogenesis. *Gene Expr Patterns. 2009 Apr 22.*

Das S, Stevens T, Castillo C, Villasenõr A, Arredondo H, Reddy K. 2002. Lipid metabolism in mucous-dwelling amitochondriate protozoa. *Int J Parasitol. 2002 Jun;32(6):655-75.*

PRESENT WORK

Villasenor A, Chong D, Cleaver O. Semi-sterotyped branching of the pancreatic epithelium and vasculature. *(In preparation)*

Villasenor A, Wang Z, Ocal O, Scherer P, Cleaver, O, Wilkie TM. Rgs8 and Rgs16 gene expression in embryonic endocrine pancreas and regenerating adult islets. (*In Revision)*

Villasenor A, Dravis C, Henkemeyer M, Cleaver O. Eph and eprhin signaling modulates pancreatic Development. *(In preparation)*

Danesh SM, Villasenor A, Cleaver, O., "BMP and BMP receptor expression in the developing midgut" *(In preparation)*

LIST OF FIGURES

Chapter 1

Chapter 2

Chapter 3

Chapter 4

Chapter 5

LIST OF TABLES

LIST OF APPENDICES

LIST OF DEFINITIONS

aPKC – Atypical Protein Kinase C

E– Embryonic day

Efn – ephrin

EMT – Epithelial to Mesenchymal Transition

Eph – Erythropoietin-Producing Hepatocellular

ephrin – Eph family Receptor Interacting protein

FGF – Fibroblast Growth Factor

GAPs – GTPase activating protein

GFP – Green Fluorescence Protein

GPCR – G protein-coupled receptor

GPI – Glycosylphosphatidylinositol

GSIS – Glucose Stimulated Insulin Secretion

ip – intraperitoneal

Isl1 – Islet1

MPC – Multipotent Precursor Cells

Ngn3 – Neurogenin 3

Pdx1 – Pancreatic and duodenal homeobox 1

RGS – Regulators of G-protein signaling

RTK – Recptor tyrosine kinase

Shh – Sonic Hedgehog

SMP – Splanchnic Mesodermal Plate

VDACs – Vessel and ductal-associated cells

Chapter 1: "THE PANCREAS"

Why study the pancreas? In particular, why are we trying to elucidate new mechanisms that regulate pancreatic development? Or spend years trying to understand the cellular and molecular basis of how the organ grows and differentiates? The answer is simple: it lies in the reward of seeing little pieces of a larger puzzle come together and in the realization that instead of yielding a definitive answer, most questions engender five additional ever more interesting questions that we then also strive to answer. However, there is also a grander and more significant reason: a better understanding of the pancreas will facilitate the development of new therapies to treat pancreatic disease. There is a clear necessity for the development of efficient treatments for diabetes, as it affects over 246 million worldwide (www.idf.org) and currently, there is no cure for this disease. There are palliative remedies that help ameliorate the symptoms of the disease, however, as we speak there are millions of diabetic patients dying or waiting for cadaver-derived islets to replace their malfunctioning ones to properly regulate their blood glucose levels. Groundbreaking research has advanced our ability to derive pancreatic cells from stem cells (D'Amour et al., 2005; D'Amour et al., 2006; Kroon et al., 2008) however much remains unknown regarding the generation of functional islets for replacement therapies. Understanding pancreas development, in combination with clinical and stem cell research, is critical for facilitating the generation of regenerative therapies to treat diabetic patients. In this thesis, an overview of the development of the pancreas is

presented. Each chapter of this thesis characterizes less understood aspects of pancreatic development and explores regulatory factors that participate in pancreas development.

1.1 General description of the pancreas

The pancreas is a glandular organ in the digestive and endocrine system of vertebrates. It is composed of two major tissues: the exocrine and the endocrine. Exocrine tissue is composed of acinar and duct cells, and constitutes about 95-99% of the total mass of the organ (Bonal and Herrera, 2008). The main function of this tissue is to provide digestive and pro-enzymes (amylase, trypsin, lipases, pepsinogen, DNAse and RNAse nucleases) to the small intestine for food digestion and absorption. Acinar cells secrete these enzymes in a bicarbonate-based solution while duct cells deliver them, through an elaborate ductal network into the duodenum. The exocrine tissue resembles a ‘tree-like” structure where a large central duct connects the duodenum in a ‘trunk-like’ manner to an extensive array of smaller branches, which terminate into acini at the tips of the branches. Intercalated ducts (centroacinar cells) extend from the center of the acini cluster (acinus) into the ductal network, which is composed of intralobular and interlobular ducts (Bonal and Herrera, 2008) (Cleaver and MacDonald, 2009).

The endocrine tissue is composed of islets of Langerhans and represents about 1-5% of the total mass of the organ. These islets are scattered throughout the exocrine tissue and are connected to blood vessels. Their main function is to maintain metabolic

homeostasis through the production of hormones that regulate blood glucose levels. Pancreatic islets are composed of five major endocrine cell types: **α-cells** produce glucagon and make up 15-20% of the islet; **β-cells** constitute the major cell type in the islet (about 60-80%) and secrete insulin; **δ-cells** make up about 5-10% of the total islet cells and produce somatostatin; **ε-cells** release ghrelin comprise less than 2% of the islet mass; and **PP-cells** produce pancreatic polypeptide and account for about 15-20% of cell mass (Bonner, 2004) (Collombat et al., 2006; Edlund, 2002). Insulin and glucagon are the main hormones that control glucose homeostasis. Islets are densely vascularized with fenestrated capillaries that are highly permeable and allow for rapid islet blood flow. Islet cells can then quickly respond to changes in blood glucose levels. As glucose levels rise (hyperglycemia), β-cells secrete insulin into the blood stream. Insulin signals peripheral tissues stimulating the uptake of glucose. The liver stores glucose through glycogenesis; skeletal muscle uptakes glucose and increases protein synthesis; and fat cells undergo lipogenesis. As glucose levels decrease (hypoglycemia), β-cells are inhibited and α-cells are stimulated. Glucagon is secreted by α-cells, which act on hepatocytes that convert the stored glycogen and lactic acid into glucose, which is then in turn secreted into the blood stream to restore normal glucose levels (Tortora and Grabowski, 1996). The other islet hormones function in conjunction with α- and β-cells to regulate glucose metabolism: somatostatin and ghrelin inhibit insulin release while pancreatic polypeptide inhibits secretion of somatostatin and digestive enzymes. It is the continuous and dynamic action of the islet, and particularly of insulin and glucagon, that keeps glucose levels under control.

1.2 Pancreatic development

The mature vertebrate pancreas forms from the fusion of the dorsal and ventral buds that evaginate from the primitive gut endoderm (Zaret, 2008). Pancreas development is a complex process during embryonic organogenesis that involves both intricate morphogenetic changes and a series of cell fate decisions that ultimately generate the different tissues that constitute the organ. Together, these events create a pool of progenitor cells produce exocrine, endocrine and ductal tissues. Below, the embryonic anatomy of the developing pancreas and the morphological processes that transform a single layer of epithelial cells into a functional organ are discussed.

1.2.1 From endoderm to bud

The pancreas develops from the embryonic endoderm. During gastrulation endodermal cells migrate out of the primitive streak to form an outer layer of cells (definitive endoderm) on the ventral surface of the embryo. At this early stage (E8.0-8.25) the endodermal epithelium is already fated into different progenitor domains that will give rise to the different organs within each embryo. The pancreas arises from several regions of the definitive endoderm (Fig. 1.1). The ventral pancreatic bud arises from two paired domains that are lateral, and adjacent to, the liver domains in the prospective ventral endoderm; and the dorsal pancreatic bud arises from the midline foregut in the dorsal endoderm (Zaret, 2008; Zaret and Grompe, 2008). After gastrulation, the definitive endoderm, consisting of a thick single-cell layered sheet of

epithelial cells (Kim et al., 1997a), folds into a primitive gut tube from which the dorsal and ventral pancreatic buds will evaginate.

The dorsal pre-pancreatic endoderm is in direct contact with the notochord, and is adjacent to both the somites and the paraxial mesoderm. The notochord inhibits endodermal Sonic Hedgehog (*Shh*) signaling by secreting activin βB and FGF2, subsequently allowing pancreatic development (Hebrok et al., 1998; Kim et al., 1997a). Chick experiments where the notochord was removed from this pre-prancreatic endoderm eliminated the expression of pancreatic genes Pdx1, Insulin, Isl-1, Pax-6, CarbA, and Glucagon (Kim et al., 1997a; Kim et al., 1997b). In addition, experiments where non-pancreatic endoderm was exposed to cylopamine, a *Shh* inhibitor, resulted in the conversion of endoderm toward the pancreatic fate (Kim and Melton, 1998). The notochord remains in direct contact with the dorsal endoderm until they become separated by the midline fusion of the paired aorta at about E8.75. The dorsal aortae at this point are in direct contact with the dorsal pancreas and provide instructive signals for its development. At this stage pancreatic budding is initiated. Studies showed that removal of the dorsal aorta from *Xenopus* embryos inhibited endocrine gene expression in the underlying endoderm and *in vitro* studies where dorsal endoderm was recombined with aortic endothelium resulted in endocrine differentiation (Lammert et al., 2001)

The ventral pre-pancreatic endoderm becomes specified at about the 5-somite stage (E8.0) when two clusters of *pancreatic duodenal homeobox* (*Pdx1*) expressing cells are clearly detected (Villasenor et al., 2008) (and see Chapter 3 of this thesis). However, ventral budding occurs later at about E9.25 (20-somite stage) (Edlund, 2002; Slack, 1995). The development of the ventral pancreas also requires *Shh* repression. Contrary to

the dorsal endoderm, the ventral endoderm is thought to have a default program for pancreatic fate (Deutsch et al., 2001; Hebrok et al., 1998). However, the ventral pancreatic program is inhibited by the expression of *Shh* from the cardiac mesoderm. The cardiac mesoderm expresses FGFs that induce high *Shh* expression. As the ventral endoderm moves away from the cardiac mesoderm it is then able to adopt the pancreatic fate program. The ventral endoderm gives rise to two ventral pancreatic buds, however, at about E9.5 one disappears coincidentally with the regression of its adjacent left vitelline vein (Lammert et al., 2003).

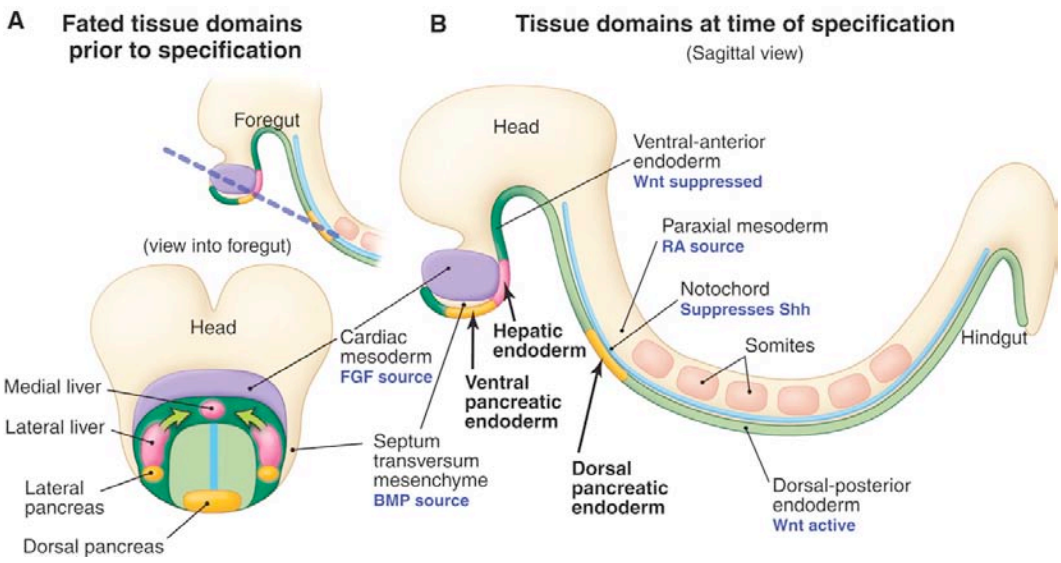

Figure 1.1 Pancreatic buds arise from different domains in the endoderm. Figure from (Zaret and Grompe, 2008). A) E8.25 (3s-4s) fate map showing the dorsal and ventral pre-pancreatic endoderm (orange domain) in the foregut of the embryo. Arrows indicate movement of progenitor regions. B) Saggital view of fate map in a 6s stage embryo.

1.2.2 From bud to organ

During early growth of the pancreatic bud, the pancreas acquires its initial form and it expands its progenitor cell pool. This early developmental window (E9.5-E12.5) has been termed the 'first transition' of pancreatic development, and generation of early 'first wave' endocrine cells occurs during this period. This time period has also been termed the 'proto-differentiated' stage, when epithelial cells become committed to the pancreatic fate and are mostly proliferative. Expanded progenitors later participate in 'second wave' of differentiation that will occur during the 'secondary transition' (E12.5-E15.5). During the secondary transition, the pancreatic buds undergo a dramatic morphological transformation where the "proto-differentiated" pool of pancreatic progenitors cells differentiates into the three main cell-types that constitute the pancreas: the endocrine, acinar and duct cells. During this stage, the pancreatic epithelium branches extensively, giving rise to a tree-like, tubular epithelial network that grows and rapidly expands (Kim and MacDonald, 2002). At later stages of development (E16.5-birth) cellular differentiation decreases but proliferation remains high, expanding the different tissues of the pancreas.

The "Proto-Differentiated" State and the 'first wave' of endocrine cells. (E9.5-E12.0)

By E9.5, two pancreatic protrusions have evaginated from the primitive gut endoderm: the dorsal and the ventral bud. The buds are surrounded by condensed mesenchyme. At this stage, the first wave of endocrine cells appear. These endocrine cells are different from the ones observed during the secondary transition and only occur

in certain organisms. For example, they are not found in humans, but they are found in mouse and rat (Cleaver and MacDonald, 2009). These endocrine cells first initiates glucagon expression, with subsets of cells transiently co-expressing insulin, pancreatic polypeptide or peptide YY (Gittes and Rutter, 1992; Golosow and Grobstein, 1962). It is controversial whether first wave endocrine cells contribute to mature islets (Gu et al., 2002; Herrera, 2000).

At E10.0, the mesothelial layer of cells that surrounds the mesenchyme on the left side of the dorsal bud thickens and its cells columnarize forming the splanchnic mesodermal plate (SMP) (Hecksher-Sorensen et al., 2004). It is thought that the SMP drives the future lateral growth of the dorsal pancreas towards the left side and supports situs-specific organogenesis (Hecksher-Sorensen et al., 2004). Indeed at this stage, the dorsal bud breaks bilateral symmetry and grows into the mesenchyme to the left of the embryonic midline.

By E10.5, the onset of pancreatic branching occurs. Branching is thought to occur either by looping and dense folding of the single-layered pancreatic epithelium (Pictet et al., 1972) or by micro-lumen fusion within a highly stratified epithelium (Hogan and Kolodziej, 2002; Jensen, 2004) (Fig. 1.2). A detailed description of pancreatic epithelium, branching, and lumen formation, as well as an alternative model for pancreatic branching, is given in Chapter 2 of this thesis.

By E11.5, the gut tube turns, further breaking bilateral symmetry of the gastrointestinal tract. This process brings together the dorsal and ventral bud and permits the fusion of their proximal ducts. The neck of the dorsal bud constricts producing an enlongated “bat-like” shaped dorsal pancreas that is completely covered by small

lobulations. The dorsal pancreas at this stage lies along the left flank of the stomach and extends towards the spleen. It has two lobes: the gastric and the larger more prominent splenic. The ventral bud is composed of a single lobe and expands its long fine branches extensively along the proximal duodenum.

During this 'proto-differentiated' state differentiation is mostly repressed, and pancreatic cells are almost entirely proliferating in order to expand the progenitor pool for the secondary transition. At this stage pancreatic cells are multipotent and capable of generating all pancreatic cell types. The gross size of the pancreas depends on the number of progenitor cells at this stage and before the secondary transition (Cleaver and MacDonald, 2009).

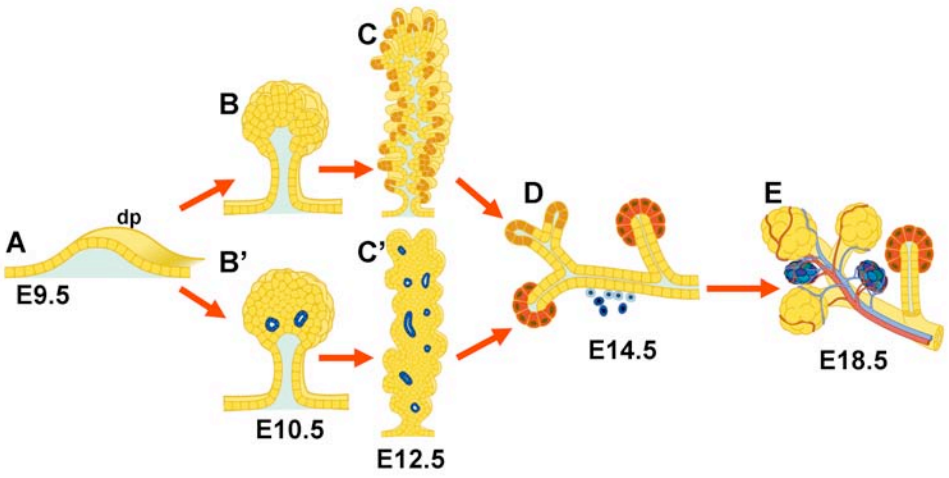

Figure 1.2 Schematics depicting two current models of pancreatic epithelial development. Figure adapted from (Cleaver and MacDonald, 2009) **(A)** Bud evagination from endoderm at E9.5. **(B)** Initiation of branching or **(B')** epithelial stratification and micro-lumen formation. **(C-C')** Onset of secondary transition**. (D)** Growth, branching, differentiation and endocrine delamination **(E)** Mature organ with acini, islets and associated vasculature. Dp= Dorsal pancreas.

The Secondary Transition (E12.5-E15.5)

Throughout the secondary transition, the cellular anatomy of the pancreas is extremely dynamic. Around E12.5, epithelial branches emerge from the stratified pancreatic epithelium and become distinguishable at the gross morphological level. These branching tips are formed from groups of $Cpa1^+$ multipotent precursor cells (MPC) that are not yet committed. Genetic linage tracing experiments performed by Melton's group (Zhou et al., 2007) show that MPCs at this early stage have the ability to give rise to all three pancreatic lineages: exocrine, ductal and endocrine around E12.5. However, as the MPCs continue branching, they become depleted and begin to differentiate. Experiments by the same group have shown that lineage tracing of $Cpa1^+$ cells after E14.5 give rise exclusively to exocrine cells, suggesting that during late stages of the secondary transition the branching tips lose their multipotency and undergo restriction of cell fate to the exocrine lineage (Zhou et al., 2007). Branching tips are highly proliferative and as they grow outwards, they progressively generate more differentiated cells, the tubular ductal epithelium and endocrine cells, in their wake. At later developmental stages, the branching tips differentiate into pro-acini and later into mature acinus. The acinus is made by a group of acinar cells that form a cap and engulf the terminus of the intercalated ducts (centroacinar cells) (Fig. 1.3)

During the secondary transition, a secondary wave of endocrine cells appear. Scattered individual cells within the ductal epithelium differentiate into the endocrine fate. Endocrine differentiation occurs only after inhibition of *Notch* signaling and expression of high levels of the transcription factor *Neurogenin 3* (*Ngn3*). After

delamination, endocrine cells aggregate into ribbon-like cords (Jensen, 2004) and remain in close proximity to the tubular epithelium. Later, they coalesce into small islet-like clusters that progressively join and proliferate into larger islet aggregates. The mechanisms for endocrine delamination, migration, aggregation and islet formation are basically unknown.

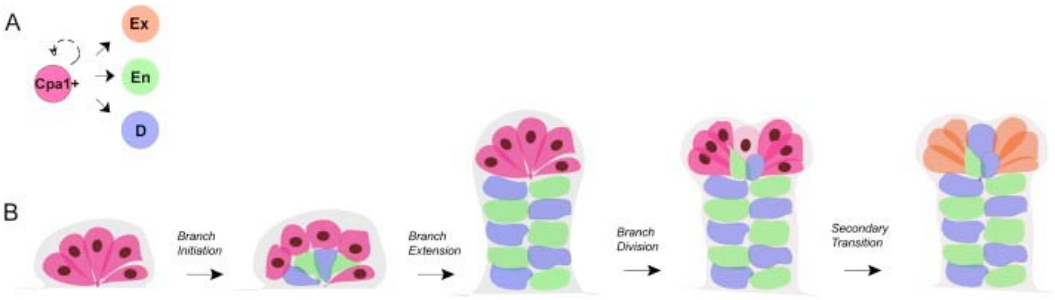

Figure 1.3 Model for multipotent Precursor cells (MPC) in branch tips. Figure from (Zhou et al., 2007) **(A)** Multipotent cells can give rise to all three pancreatic cell lineages. **(B)** In the 'proto-differentiated' state the pancreatic bud is composed mainly of proliferative multipotent progenitor cells. At the beginning of branching morphogenesis MPCs branching tips grow outwards from the pancreatic epithelium, cells left behind become: ductal and endocrine cells while cells at the tip (~E14.0) restrict to the exocrine fate.

The secondary wave endocrine cells are known to be different from the first wave endocrine cells. During the secondary transition, endocrine cells primarily differentiate into β-cells, while first wave endocrine cells are mostly α-cells. In addition both types of endocrine cells are thought to have different methods of separation from the epithelium: First wave endocrine cells have been observed to 'bud' out as groups of cells

from the epithelium, while secondary cells delaminate individually.

There are two proposed mechanism for second wave endocrine delamination. The first one includes Epithelial- Mesenchymal Transition (EMT) and the second involves orthogonal asymmetric cell division from the pancreatic epithelium. EMT is a common mechanism for cellular delamination from an epithelial sheet. During EMT, epithelial cells lose their polarity and tight junctions, they change their morphology and become motile. The evidence that EMT is the main mechanism for endocrine delamination is only correlative. In the pancreas, the second wave endocrine cells are known to be unpolarized (Pictet et al., 1972) and highly motile (Puri and Hebrok, 2007). In addition, during the secondary transition, Snail2, an inducer of EMT, is co-expressed in *Ngn3*$^{+}$ progenitor cells within the ductal epithelium (Rukstalis and Habener, 2007). Furthermore, experiments in endocrine cell lines have shown that Snail modulates insulin and glucacon expression (Rukstalis and Habener, 2007).

The second one explains the process of endocrine delamination by asymmetrical cell division and it was proposed in the early 1970s by Pictet and Rutter (Pictet et al., 1972). In this model, when delaminating endocrine cell divides it changes its axis of cell division, from longitudinal – or in the plane of the epithelium – to perpendicular – or at a 90˚ angle from the plane of the epithelium. Following orthogonal cell division, one daughter cell will remain bound to the epithelium while the other is released.

During the secondary transition, epithelial branching and endocrine differentiation is concomitant with ductal development. As tips grow and expand out, and endocrine cells delaminate, the tubular proto-differentiated epithelium starts to acquire its more mature ductal/tubular characteristics. At later developmental stages, it is possible to

find three main types of ducts: the intercalated, intralobular and interlobular. As the organ matures, these tubes connect and form the pancreatic ‘tree-like’ ductal network. However, the cellular mechanisms for ductal specification and development are still poorly understood.

The Differentiated State (E16.5-postnatal)

After the major wave of exocrine and endocrine differentiation that occurs during the secondary transition, the distinct fate of pancreatic cells is largely established. The different tissues of the pancreas, especially the exocrine tissue, remain highly proliferative contributing to the growth and expansion of the organ. During this state, the tubular network assembles, the exocrine mass increases enormously, and islets start to organize. During postnatal development, these clusters coalesce and take on recognizable islet anatomy. In mice, this consists of a core of insulin-expressing β−cells surrounded by a mantle of mostly α-cells, but also δ-, ε- and PP cells. (Collombat et al., 2006; Oliver-Krasinski and Stoffers, 2008)

Finally, in adults, most proliferation of pancreatic cell types has ceased. Indeed, there is little endocrine proliferation and/or differentiation, unless the pancreas detects metabolic stresses that challenge glucose homeostasis. For example, during pregnancy, maternal β−cell expansion compensates for increased metabolic demands of the developing fetus (Karnik et al., 2007). In type 2 diabetes, β−cell expansion transiently controls elevated glycemic levels before β−cell failure (Chua et al., 2002). In type 1 diabetes, β−cells continually replenish in a futile effort to manage hyperglycemia resulting from β−cell destruction by the immune system (von Herrath and Homann,

2004). The cellular origin of new β−cells remains controversial. One group favors the idea of a progenitor cell located in the pancreatic duct (Bonner-Weir et al., 2004) while the second group suggests that new β−cells derive from replication of pre-existing β−cells (Dor et al., 2004; Teta et al., 2007). The identification of signaling pathways that control pancreatic β−cell expansion would be extremely useful for the development of therapies to treat pancreatic disease.

1.2.3 The pancreatic epithelium and its surrounding mesenchyme

Mesodermal signals also play an important role in pancreatic specification and subsequent development. The dorsal bud receives signals from the dorsal mesoderm and mesodermal-derived tissues, while the ventral bud receives signals from the splanchnic and procardial mesoderm. It has been shown that signals from the lateral plate mesoderm are required for the expression of *Pdx1, Ptf1a, Nkx6.1*, glucagon and insulin pancreatic genes (Kumar et al., 2003).

Mesenchymal signals are not only necessary for pancreatic specification, but they are also necessary for proper pancreas development throughout embryonic organogenesis. During its development, the pancreas is continuously surrounded by mesenchymal cells. At early budding stages, the pancreatic buds grow into a condensed mesenchyme layer. As development proceeds, the mesenchymal layer thins out until it becomes barely discernible. Early studies in pancreatic development showed that if the mesenchyme was removed from the epithelium, pancreas proliferation decreased. In addition, mutant mice that are deficient in dorsal pancreatic mesenchyme such as *Islet 1*

(*Isl1*) and *N-cadherin* null mice showed lack of bud development (Ahlgren et al., 1997; Esni et al., 2001). Furthermore, mesenchyme signaling has been shown to inhibit endocrine differentiation (Scharfmann, 2000), and to promote pancreatic progenitor proliferation (Elghazi et al., 2002; Ye et al., 2005) and in this way regulate total β-cell numbers (Attali et al., 2007).

More evidence for the importance of mesenchymal signaling in pancreatic development comes from studies in *Fgf10* null mice. *Fgf10* is transiently expressed in the pancreatic mesenchyme around E10.0. *Fgf10*$^{-/-}$ mice display an arrest in the proliferation and differentiation of the pancreatic epithelium (Bhushan et al., 2001). The technical difficulty inherent in the manual separation of mesenchyme from pancreatic epithelium, during and after the secondary transition, has restricted the study of epithelial-mesenchymal interactions in the pancreas.

1.3 Regulatory Genes

In the previous sections, I discussed both the morphogenesis of the pancreas and the differentiation of its various lineages, as well as the regulation of these processes by extrinsic signals. The following section briefly discusses some of the key pancreatic genes used throughout this thesis. Background information presented here will familiarize the reader with the tools we have used to assess pancreatic development in our studies.

1.3.1 *Pdx1*

Pdx1 is one of the most studied transcription factors in pancreatic development. It is a homeodomain transcription factor necessary for proper pancreatic development. At early stages of pancreatic development, *Pdx1* is clearly expressed throughout the pancreatic epithelium but then becomes restricted to β-cells, δ-cells, and PP cells (Ahlgren et al., 1997; Guz et al., 1995). *Pdx1* null mice show initiation of pancreatic budding and differentiation of first wave endocrine cells, but further pancreatic development is arrested (Jonsson et al., 1994; Offield et al., 1996). This indicates that *Pdx1* function is not essential for the specification of early endocrine cells or for pancreatic induction; however, its function is required for the development of all three pancreatic lineages. Ablation studies by Stanger et al. demonstrated that Pdx1+ was a marker of progenitor cells and the *Pdx1+* progenitor pool is generated in the proto-differentiated state (Stanger et al., 2007).

Elegant studies by Gu et al to determine the influence of *Pdx1+* in pancreatic fate showed that cells that expressed *Pdx1+* between E9.5-E11.5 are capable of giving rise to all three pancreatic cell lineages: exocrine, endocrine and ductal. However, cells that expressed *Pdx1* at E8.5, E12.5 and thereafter gave rise to exocrine and endocrine tissue but not ducts. These results indicated that *Pdx1+* progenitor cells for ducts and for exocrine/endocrine are separated during pancreatic development, specifically at the onset of secondary transition (~E12.5) (Gu et al., 2002). However, ectopic expression of *Pdx1* in non-pancreatic endoderm is not sufficient to promote full endocrine and exocrine cytodifferentiation (Grapin-Botton et al., 2001) indicating that *Pdx1* acts in coordination

with other pancreatic transcription factors to promote the full pancreatic program. Indeed, Hale et al. showed that depletion of *Pdx1* at E12.5 and E13.5 arrested exocrine development as a result of suppressed *Ptf1a* induction (Hale et al., 2005). This relationship between both transcription factors, *Pdx1* and *Ptf1a*, is not only observed during secondary transition, but it is also observed at early stages of development, where it has been shown that the interdependent cooperation between *Pdx1* and *Ptf1a* maintains the pancreatic progenitor pool (Burlison et al., 2008). How do these transcriptions factors regulate each other during pancreatic development is poorly understood, however, recent work by Wiebe et al shows that *Ptf1a* is able to bind *in vitro* and *in vivo* to area III of the *Pdx1* promoter and that this particular region is sufficient to drive *Pdx1* expression at early developmental stages (E9.5-E11.5) (Wiebe et al., 2007).

1.3.2 *Sox9*

Sox9 is a transcription factor involved in pancreatic development and cell fate determination. *Sox9* is expressed throughout the pancreatic epithelium as early as E9.0 and until late gestational stages (E18.5) where it becomes restricted to islets, a sub-population of ductal cells and some exocrine cells (Lioubinski et al., 2003). *Sox9*, similar to *Pdx1*, marks the pancreatic progenitor cell pool (Lioubinski et al., 2003; Seymour et al., 2007). Studies by Seymour et al showed that depletion of *Sox9* in *Pdx1* expressing cells impaired pancreatic growth and endocrine differentiation. In addition, they showed that *Sox9* is necessary for maintenance of the pancreatic cell pool, since progenitor cells with depleted *Sox9* had reduced cell proliferation and increased cell death (Seymour et al., 2007). In addition, work by the Sander group showed that there is a *Sox9* dosage-

dependent requirement for proper development of the endocrine compartment. Pancreas epithelium with reduced *Sox9* gene dosage had an overall reduction of endocrine cells, but normal exocrine development (Seymour et al., 2008). Recent work from Sander's group proposes a role for *Sox9* in *Ngn3* regulation where *Sox9* positively regulates *Ngn3* and is thus required for endocrine differentiation. Whether *Sox9* acts in a cell autonomous fashion regulating *Ngn3* directly or in a non-autonomous fashion regulating Hes1 and indirectly regulating *Ngn3* expression, still needs to be determined. In addition, work from the Sander lab also showed that *Sox9* expression is excluded from the branching tips as they become specified towards the exocrine fate, while *Sox9* expression remains high in the tubular epithelium that generates endocrine cells. They proposed that loss of multi-potency in the branching tips is due to loss of distal *Sox9* expression.

1.3.3 *Ngn3*

Nng3, or *neurogenin3,* encodes a basic-helix-loop-helix (bHLH) transcription factor that is critical for endocrine specification (Apelqvist et al., 1999; Grapin-Botton et al., 2001; Schwitzgebel et al., 2000). *Ngn3* is expressed in scattered cells of the pancreatic epithelium as early as E8.25 and its expression peaks during secondary transition (13.5-14.5) (Schwitzgebel et al., 2000; Villasenor et al., 2008), after which its expression decreases dramatically. *Nng3* expression in the adult islet is controversial, early work has shown a lack of *Ngn3* expression in the adult islet (Gradwohl et al., 2000; Schwitzgebel et al., 2000), however work by Gu et al. and our laboratory detects low levels of *Ngn3* expression in islets (Gu et al., 2002; Wang et al., 2009) (and data not

shown). This discrepancy is probably the result of different technical approaches used to analyze *Ngn3* expression. For a more careful description of *Ngn3* expression in the developing pancreas, please refer to chapter 3 of this thesis. The role of *Ngn3* as an endocrine fate determinant primarily came from studies of *Ngn3* null mice. Mice lacking the function of *Ngn3* also lack all four pancreatic endocrine lineages (glucagon, insulin, somatostatin and pp). In addition, these mice lacked early endocrine markers (Pax4, Pax6, NeuroD), but showed proper exocrine development (Gradwohl et al., 2000). These data indicate that *Ngn3* is required exclusively for the development of the endocrine cell lineage. In addition, these results indicate that *Ngn3* is likely to lie upstream of the other pancreatic endocrine gene networks. Work by Apelqvist et al showed that *Ngn3* is negatively regulated by *Notch* signaling (Apelqvist et al., 1999) since mice defective in *Notch* signaling showed accelerated endocrine differentiation and high levels of *Ngn3* expression. It was then assumed that endocrine differentiation occurred by lateral specification through the *Notch* signaling pathway in a similar fashion as neuronal differentiation. However, recent work in the pancreatic field by Palle Serup challenges this idea. The Serup group has found that not all mutants defective in *Notch* signaling pathway show accelerate endocrine differentiation. He found a 80-90% decrease in *Ngn3* expression in *Dll1* mutants, supporting an alternative mechanism rather than *Dll1*-mediated lateral inhibition for *Ngn3* regulation and endocrine differentiation.

The mechanisms by which *Ngn3* determines endocrine specification are poorly understood. However, elegant experiments by Grapin-Botton's group showed that the pancreatic progenitor pool has different temporal competence windows and responds

differently to *Ngn3* actions at different times. When *Ngn3* expression was induced at early stages of pancreatic development using a transgenic approach in an *Ngn3* null background, the resulting endocrine cells mostly differentiated into α-cells. When *Ngn3* was induced from E11.5, endocrine differentiation favored β-cells and PP cells. When *Ngn3* was induced from E14.5, endocrine cells differentiated into somatostatin cell types and α-cell differentiation is dramatically decreased (Johansson et al., 2007). This work proposes that temporal control of *Ngn3* as well as different competency between pancreatic progenitors determines endocrine cell type fate.

1.3.4 Nkx genes

Nkx genes have been shown to be expressed in, and critical to, the developing pancreas. *Nkx2.2* is an *Nkx* homeobox transcription factor involved in the endocrine commitment of α- , β-, and PP cells. *Nkx2.2* is expressed early throughout the early pancreatic epithelium (E9.5-E12.5) and later in all the β-cell population, but it is only partially co-expressed in subsets of α- and PP cells. It is also expressed in adult islets. *Nkx2.2* null mice display islet mass reduction due to a decrease in *α-*, *β-*, and PP cells. δ-cell number appeared normal, but there is a great increase in the number of ghrelin-expressing cells. In addition, these mice were incapable of producing insulin (Sussel et al., 1998).

Nkx6.1 is expressed early throughout the pancreatic epithelium (E10.5-E12.5); around secondary transition its expression peaks and restricted to *β*-cells. At E15.5 two populations of *Nkx6.1* can be found: one that co-expresses insulin and *Pdx1*; and a second one that co-expresses *Ngn3* and is located at the tubular epithelium. *Nkx6.1* null mice exhibit reduced β-cell numbers perceivable only after secondary transition; but the number of the other endocrine cells remains normal. Double Nkx null mice (*Nkx2.2*$^{-/-}$ and *Nkx6.1*$^{-/-}$) had an identical phenotype to *Nkx2.2* single mutant indicating that *Nkx2.2* is upstream of *Nkx6.1* for β-cell development (Sander et al., 2000; Sussel et al., 1998)

Lastly, *Nkx6.2*, the paralog of *Nkx6.1*, is expressed in the pancreatic epithelium and the majority of *Nkx6.2*+ cells co-express *Pdx1*+ but not glucagon at E10.5. However, at later developmental stages (12.5-E15.5) *Nkx6.2* co-express glucagon, in addition at E15.5 *Nkx6.2* co-expresses amylase indicating that *Nkx6.2* function is not restricted to the endocrine lineage. Lineage tracing studies reveal a transient expression of *Nkx6.2* in insulin and *Ngn3* expressing cells. (Henseleit et al., 2005). *Nkx6.2*+ null mice show no apparent phenotype since their pancreas develops normally. However, double null mice (*Nkx6.1*$^{-/-}$ and *Nkx6.2*$^{-/-}$) exhibit an increase in β-cell reduction and an additional decrease in α-cell number indicating a role for *Nkx6.2* in α-cell formation.

1.4 Final remarks

This chapter provides a comprehensive introduction of pancreatic development and helps in the future appreciation of the work presented in this thesis. The work in the next chapters expands the understanding of pancreatic development by studying in detail the morphological changes of pancreatic growth (chapter 2), analyzing the dynamic expression of key transcription factor genes (chapter 3); and establishing a role for new signaling cascades in pancreatic development (chapter 4 and 5). We hope that the work presented in this thesis contributes to a better understanding of the pancreas and presents new ideas to the researcher for the development of therapies to treat pancreatic disease.

Chapter 2. PANCREATIC ORGANOGENESIS: EPITHELIAL POLARITY, LUMEN FORMATION AND BRANCHING MORPHOGENESIS.

2.1 INTRODUCTION

The pancreas is a branching organ composed of two types of tissue: the exocrine (acini and ducts) and the endocrine (Islets of Langerhans). Both tissues carry out specific functions: the exocrine tissue produces digestive enzymes that are collected by the ducts, and the endocrine tissue produces hormones that regulate glucose homeostasis. The mature pancreas, like many other branching organs, consists of ramifying tubular networks that conduct fluids. These tubes are constructed from monolayer of single cell thick epithelia that form a tree-like structure, where the tubular ramifications are closed at one end by a cap of exocrine cells (acinus). Lumens are interconnected and form a continuous cavity that directly connects to the primary duct, which empties into the duodenum (Pictet et al., 1972). The formation of the pancreas then requires the coordination of branching morphogenesis, lumen formation, cellular polarity establishment, and cellular differentiation.

The first appearance of the organ starts at developmental stage E8.75 when the dorsal epithelial bud evaginates out from the endodermal gut tube. Approximately 12 hours later, the ventral pancreatic bud emerges. The pancreas develops from the fusion of these two buds and undergoes several developmental stages of growth to produce the

mature organ (Edlund, 2002; Slack, 1995). These developmental stages include: 1) the primary transition (E9.5-E10.5) where epithelial cells become specified for pancreatic fate, levels of acinar enzymes are low, and the initial appearance of glucagon cells occurs; 2) the proto-differentiated state (E9.5-E12.5) where pancreatic epithelial cells mostly proliferate to expand the progenitor cell pool; 3) the secondary transition (E12.5-E15.5) where there is a major wave of endocrine and exocrine differentiation; and 4) the perinatal growth and differentiation state (E16.5-birth) where the pancreas continues to grow and develop. (Cleaver and MacDonald, 2009)

The gross anatomy of the embryonic pancreas remains only vaguely understood. It has long been hypothesized that pancreatic branching is random occurring as a result of folding and buckling of the endodermal epithelium (Pictet et al., 1972), in contrast to many organs that branch in a highly stereotyped and reproducible way. For instance, the lung and kidney exhibit strikingly reproducible budding and branching events (Costantini, 2006; Metzger et al., 2008; Warburton et al., 2005). However, recent real-time imagining studies by Puri et al. showed that lateral branching is the predominant way of branching of the pancreas and that only about 20% of branching events are bifid (Puri and Hebrok, 2007)

Lumen formation is necessary for the building of functional epithelial tubes. It occurs concomitant to branching morphogenesis as in the lung, or secondary to branching as in the mammary or salivary gland (Affolter et al., 2003; Cutler and Mooradian, 1987; Hogg et al., 1983; Mailleux et al., 2008). In the pancreas, as branching morphogenesis, lumen formation is also poorly understood. Currently, there are two models that explain lumen formation in the pancreas. The first one proposes that the pancreatic bud is a

compact ball of highly branched single epithelium within a confined space creating lumens and branches as folding occurs (Pictet et al., 1972). The second one suggests that the pancreas is actually a stratified epithelium, with multiple cell layers that give rise *de novo* to microlumens (Hogan and Kolodziej, 2002; Jensen, 2004)

In order to understand lumen formation, is important to study cell polarity. Apical-basal polarity of the epithelium is necessary for tubulogenesis in many branching organs such as the kidney, lungs, and the *Drosophila* traquea system (Bryant and Mostov, 2008; Kim et al., 2007; Zegers et al., 2003). Cellular polarity is acquired when the intracellular organelles, the cytoskeleton and the cell surface of a cell are asymmetrically organized, producing an apical and a basal side. The basal side interacts with the basement membrane and the extracellular matrix (ECM) while the apical side faces the lumen (Bryant and Mostov, 2008; Hogan and Kolodziej, 2002). Cell polarization in the pancreas has been proposed to occur after *de novo* lumen formation as in the case of the mammary gland, hair follicle and submandibular gland (Hogan and Kolodziej, 2002; Jensen, 2004). In addition, it has been suggested that endocrine cells are not polarized and that they separate from the pancreatic epithelium by an inversion of the polarity of the axis of cell division of the endocrine cells from epithelium (Pictet et al., 1972). However, a careful description of epithelial cell polarity in the pancreas is still lacking in the field.

Here, we have carefully studied the development of the pancreatic epithelium and have found unique features of epithelial stratification and lumen formation. We propose a new model for pancreatic lumen formation where the major lumen is formed as a combination of epithelium folding from the gut endoderm followed by the creation of

new lumens through cellular rearrangements and microlumens fusion. Our work also includes a macroscopic analysis of the anatomy of pancreatic branching. We provide an anatomical template that describes the basic morphology and growth/branching parameters of the embryonic pancreas. We believe that our work will serve as reference for future comparison and analysis of mutants allowing for a better understanding of the mechanisms for pancreatic branching morphogenesis.

2.2 RESULTS

MACROSCOPIC ANALYSIS OF THE PANCREAS

Different biological tools available in the field were compared in order to access the macroscopic branching of the embryonic pancreas. These tools included the *Pdx1*-LacZ mice (Offield et al., 1996), the *Ngn3*-EGFP mice (Lee et al., 2002), immunofluorescence technique using the ductal marker mucin-1, and *in situ* hybridization with *Ngn3* (Fig. 2.1). The clearest visualization of the pancreatic epithelium was accomplished using the *Pdx1*-LacZ mice for our studies for the following reasons: 1) β-galactosidase staining of the branches of the pancreas was simpler; 2) the pancreas required less handling before having a distinguishable coloration, helping dissection and preventing the breakage of the branches; and 3) even though it is known that Pdx1 expression becomes restricted to β-cells after the secondary transition (Ahlgren et al., 1998; Hale et al., 2005; Ohlsson et al., 1993), β-galactosidase staining of *Pdx1*-LacZ embryos stained the complete pancreas up to the E18.5 stage (the last stage assayed). At older stages (E15.5-E18.5), Pdx1 staining intensity was lower in the exocrine tissue and higher in islets (Fig. 2.4J-J’’).

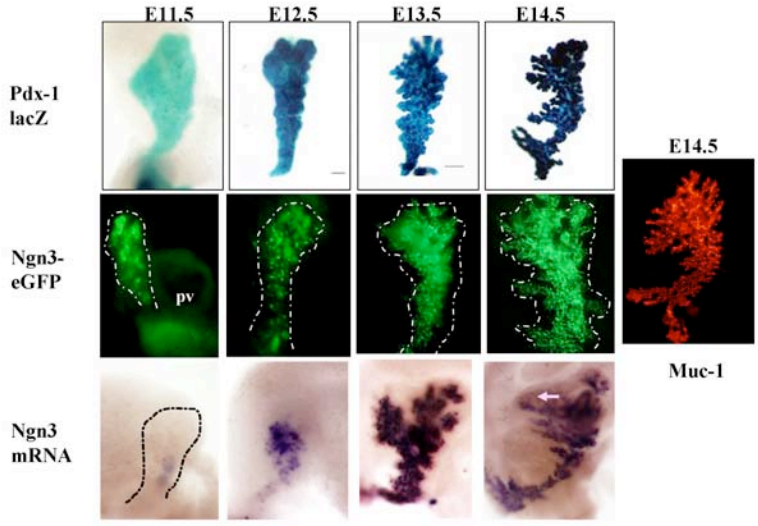

Figure 2.1. **Pancreatic branching assessed using *Pdx1*-lacZ, Muc-1 and *Ngn3* expression.** Assessment of different biological tools for analysis of pancreatic morphology through (E11.5-E14.5). First row: Whole mount β-galactosidase staining of isolated *Pdx1*-lacZ dorsal pancreas. Second row: Isolated dorsal pancreatic buds from Ngn3-GFP mouse line. Third row: *In situ* hybridization of *Ngn3* at different developmental stages. Fifth column: mucin (Muc-1) staining of isolated dorsal pancreas. Pv=portal vein.

2.2.1 Developmental pancreatic gross morphology

Over 200 *Pdx1*-LacZ embryonic pancreata (S2.1-S2.4 and data not shown) were analyzed and even though the pancreata showed limited variability in the number of branches and branch lengths, the overall pancreatic morphology followed predictable trends of growth (Fig.2.2 and 2.4). The initial stages of pancreatic development (E9.5-E11.5) showed highly stereotyped and simple morphology (Fig. 2.2A-C; 2.4A-C'; S2.1); mid- gestation stages of embryonic pancreas development (E12.5-E14.5) showed the most variability, with pre-branch lobulations of varying lengths and locations (Fig. 2.2D-

F; 2.4D-F’’’; S2.2-S2.3); and during later stages of development (E15.5-E18.5) branching re-aligned into recognizable and defined pancreatic branches (Fig. 2.2G-H; 2.3G-J’’; S2.3-S2.4). Just prior to birth, the embryonic pancreas acquired a predictable morphological shape that continued into postnatal stages.

Initial stages (E9.5-E11.5): Around E8.75 the cuboidal endodermal cells of the dorsal pancreas have obtained a columnarized shape and evaginated out from the gut tube into the visceral mesoderm (Jensen, 2004; Kim and MacDonald, 2002) forming, by E9.5, a “fin-like” bud (Fig. 2.2A). At E10.5, the neck of the bud constricted acquiring a “fist-like” form (Fig. 2.2B). By E11.5, the neck continued to constrict even more and the bud elongated out into a “bat-like” structure (Fig. 2.2C). During early developmental stages (E9.5-E11.5), the bud epithelium is surrounded by a thick layer of mesoderm, which includes both an inner layer of mesenchyme and an outer layer of mesothelium (Fig. 2.2I-L) and as the pancreas grows and branches, this mesodermal layer becomes thinner (Fig. 2.2M-N) until it is almost negligible by E18.5 (Villasenor et al., 2008) and data not shown).

Mid-gestation stages (E12.5-E14.5): By E12.5 the pancreas continued to extend to a “bat-like” shape (Fig. 2.2D, S2.2) and numerous lateral branches formed perpendicular to the main pancreatic axis. These branches displayed relatively homogenous lengths and protruded at regular intervals along the proximal-distal axis of the pancreas. In addition to these longer branches, the entire surface of the pancreas is covered by small lobulations that resemble blunt twigs. At E13.5, the pancreatic bud epithelium undergoes

a dramatic morphological transformation, going from a smoother bud to a highly branched tree-like form. At this point, many lateral branches have grown and extended out from the axis of the bud, while others have remained short, yielding a variety of branches of heterogeneous lengths. The surface of these branches remains covered by many perpendicular/lateral lobulations giving each branch of the pancreas a bumpy, rough appearance (Fig. 2.2E, S2.2). At E14.5, pancreatic lobulations remained evident on the surface of the pancreas (Fig. 2.2F), however the lateral branches have continued to extend and the organ has become larger and denser. At this developmental stage, there is considerably less variability in overall shape, as the pancreatic shape converged from individual to individual. During this stage, the embryonic pancreas acquired its conventional morphological form, which has been defined based on meta-analysis of large numbers of pancreatic anlagen, as composed of a distal ‘anvil-shaped’ tail; a lateral ‘ridge’ that runs along the proximo-distal axis; a distal ‘cap’, ‘left lateral branches’; and a proximal ‘gastric branch’ (Fig. 2.2P). These morphological features are described in detail later in the text.

Late stages (E15.5-E18.5): During these late gestational stages, the pancreas grew larger and became denser, but it maintained the same overall morphological shape that it acquired by E14.5 (Fig. 2.2G-H). The only exception is the ‘cap’ that disappeared as the mesenchyme thinned out.

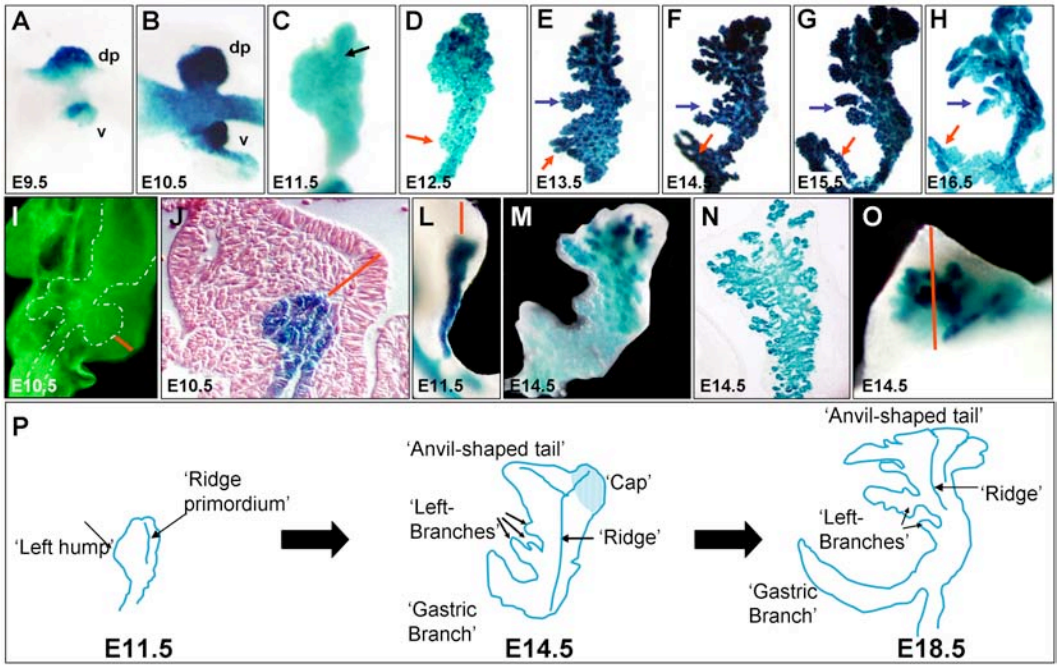

Figure 2.2. Macroscopic trends in pancreatic growth and branching. **(A-H)** Whole mount β-galactosidase staining of dissected *Pdx1*-lacZ guts from E9.5 to E16.5. Guts **(A-B)** show pancreatic epithelium and mesenchyme while guts **(C-H)** show only pancreatic epithelium. **(A-B)** Dissected gut tubes, anterior is to the left, dorsal is up; **(C-H)** isolated dorsal pancreatic bud. Black arrow in **(C)** denotes the 'ridge primordium'. Blue arrows in **(E-H)** indicate lateral branch, red arrow in **(D-H)** point to gastric branch. **(I)** whole pancreatic gut. The gut endoderm is outlined with a white dotted line. **(J)** H& E staining of a cross-section of an E10.5 *Pdx1*-LacZ dorsal pancreatic bud. **(L)** Whole mount β-galactosidase staining of an E11.5 *Pdx1*-lacZ dissected gut. Pancreas is facing right. Red line in **I-L** marks the thickness of the mesenchymal layer. **(M-O)** E14.5 *Pdx1*-Lacz dorsal pancreas **(M)** isolated dorsal bud, notice the translucent layer of mesenchyme surrounding the complete organ; **(N)** cross section of E14.5**; (O)** top view of the pancreatic tail. Red line marks the altitude of the head. **(P)** Cartoon Model showing the major morphological trends in pancreatic development. dp, dorsal pancreatic bud; v, ventral pancreatic bud.

2.2.2 Morphological features of the embryonic pancreas.

Large numbers of pancreatic anlagen were examined and many distinct, albeit sometimes transient, landmark morphological features were identified as characteristic of certain stages. To refine the anatomical model of pancreatic branching and overall development, these features were named and are noted in Fig. 2.2P.

The anvil-shaped tail (E14.5-birth): The pancreatic tail is defined as the distal end of the dorsal pancreatic anlagen, located near the spleen in close association with the left lateral side of the stomach. Although early in development, pancreatic tails displayed either a bi-furcated or blunt phenotype (Fig. 2.4C-D'), both types grew to form the characteristic 'anvil-shape' tail that typifies all pancreata observed. This 'anvil' shape is pyramidal in shape, as the distal pancreas is nestled between a loop of the proximal duodenum and the left kidney. The anvil-shaped tail is composed of three principal groups of branches: a left group that spreads 45° out towards the caudal part of the stomach and is made of 3-5 individual branches; and two right groups which overlap each other within a common mesenchyme (Fig. 2.2P and Fig. 2.3.).

The ridge (E11.5-birth): The pancreatic ridge is defined as a morphological feature of the outer flank of the dorsal pancreas, comprising the apex of the pyramidal shaped tail, separating the 'left' from the 'right' side of the bud. These two different 'sides' of the dorsal pancreas displayed recognizable features. The 'left' side of the pancreas is flattened against the caudal part of the stomach and is composed of long lateral branches, while the 'right' side of the pancreas is thicker, with shorter branches, and is located nearer the fundus of the stomach (Fig. 2.2F-H, M, P; Fig. 2.3). One can picture the right and left sides of the pancreas as sides in an isosceles triangle, where the

'ridge' is the vertice where both sides join (when the altitude of the triangle is at max) (Fig. 2.2O). The ridge is initially formed around E11.5 from mesothelial thickening as described by Hecksher-Soresnsen and appears as an exacerbation of bulging on the 'right' side of the pancreas ('ridge primordium' Fig. 2.2C black arrow, 2.2P).

The cap (E13.5-E15.5): The cap is defined as a distal feature of the 'right' side of the pancreatic tail. It is a thick, rounded lobe of mesenchyme located near the spleen, on the right side of the 'anvil-shaped' tail (Fig. 2.2P, Fig. 2.3C). It defines the 'right' thicker, blunt edge of the 'anvil', in contrast to the 'left' side is wedge-shaped and tapers down along the flank of the stomach.

Interestingly, the identification of the 'ridge' and the 'cap' structures was not only based on the visual analysis of the epithelium of *Pdx1*-LacZ embryonic pancreata, but also on the restricted expression of mesenchymal genes (Fig. 2.3). In situ hybridization for mRNA expression of Hox11, Barx1, and *ephrinB1* at E14.0 revealed different mesodermal domains within the pancreatic anlagen. *Barx1* marked the 'left' side (Fig. 2.3B), *Hox 11* marked the 'cap' (Fig. 2.3C), and *ephrinB1* marked the 'right' side and had a higher concentration of expression at the 'ridge' (Fig. 2.3D).

The left lateral branches (E13.5-birth): The left lateral branches are defined as the long branches located near the caudal end of the stomach, which extend midway between the distal anvil-shaped tail and the proximal gastric branch (Fig. 2.2P). These lateral branches of the pancreas continued to grow throughout development. However, these epithelial extensions occurred mainly on the 'left' side of the pancreas. The branches of the right side grow initially, but ceased to extend during mid-gestation, as the pancreas takes shape (Fig. 2.2F-H, 2.2P). At older embryonic and postnatal stages, the right side of

the pancreas displayed limited ‘right’ branches, but these are invariably shorter and more blunt (Fig. 2.2H; Fig. 2.4J)

The gastric branch (E14.5-birth): It is the longest and most easily identifiable branch in the pancreas (Fig. 2.2F-H, 2.2P) that branches from the most proximal portion of the dorsal pancreatic bud. Its growth is perpendicular to the proximo-distal axis of the pancreas and it curves up following the edge of the stomach and sometimes, at older stages, it can be found connected to the ‘anvil-shaped’ tail or to the ‘left branches’.

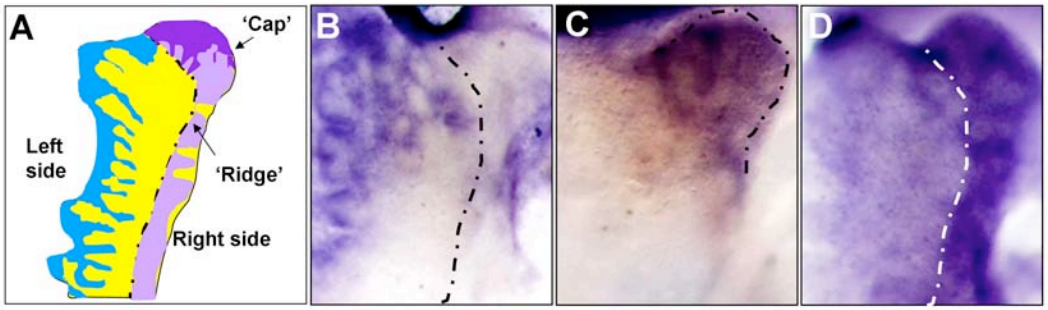

Figure 2.3. Distinct pancreatic domains revealed by mesenchymal gene expression. In situ hybridization for different mesenchymal genes. **(A)** Model of mesenchymal pancreatic areas. **(B-D)** Close-up of E14.0 dorsal pancreata **(B)** *Barx1*; **(C)** *Hox11*; and **(D)** *ephrinB1*. Dotted lines in A,B, and D outlines the position of the `ridge´ and on C the `cap´.

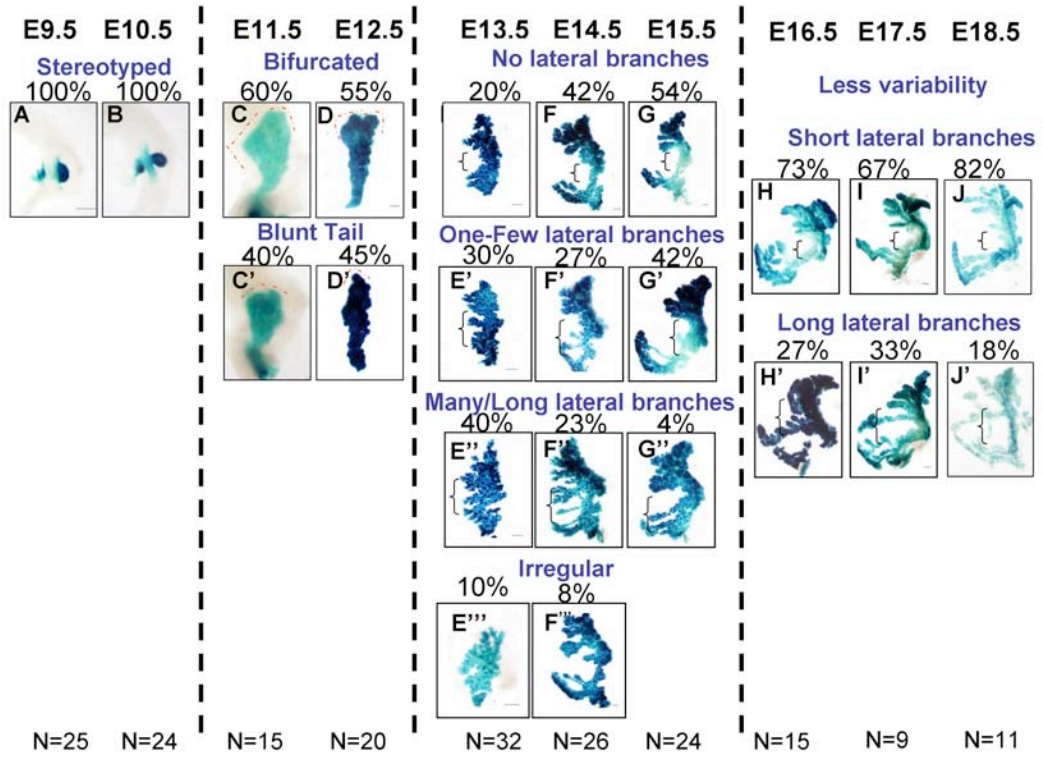

Figure 2.4 Analysis of gross dorsal pancreas morphology during development. (A-J'') Whole mount β-galactosidase staining of isolated *Pdx1*-lacZ guts from E9.5 to E18.5, as indicated along top of figure. **(A-B)** Dissected early gut tubes showing pancreatic epithelium (blue) and mesenchyme (brown), anterior is up, dorsal is to the right **(C-C'')** Dissected E11.5 dorsal pancreas with mesenchyme. Red lines delineate pancreatic tail **(D-J')** Isolated dorsal pancreas showing only the pancreatic epithelium. **(E9.5-E10.5)** All pancreas show similar morphology; **(E11.5-E12.5)** Pancreas are categorized based in their tail shape, note red lines; **(E13.5-E15.5)** Pancreas are categorized based on their lateral branches: 1st row) No lateral branches; 2nd row) One to few lateral branches (black arrow); 3rd row) Many or long lateral branches (red arrows); and 4th row) irregular shape; **(E16.5-E18.5)** pancreas are categorized based on lateral branches 1st row) short branches and 2nd row) long branches. Brackets mark lateral branches.

2.2.3 Trends in pancreatic branching patterns.

Meta-analysis of large numbers of pancreatic anlagen, demonstrated that while the pancreas did not branch in a strictly 'stereotyped' manner, it did display recognizable features through its development that were evident in all individuals examined. To classify the branching patterns of the pancreatic anlagen, different categories based on either the presence of lateral branches or the shape of its tail were assigned (Fig. 2.4).

At the earliest stages, E9.5 and E10.5, all pancreata examined showed the same morphology, with little to no variability (Fig. 2.4A-B, S2.1). However, at E11.5-E12.5 two principal forms became distinguishable: 1) one in which the tail of the pancreatic anlagen showed a 'left hump' and was wider, essentially presenting a 'bifurcated' tail (Fig. 2.2C,P; 2.4C-D), and 2) a second in which there were no obvious extensions or bulges off the distal pancreatic tail (Fig. 2.4C'-D'). While these differences between the bifurcated and blunt tail were clear at E11.5-E12.5, they became almost unrecognizable by E13.5. At this stage, the morphology of the pancreas was quite variable from one embryo to the next, and the growth of individual branches was not stereotyped (compare branches in Fig. 2.4E vs. 2.4E'). Slightly later, from E14.5, the overall morphology of individual pancreata converged and distinct patterns were recognizable. In general, however, from E13.5 to E15.5 gross anatomy was classified based on position and length of 'left lateral" branches: 1) no/short lateral branches (Fig. 2.4E-G); 2) few branches midway along the pancreatic axis (Fig. 2.4E'-G'); 3) many/long lateral branches (Fig. 2.4E''-G''); and 4) irregular pancreatic morphology (Fig. 2.4E'''-F'''). By later stages of pancreatic development E16.5-E18.5 much of these differences have resolved and pancreatic anatomy was less variable. The pancreatic lobulations found in the 'no-lateral

branches' group of pancreata have grown into small branches, and classification can be simplified into two groups: 1) short left-branches (Fig. 2.4H-J') and 2) long left-branches (Fig. 2.4H-J'')

MICROSCOPIC ANALYSIS OF THE PANCREAS

2.2.4. The pancreatic epithelium

To further understand the cellular basis for the changes that were observed in the macroscopic anatomy of the pancreas, the pancreatic epithelium was examined at higher resolution using immunofluorescence studies at key developmental stages (Fig. 2.5). Both E-cadherin (an epithelial adhesion molecule and an accepted epithelial marker) and laminin (a basement membrane molecule which marks the basal aspect of cells) were examined.

Prior to pancreatic budding, at E7.5 (2s) when the gut tube epithelium is open and the embryo has not yet turned, the pre-pancreatic endoderm was composed of a single layer of cuboidal epithelial cells that were polarized (Fig. 2.5A, white arrows). These cells were polarized, as assessed by abundant basal laminin accumulation (Fig. 2.5A) and by the apical intercellular tight junction protein ZO-1 (data not shown). By E8.75, pancreatic cells became columnar and formed a 'placode' or a 'plate-like' epithelial thickening (Fig. 2.5B), which evaginated out from the primitive gut epithelium as a protrusion of epithelial cells. While this placode was initially a single cell layer thick, it began to stratify, acquiring multiple layers of cells between the lumen and the basement membrane. The basal (or more dorsal) cells within this cluster remained polarized, as

seen by maintenance of laminin along the surface of the bud, while the stratifying (or more ventral) cells were mostly unpolarized at this stage, as assessed by the absence of staining for either apical or basal markers (Fig. 2.5C-D; 2.9A-B, white arrow, and data not shown).

As development continues during the proto-differentiated stages (E9.5-E11.5), the number of cell layers which the stratified epithelium of the bud continued to increase (Fig. 2.5C-F) and the bud resembled a bag of compact stratified epithelium as previously described (Hogan and Kolodziej, 2002; Jensen, 2004). Subsequently, during the secondary transition, the thick multi-layered pancreatic epithelium began to decrease in thickness (Fig. 2.5G) as epithelial cells rearranged around newly formed lumens (*de novo* microlumens). These changes were coincidental with differentiation of both secondary wave endocrine cells as well as with segregation of exocrine acini and ductal networks (Fig. 2.5G, pink arrows). By E15.5 the pancreatic epithelium has largely resolved back to a single cell layer in thickness (Fig. 2.5H).

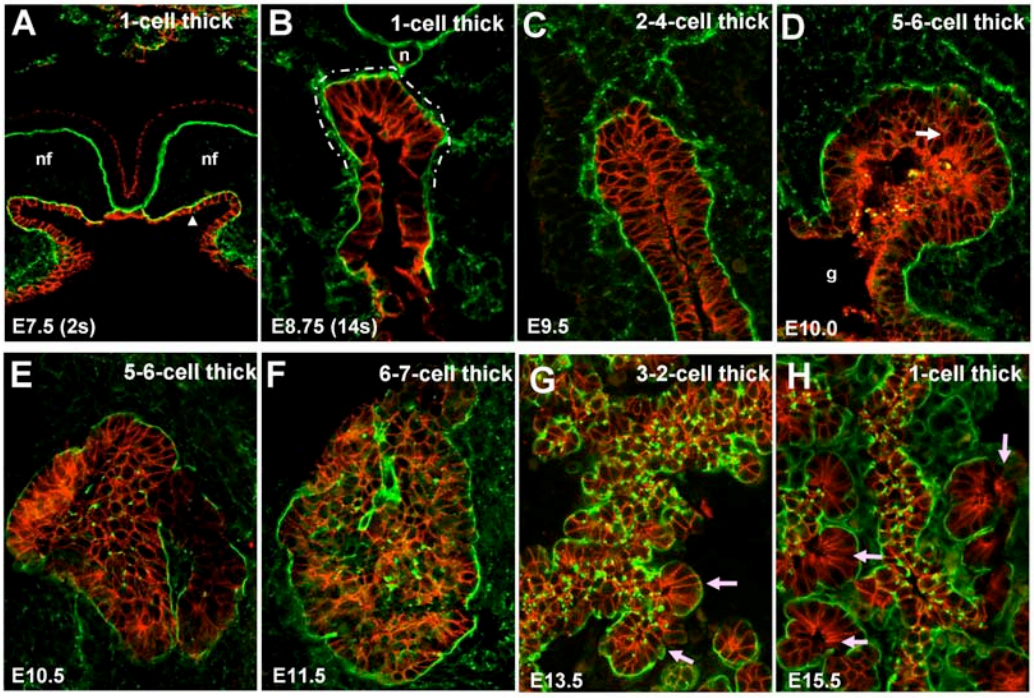

Figure 2.5. Pancreatic epithelial stratification: Loss of epithelial polarization, but not epithelial adhesion. Immunostainings of Laminin (green) and E-cadherin (red) on **(A-C)** transverse sections and **(D-H)** saggital sections of dorsal pancreatic buds throughout development. Sections in **A-F** show pancreatic stratification, while sections in **G-H** show cellular re-arrangements and de-stratification. Arrowhead in **A** mark single cuboidal epithelium layer. Pink arrows show newly form acini and white arrow marks and example of an 'unpolarized' cell within the stratified epithelium. White line in **B** delineates pancreatic 'placode'. Nf, neural folds, n, notochord, g, gut tube.

2.2.5 Pancreatic epithelial cell polarity.

In order to understand the epithelial changes observed during formation of the pancreatic tubular network, cellular polarity at different developmental stages was explored by immunofluorescence analysis of several known intracellular junctional complexes. Two key stages of pancreatic development: E10.5, when the bud is composed

of a multilayered stratified epithelium, and E13.5, when the pancreatic epithelium begins to re-organize itself into a single epithelium, were compared (Fig. 2.6).

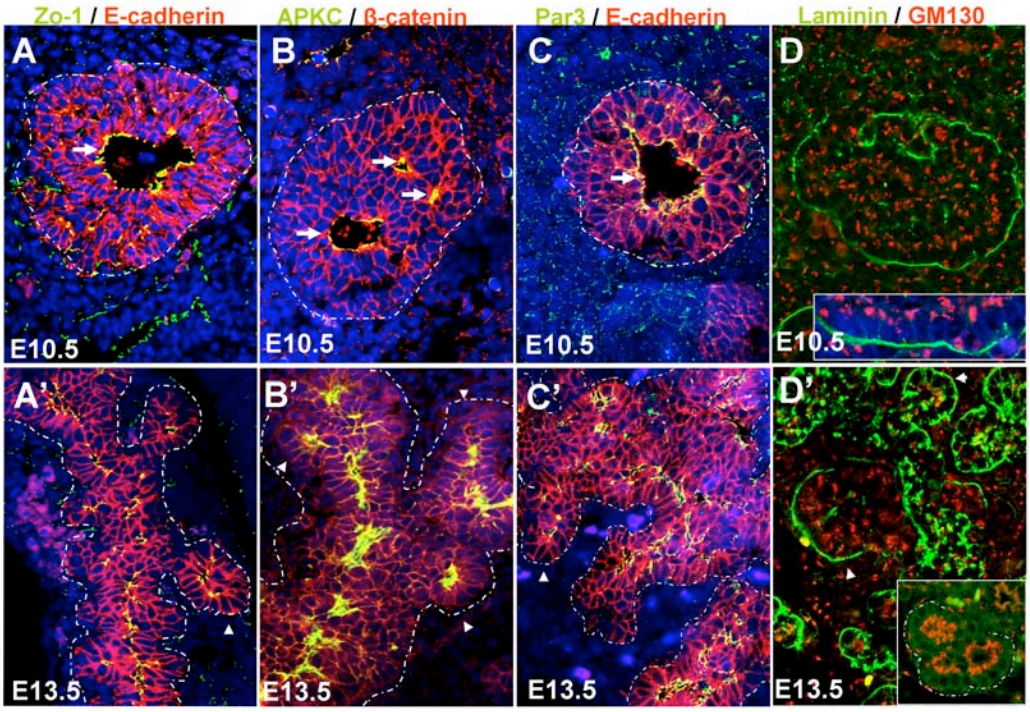

Figure 2.6. Pancreatic polarization is lost in subset of epithelial cells during epithelial stratification. Immunofluorescent assays on E10.5 (top panel) and E13.5 (bottom panel) pancreatic sections of the following cell polarity markers: **(A-A')** ZO-1 (green) and E-cadherin (red) **(B-B')** APKC (green) and β-catenin (red); **(C-C'')** Par3(green) and E-cadherin (red); **(D-D'')** Laminin (green) and GM130 (red). In all cases, the pancreatic epithelium is outlined with a dotted line, except in D-D' where the pancreatic epithelium is outlined by laminin staining. White arrows mark microlumens, and white arrowheads show newly form acini florets.

Prior to epithelial stratification, the pancreatic cells displayed typical apical-basal polarity (Fig. 2.5A-B). As new layers of epithelial cells were being formed, epithelial cells loose their polarity partially or completely depending on their location. Epithelial cells that remained in direct contact with the basal membrane kept their basal polarity as assessed by laminin (Fig. 2.5D, 2.6D and 2.7A) as well as basal nuclear localization (Fig. 2.6D, 2.7C,D,G,H), however these cells lost apical polarity, as noted by lack of ZO-1, APKC, and PAR3 staining. It is important to mention, that although these cells lost their tight junction proteins or apical polarity complexes, their intracellular organelles kept an apical asymmetric organization, as observed by GM130 golgi staining (Fig. 2.6D, inset). In contrast, cells that were in direct contact with the lumen retained their apical polarity as assessed by expression of ZO-1, PAR3 and APKC (Fig. 2.6A-C), but lost their basal markers such as laminin (Fig. 2.5D, white arrowheads). Strikingly, the cells between these two 'semi-polarized' layers displayed no apical or basal polarity, since they did not express neither basal laminin nor apical markers, but they remainned 'epithelial', as they retained epithelial adhesion molecule expression, such as E-cadherin (Fig. 2.7A-C, arrows) and lack expression of mesenchymal markers (Fig. 2.7B). The same arrangement of cellular polarity within the stratified bud was observed through all the proto-differentiated developmental stages (Fig. 2.5C-F and data not shown).

During the secondary transition, however, the 'unpolarized' epithelial cells within the stratified bud gained their cellular polarity as the epithelium decreased in thickness and allowed them to become in direct contact with the basal membrane or the lumen (Fig. 2.5G,H; Fig. 2.6A'-D' and Fig. 2.7 A,E). By E15.5 the pancreatic epithelium was mostly single cell layered in thickness and it showed clear apical-basal polarity (Fig.

2.6 D’ inset and data not shown). At E13.5 polarized pro-acini (Fig. 2.6A’-D’, white arrowheads) formed as exocrine cells differentiated from the pancreatic epithelium. These pro-acini will give rise to the mature acinar cells observed in the adult.

In order to better understand the coordination of endocrine differentiation and how it correlates with the dynamics of the changing pancreatic epithelium, the relationship between endocrine cells and the pancreatic epithelium at two different developmental stages: E11.5 (first wave of endocrine cells) and E15.5 (second wave of endocrine cells) was investigated.

At both developmental stages, endocrine cells showed low levels of E-cadherin and β-catenin during their differentiation and exit from the pancreatic epithelium (Fig. 2.8 and data not shown). This observation suggests that a loss or change in adhesion properties is necessary for proper detachment of endocrine cells from the pancreatic epithelium. Unexpectedly, nascent endocrine cells showed varying degrees of cell polarity during their exit from the epithelium. At E11.5 polarized (Fig. 2.8A-A’’, arrow) and non-polarized (Fig. 2.8A-A’’, bottom aggregates) endocrine aggregates were observed as assessed by positive laminin staining bordering the endocrine aggregate. However, at E15.5 most individual endocrine cells showed no laminin staining and have an irregular shape (Fig. 2.8B-B’, white arrows).

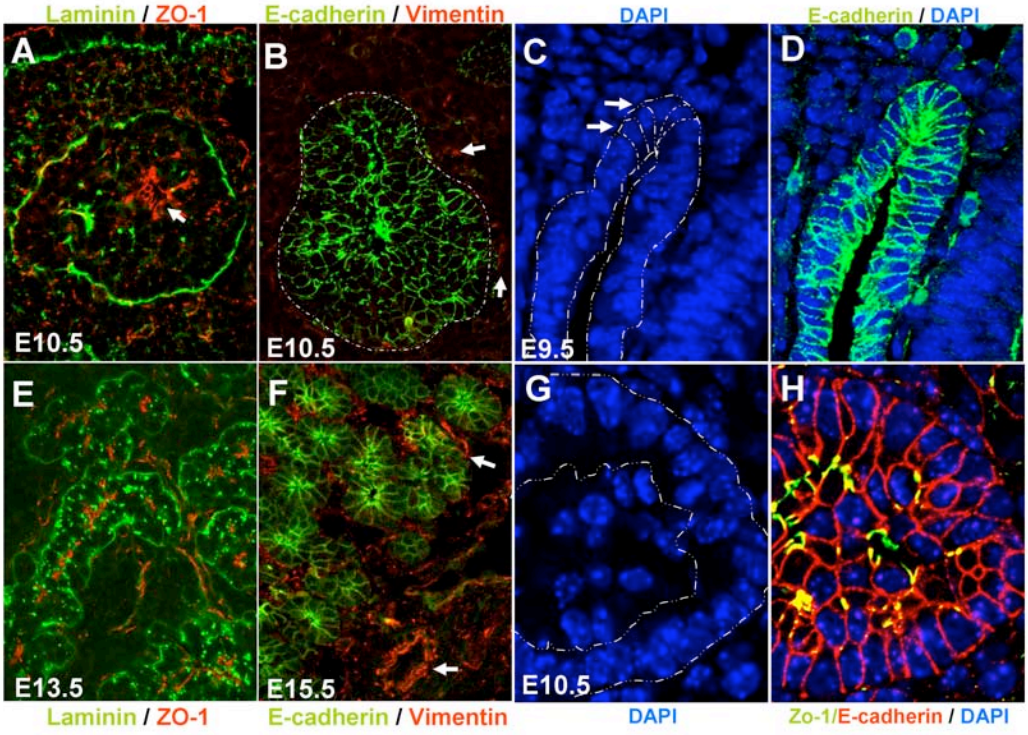

Figure 2.7 Stratified epithelial cells lose their cell polarity during stratification, without losing their epithelial character. **(A-B)** Saggital sections of E10.5; **(E)** E13.5 and **(F)** E15.5 dorsal pancreatic bud. **(A,E)** ZO-1 (red) and Laminin (green). Arrows in A show microlumen. **(B,F)** vimentin (red) and E-cadherin (green). Arrows in B and F show mesenchymal cells positive for vimentin outside the pancreatic epithelium. The pancreatic epithelium is outlined in B. **(C-D)** Transverse sections of E9.5 and **(G-H)** Saggital sections of E10.5 pancreatic bud showing basal nuclear localization. **(C-D)** E-cadherin (green) and DAPI (blue). Arrows in C show cells within the pancreatic epithelium with nucleus located basally. **(G-H)** ZO-1(green), E-cadherin (red) and DAPI (blue). The pancreatic epithelium is outlined with a white dotted

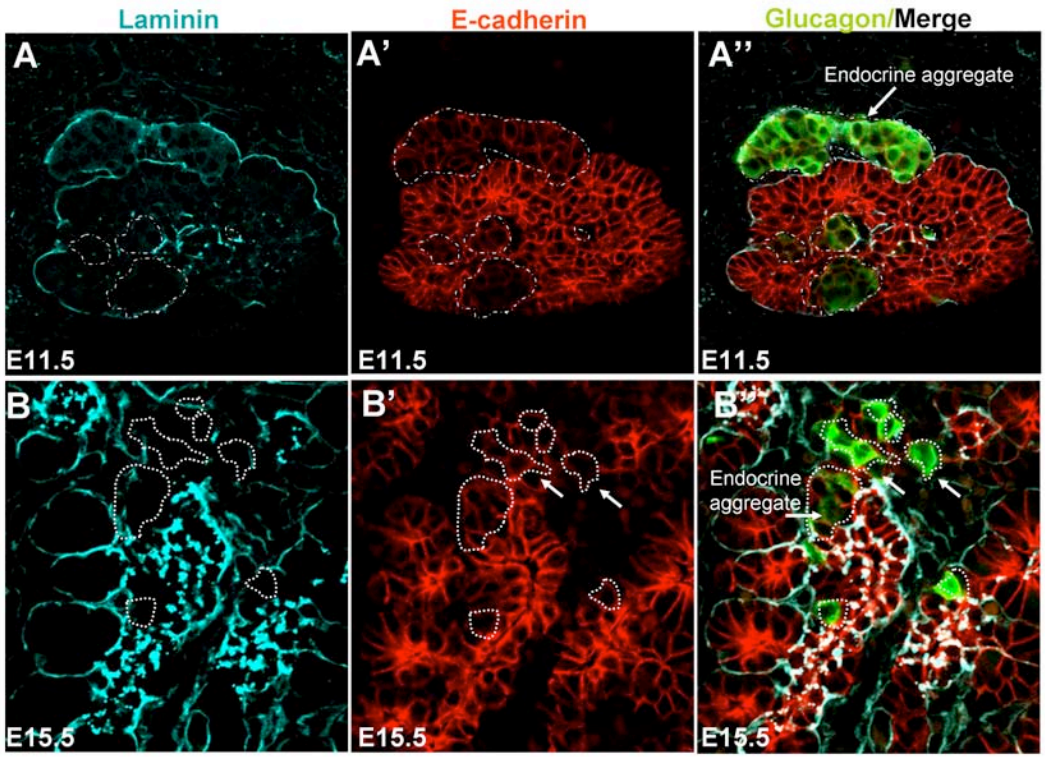

Figure 2.8 Differential cell adhesion underlies endocrine delamination. Immunofluorescence stainings of laminin (blue), E-cadherin (red) and glucagons (green) in **(A-A'')** E11.5 and **(B-B'')** E15.5 dorsal pancreatic sections. Endocrine cells and aggregates are outlined by white dotted lines.

2.2.6 Lumen formation

Epithelial tube formation, or tubulogenesis, within the pancreas at different developmental stages was examined (Fig. 2.9) in order to understand the process of lumen formation within the stratified pancreatic epithelium. At E8.75 all embryonic endodermally derived epithelium expressed E-cadherin (Fig. 2.9A). Soon after budding, a Principal Central Lumen (PCL) was formed, which followed the proximo-distal axis in the center of the dorsal bud. The PCL connected directly to the gut lumen as observed by

ZO-1 staining in both saggital (Fig. 2.9D) and transverse sections (Fig. 2.9I, Fig. 2.10) of the E10.5 dorsal pancreatic bud.

At this stage, the stratified epithelium folded and expanded around the PCL. Transverse sections of the E10.5 midgut region showed that the ventral pancreatic bud also had a central lumen that connected to the gut lumen and at a certain point these three lumens intersected (dorsal, ventral and gut) (Fig. 2.9I, 2.10E-F). Note that the epithelium of the gut tube in this region, including that of the stomach and duodenum is never stratified (Fig. 2.10)

It has been proposed by Jensen and Hogan that lumens in the pancreatic anlagen arise by *de novo* microlumen formation (Hogan and Kolodziej, 2002; Jensen, 2004). Indeed, after E10.5, we observe this phenomenon distal to the PCL within the thick multi-layered stratified epithelium (Fig. 2.6B white arrows and Fig. 2.9I). Sequential cross sections of an E12.0 dorsal pancreatic bud showed the formation of pancreatic lumens (Fig. 2.9E-G,H) that resembled the formation of the intestinal lumen in Zebra fish (Horne-Badovinac et al., 2001). Distal sections of the dorsal pancreas showed the formation of foci of tight junctions as shown by ZO-1 aggregates locally between cells (Fig. 2.9E) but not lumens. These foci located apically in the cells and as in zebra fish, seem to merge with other foci until there is a single cluster of tight junctions in the middle of a rosette (Fig. 2.9E-F, outline rosette). After, the lumen opens within the tight junction aggregate giving rise to a microlumen (Fig. 2.9F white arrows) (Fig. 2.9F, white arrows). Proximal sections showed the PCL interconnected with duodenum lumen (Fig. 2.9G). Later, the microlumens formed distally will coalesce with the PCL establishing an interconnected tubular system.

In order to address whether these lumens are formed by apoptosis, as in other similar tubular organs (Humphreys et al., 1996; Jaskoll and Melnick, 1999; Mailleux et al., 2007), two hallmarks of apoptosis: DNA break points and caspase 3 activation were assayed. DNA break points or caspase 3 activation at both developmental stages assayed (E10.5 and E13.0) was not detected in the pancreas indicating that apoptosis does not play a role for pancreatic lumen formation (Fig. 2.11 and data not shown).

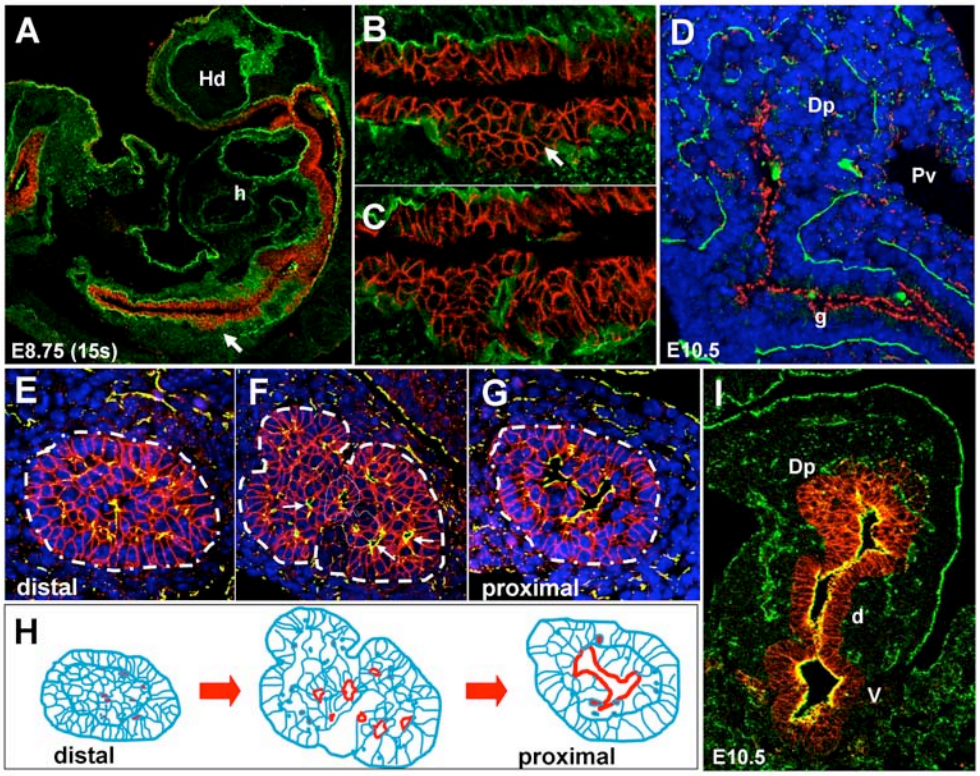

Figure 2.9. Lumen formation and branching initiation. (A) Saggital section of E8.75 embryo showing laminin (green) and E-cadherin (red) staining. **(B-C)** Close-ups of the early pancreatic evagination. White arrow in A-B points to the pancreatic bud. White arrow in C points to microlumen. **(D)** Saggital section of E10.5 showing establishment of a major lumen, detected by ZO-1 (red) staining, connected to the gut. The pancreas is outlined by laminin (green) staining. **(E-G)** Immunostainings of E-cadherin (red) and ZO-1 (green) stainings in sequential sections of E12.0 dorsal pancreatic bud from distal **(E)** to proximal **(G)** The pancreatic epithelium is outlined by a dotted line. **(H)** Cartoon of lumen formation. Lumens are in red, epithelial cells are in blue. **(I)** Cross-section of E10.5 bud showing fusion of dorsal pancreas, ventral pancreas, and gut lumens. E-cadherin in red and ZO-1 in green. Hd=head; h=heart; Dp=Dorsal pancreas; Pv=Portal vein; g=Gut tube; d=duodenum; v=ventral bud.

2.3 DISCUSSION:

2.3.1 Embryonic gross pancreatic morphology.

For a long time pancreatic branching has been considered to occur randomly and not be stereotyped (Pictet et al., 1972). However, simple observation of the embryonic pancreas revealed at least some level of common gross morphological features. This chapter provided a careful description of gross pancreatic development and constructed an anatomical model that will aid in the future analysis of the organ. Before the secondary transition, during the proto-differentiated state, pancreatic morphology was quite stereotyped. Especially, at early stages of pancreatic development (E9.5-E10.5) there was 100% conservancy in shape between the pancreata assayed. After, at E11.5-E12.5, the pancreatic tail diverged between pancreata, but the trend of growth was still very similar. Pancreata have either a bifurcated or a blunted tail. A slight preference of growth for the bifurcated tail makes up about 55-60% of the cases versus the blunted tail that accounts for about 45-40% of the cases observed. This difference in shape was not due to a developmental delay since at later stages these subtle differences in the pancreatic tails were still identifiable indicating that the pancreatic tail has two preferential patterns of growth. For developmental stages after the secondary transition, however, pancreatic morphology was classified based on their lateral branches rather than pancreatic tail because this was clearer. During the secondary transition, especially at E13.5, there was great amount of variability in the pancreatic shape. This was probably due to the massive remodeling the pancreatic epithelium was suffering as new lumens were being formed and exocrine and endocrine cells differentiating. However, by E14.5,

the pancreas acquired its characteristic shape that will distinguish it throughout all developmental stages. After E12.5, the number and length of branches was not stereotyped between pancreata. Some had many, some had few, some had long branches while others had short. However, the pattern of branching was generalized into four major groups: 1) No/short lateral branches, 2) one/few lateral branches, 3) many/long lateral branches, and 4) irregular shape. The ratios of these groups vary between stages and litters, but still the pancreas seem to preferentially grow into the first and second group accounting for about ~70% of pancreata assayed versus ~30% of pancreata that fell into the third category. In the later stages of development, the pancreatic shape became less variable since the lobulations that cover the body of the pancreata in the 'no-lateral branches' group grew into little branches making it possible to categorize pancreata only in two groups: 1) Small lateral branches and 2) Long lateral branches. Again at these later developmental stages the pancreas preferentially grew into the first group (short branches).

2.3.2 Pancreatic epithelium, cell polarity and lumen formation.

In 1970 Raymond Pictet and Bill Ruther published a very careful study of pancreatic growth and branching (Pictet et al., 1972). Their work introduced the concept of "psedostratified" and "stratified" bud epithelium, but they proposed that this appearance was due to epithelial bulging. Developmental models of pancreatic branching after this study presented a convoluted single epithelium where branches arise from looping and folding of this single-epithelial layer and lumens arise as folding occurs. This type of branching resembled the one found in the lung where cells proliferate and expand

in a single epithelium layer that bulges and creates the branching organ. However, in 2002 Brigid Hogan and Peter Kolodzief introduced a new concept for pancreatic branching (Hogan and Kolodziej, 2002). They proposed that pancreatic development occurs in a similar way as in the mammary and salivary gland where the epithelium stratifies and tubulogenesis is the result of micro-lumen fusion. Until this date, however, there is no descriptive analysis that supports their ideas or shows the existence of micro-lumens in the pancreatic bud. As a consequence, the pancreatic field keeps debating between these two models of pancreatic development. Here, a careful analysis of pancreatic branching was carried and we propose a new model that unifies the two previous models. We propose that branching occurs through microlumen fusion and cellular rearrangements of the stratified epithelium. But in contrast to mammary and salivary gland where the central lumen and branches are only generated once microlumens are formed and fused into a cohesive system of tubes; in the pancreas evagination creates the principal lumen of the dorsal bud which only subsequently becomes linked to *de novo* formed microlumens. The stratified epithelium grows and bulges from this mayor central lumen and micro-lumen formation occurs only distally within the stratified epithelium.

Our studies established that lumens are formed differently in the pancreas than in other similar branching organs. In both mammary and salivary gland apoptosis is required for lumen formation. In the mammary gland at the terminal end bud there are high levels of apoptosis in the body cells and this phenomena is critical for ductal morphogenesis (Humphreys et al., 1996; Mailleux et al., 2008; Mailleux et al., 2007). In the salivary gland apoptotic cells are detected in the sites were new lumens are being

formed (Jaskoll and Melnick, 1999). On the contrary in the pancreas lumens are formed independent of apoptosis, as suggested before by Joan Brugge group (Mailleux et al., 2008). The absence of either TUNEL or caspase staining within pancreatic lumens suggests that lumens are instead the consequence of cellular arrangements and expansion of the apical membrane domain rather than cell death. This mechanism is very similar to the one observed in the intestine for zebra fish where lumens are formed after small foci of adherens junctions cluster, merge and open to form a new lumen (Horne-Badovinac et al., 2001).

Similar to hair follicle, mammary and salivary gland morphogenesis; the outermost layer of epithelial cells of the pancreatic bud displays basal polarity while the 'inner' cells of the stratified epithelium are unpolarized (Nanba et al., 2000; Nanba et al., 2001; Patel et al., 2006) and as in these branching organs, apical polarity in the 'inner' cells is regained and new lumens are formed. In addition, E-cadherin and β-catenin expression remains constant in all epithelial cells as observed before for the submandibular gland (Hieda et al., 1996). It has been proposed that this change in intracellular adhesion in the hair follicle, mammary and salivary gland is necessary for their morphogenesis (Nanba et al., 2001). Indeed, we believe that the decrease in adhesion in the 'inner' cells (measured by a lack in tight junctions) of the pancreatic bud allow for *de novo* lumen formation and cellular rearrangements required for branching.

Based on data, we speculate that pancreatic stratification results from orthogonal cell division of the polarized- columnar epithelial cells. The first cell divisions occur asymmetrically, creating two types of daughter cells: one that retains the basal constituents (laminin) and another one that inherits the apical cell constituents (APKC,

PAR3, ZO-1). As subsequent cell divisions occur, daughter cells are unpolarized as they do not maintain direct contact with neither the basement membrane/ ECM nor the lumen.

Here, an in depth analysis of the macro and microscopic morphology of the pancreas with a special focus on the epithelium was provided. The meta-analysis revealed semi-stereotyped branching patterns or ‘trends’ of epithelial growth in the pancreas that were summarized in an anatomical model. In addition, the microscopic analysis of the pancreatic epithelium revealed new features to pancreatic development and a better understanding of its dynamics of growth. This work provides the foundations for the analysis of mutant pancreata and leads to the discovery of new molecules involved in pancreatic/epithelial branching.

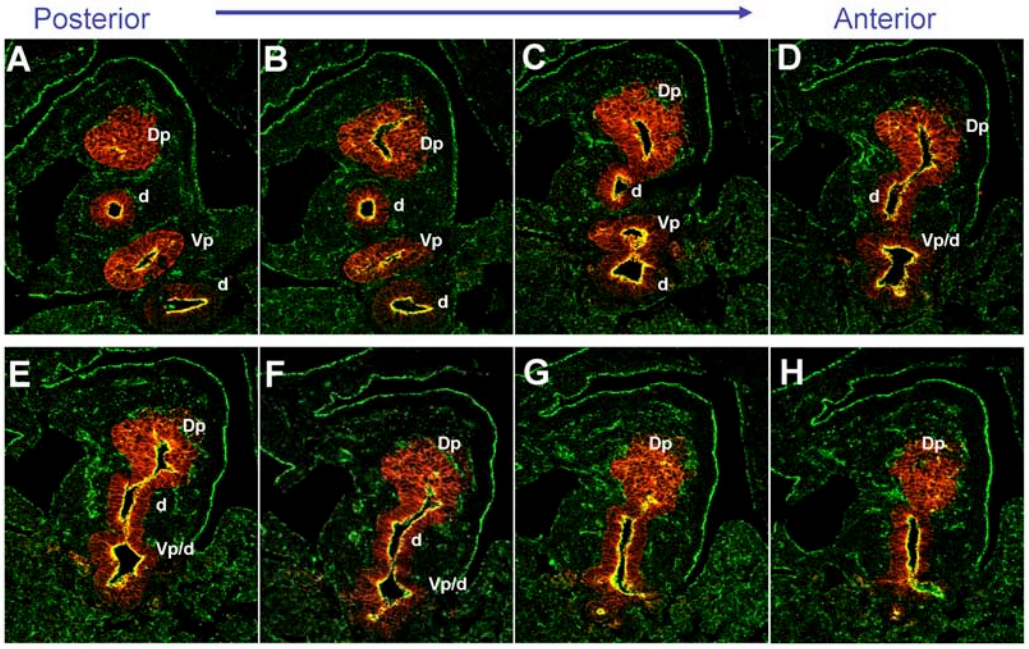

Figure 2.10. Lumen formation and branching initiation. (A-H) Cross sections of E10.5 embryo from posterior to anterior showing ZO-1 (green) and E-cadherin (red) staining. **(D-G)** Dorsal pancreatic lumen fused with duodenum and ventral lumen. Dp=Dorsal pancreas; d=Duodenum; Vp=ventral pancreas; Vp/d=ventral pancreas fused lumen with duodenum.

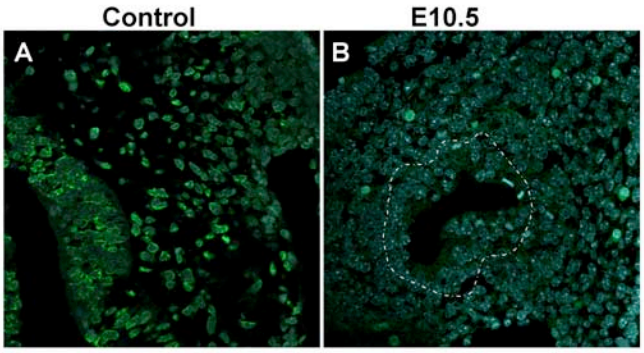

Figure 2.11. Pancreatic lumens are formed by cellular re-arrangement and not apoptosis. (A) E10.5 positive control sections showing apoptotic cells in green. **(B)** Sections of E10.5 in pancreatic epithelium or lumen**.** Pancreatic epithelium is outlined with a dotted line.

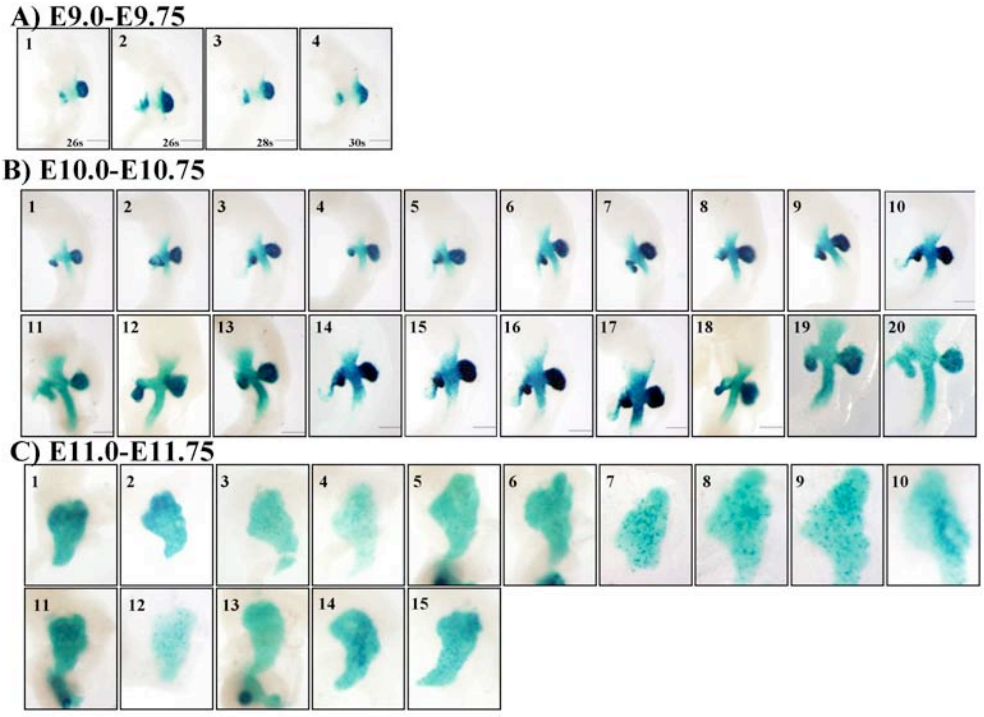

Supplementary Figure 2.1 Pancreatic morphology is stereotyped at early stages of pancreatic development (E9.5 - E11.75) Whole mount β-galactosidase staining of isolated *Pdx1*-lacZ guts from E9.5 to E11.75. **(A-C)** Dissected gut tubes showing pancreatic epithelium and mesenchyme, anterior is up, dorsal is to the right.

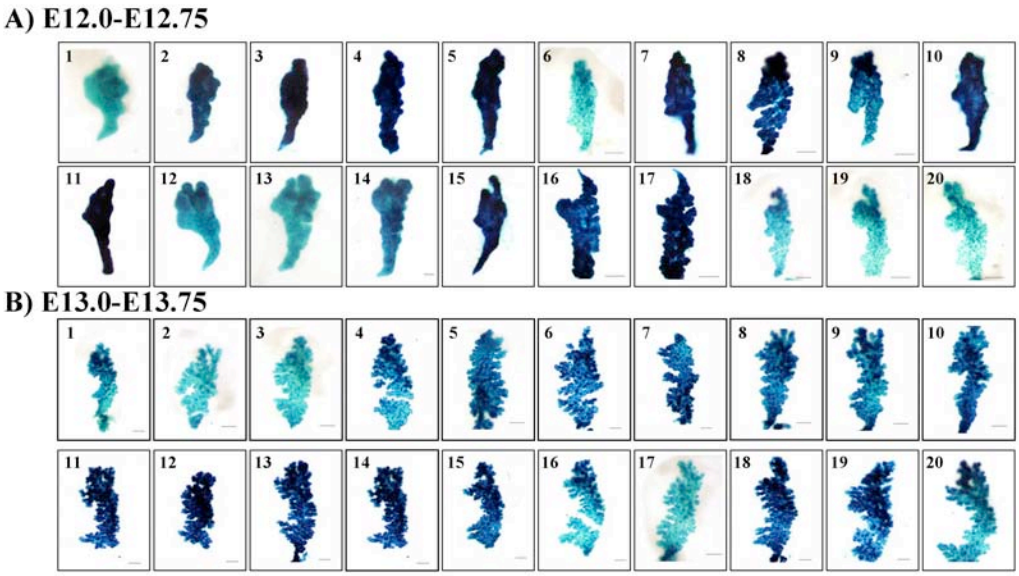

Supplementary Figure 2.2. Composite of multiple images of E12.0- E13.75
Whole mount β-galactosidase staining of isolated *Pdx1*-lacZ dorsal pancreas from E12.0 to E13.75

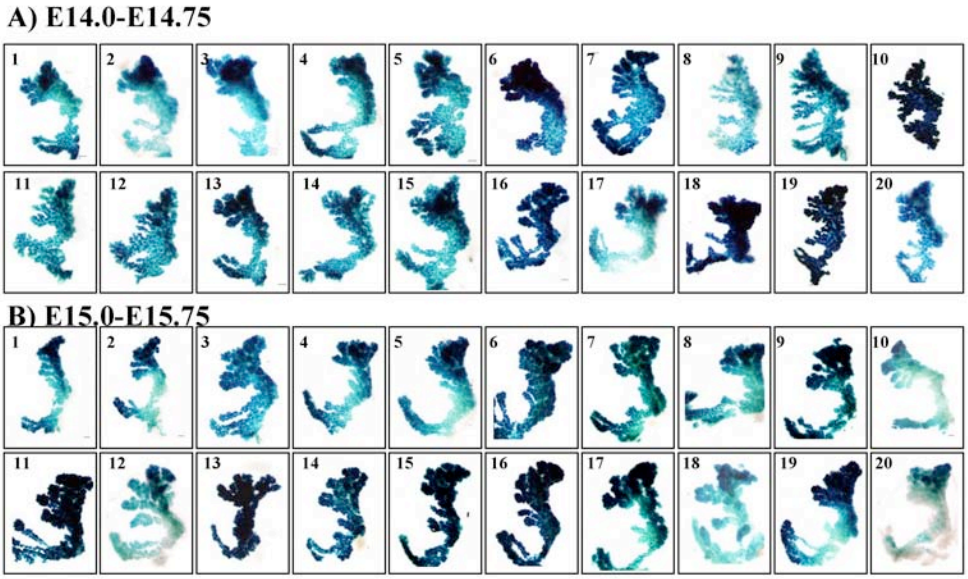

Supplementary Figure 2.3. The pancreas acquires is characteristic morphological shape (E14.0- E15.75) Whole mount β-galactosidase staining of isolated *Pdx1*-lacZ dorsal pancreas from E14.0-E15.75

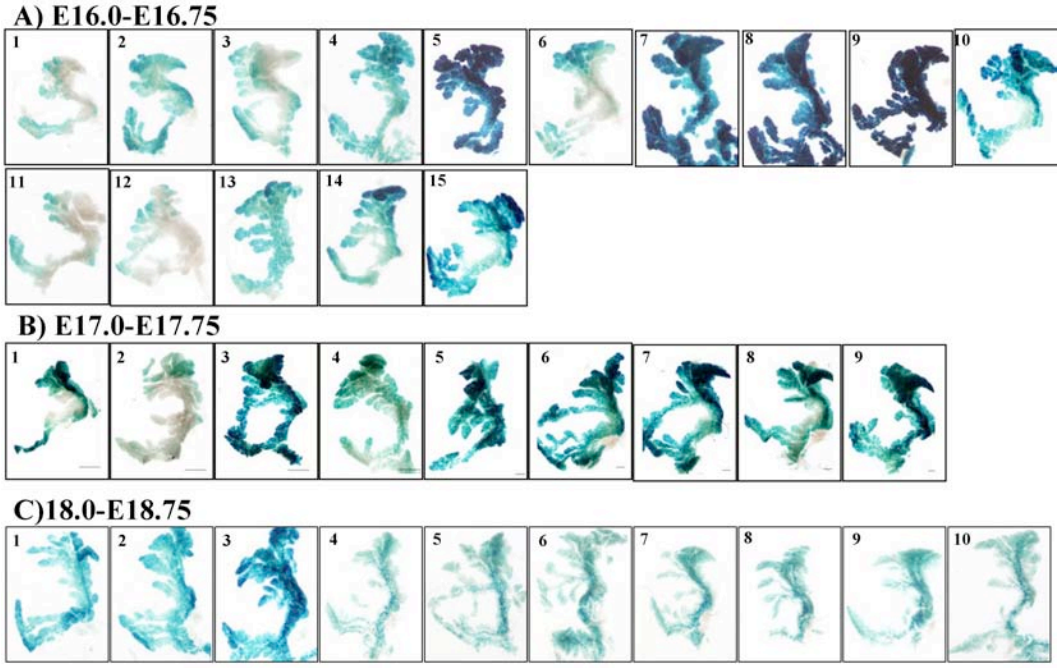

Supplementary Figure 2.4. The pancreatic shape does not change it grows. Whole mount β-galactosidase staining of isolated *Pdx1*-lacZ dorsal pancreas from E16.5-E18.75

Chapter 3. ANALYSIS OF NGN3 EXPRESSION IN PANCREATIC DEVELOPMENT.

NB: This chapter has been previously published under the title: "Biphasic Ngn3 expression in the developing pancreas". Dev Dyn. 2008 Nov;237(11):3270-9". The text has been slightly altered to suit the purposes of this dissertation.

3.1 INTRODUCTION

Ngn3 (Neurogenin3 or Neurog3) is a bHLH transcription factor critical for the specification of endocrine cells in the pancreatic Islets of Langerhans. It was first described in 1996 as a transcriptional regulator expressed in peripheral endocrine tissue of the E12.0 pancreas (Sommer et al., 1996). Later studies demonstrated that Ngn3 is expressed in the pancreatic bud as early as the first endocrine cells are observed and it is never co-expressed with endocrine hormones in pancreatic islets (Gradwohl et al., 2000; Schwitzgebel et al., 2000). Genetic ablation of Ngn3 in mouse results in the complete failure of all pancreatic endocrine cell differentiation and neonatal lethality (Gradwohl et al., 2000). Conversely, gain-of-function studies demonstrate that Ngn3 can induce differentiation of the four endocrine lineages (Apelqvist et al., 1999; Grapin-Botton et al., 2001; Schwitzgebel et al., 2000). The complete failure of both early and late endocrine differentiation in Ngn3 null embryos suggests that NGN3 is required for endocrine cell specification, during the two temporal waves of endocrine differentiation (For a detailed description of these waves of differentiation refer to Chapter 1)

Recent work in the field of pancreas development suggests that different cascades of molecular regulation regulate these two temporally separate waves of islet endocrine cell generation. For example, the transcription factor HLXB9 is transiently expressed early in the pancreatic epithelium, but diminishes following the first transition. Later, however, it reinitiates expression in differentiated b-cells, coinciding with the onset of secondary transition (Li and Edlund, 2001). In addition, the expression of many critical pancreatic transcription factors during secondary transition become differentially restricted to either endocrine or exocrine cell types. For instance, the transcription factors Pdx1, Nkx2.2, Nkx6.1 and Sox9, which are initially expressed widely in the pancreas, gradually become restricted to the endocrine lineage during this time, while Ptf1a becomes restricted to exocrine cells (Kim and MacDonald, 2002). Even more strikingly, some factors only initiate expression after the secondary transition. For example, it has been shown that the expression of the transcription factor MafA is specifically restricted to the endocrine cells of the second wave (Artner et al., 2007), thus supporting the hypothesis that there exists distinct molecular cascades underlying the first and second wave of pancreatic endocrine differentiation.

The dynamics of Ngn3 expression and its molecular function to determine the different endocrine cell lineages during these two temporal waves is poorly understood (Oliver-Krasinski and Stoffers, 2008). However, recent work on Ngn3 has highlighted differences between early versus late embryonic endocrine cells. Using a transgenic temporally-controlled ‘addback’ system to express Ngn3 in an Ngn3 null background, Grappin-Botton and colleagues demonstrated that Ngn3 expression drives endocrine precursors to differentiate, however endodermal progenitors pass through different stages

of ‘competence’, resulting in the differentiation of precursors down various lineages at different embryonic time points (Johansson et al., 2007). Early embryonic endoderm displays the capacity to generate mostly glucagon-expressing cells, while later endoderm is able to generate the full range of endocrine cell types, including β cells. This suggests that there is likely to be temporal regulation of Ngn3 expression during different stages of pancreatic development.

Previous reports describe Ngn3 expression at various stages (Apelqvist et al., 1999; Burlison et al., 2008; Gradwohl et al., 2000; Murtaugh, 2007; Schwitzgebel et al., 2000; van Eyll et al., 2006), however, no detailed characterization currently exists that examines either Ngn3 expression initiation or maintenance throughout pancreatic development. Here, a detailed developmental profile of Ngn3 mRNA and protein expression throughout all stages of pancreatic budding and branching is presented. Clarifying the temporal expression of Ngn3 expression, both during the first and the secondary transition, will advance our understanding of both early and late islet endocrine cells.

3.2 RESULTS

3.2.1 Ngn3 expression initiation

To assess early embryonic *Ngn3*, whole mount *in situ* hybridization was used and compared its expression to that of the pancreatic duodenal homeobox gene, *Pdx1* (Fig. 3.1), utilizing a *Pdx1*-lacZ reporter line (Offield et al., 1996). Mouse embryonic endoderm and budding pancreas were examined from E8.0 (5 somites, or 5s) to E9.5

(24s). It was observed that *Ngn3* expression initiated around E8.25 (Fig. 3.1A-C and Fig. 3.2), slightly earlier than previously reported (Apelqvist et al., 1999). Specifically, it initiated as early as the 9-somite stage, in a few cells within the dorsal pre-pancreatic endoderm. Soon after, at 12 somites, *Ngn3* expression became quite robust, in a rather punctate pattern, with cells expressing either higher or lower levels of transcript (Fig. 3.1C). Given that early *Ngn3* expression was clearly punctate, and thus not in all cells of the pancreatic bud, it is likely that these early cells already represent progenitors that give rise to endocrine cell lineages.

3.2.2 Delay of Ngn3 expression in the ventral pancreas

Early endodermal *Ngn3* expression in the dorsal pancreatic region, is rather remarkable at E8.5 (12s) in that it preceded pancreatic morphogenesis and it initiated long before ventral pancreas *Ngn3* expression (Fig. 3.1C, and Fig. 3.2). The dorsal bud in mouse evaginates from the pre-pancreatic endoderm at embryonic day E9.0-E9.5 (Jorgensen et al., 2007) and prior to this stage *Ngn3* expression was observed. This indicates that cells turn on *Ngn3* expression before the epithelium thickens, stratifies and begins the cellular morphogenesis that initiates pancreatic differentiation. In addition, although endocrine hormone transcription is reported to be detectable as early as E9.25 (Gittes and Rutter, 1992), endocrine precursor cells cannot yet be identified by hormone protein immunohistochemistry (Jorgensen et al., 2007).

The expression of *Pdx1*, on the other hand, initiated earlier than *Ngn3* and was also first observed only in the ventral pancreatic domain. Specifically, two clusters of

Pdx1 expressing cells in the ventral endoderm of the anterior intestinal portal (AIP) were observed, as early as the 5-somite stage (E8.0), slightly earlier than previously described (Fig. 3.1G)(Jorgensen et al., 2007; Li et al., 1999). Faint expression of *Pdx1* in the dorsal pancreatic region was detected later, around the 8-somite stage as the embryo turns (Fig. 3.1H). By 12 somites, strong *Pdx1* expression was detected in both the ventral and dorsal pancreas (Fig. 3.1I) (Apelqvist et al., 1999; Guz et al., 1995). In contrast to the close correlation of *Pdx1* and *Ngn3* expression initiation in the dorsal pancreas, there was a dramatic delay in *Ngn3* expression initiation in the ventral pancreas (compare Fig. 3.1C-E to Fig. 3.1I-K), where *Ngn3* was not detectable until about two days later (about E10.0). Interestingly, it has been shown that endocrine differentiation occurs later in the ventral pancreas compared to dorsal (Apelqvist et al., 1999; Pictet et al., 1972; Spooner et al., 1970), and the mature ventral pancreas is known to contain fewer α and β cells in many species (Beaupain and Dieterlen-Lievre, 1974; Cleaver, 2004; Stefan et al., 1982). It is likely that this notable delay in *Ngn3* expression is correlated with this differential β cell composition of the dorsal and ventral pancreas.

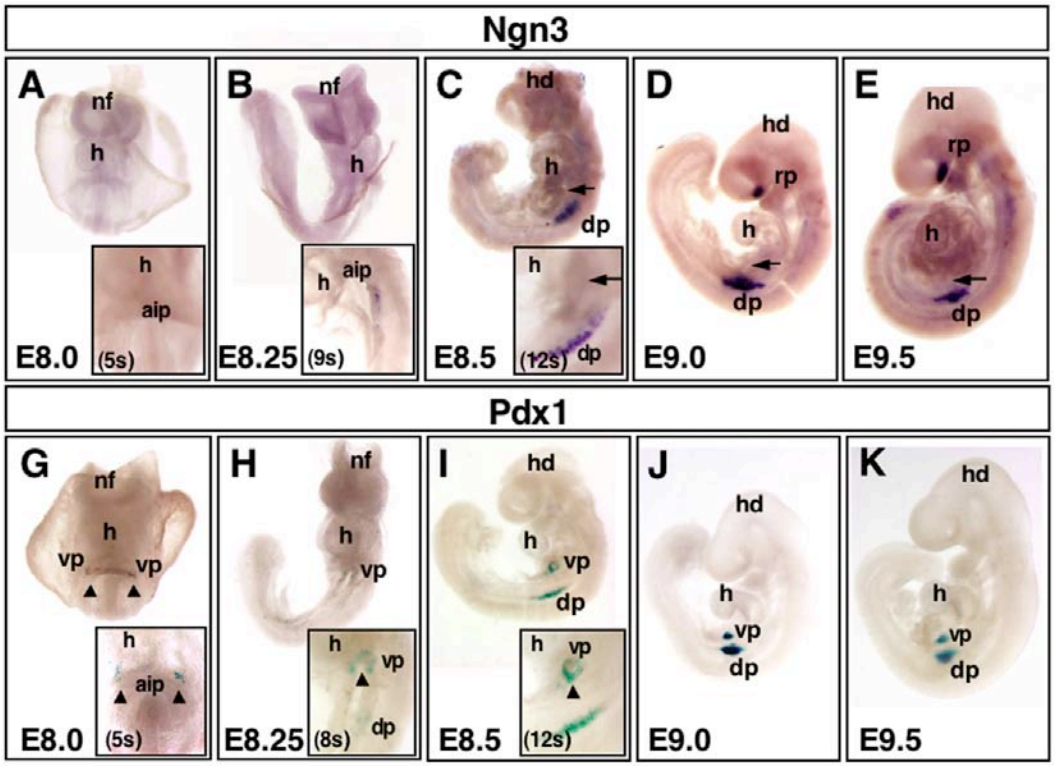

Figure 3.1. Initiation of *Ngn3* and *Pdx1* expression during embryogenesis. Developmental profile comparison of early expression of *Ngn3* and *Pdx1*, using whole mount in situ hybridization of *Ngn3* (A-E) and whole mount β-galactosidase staining of *Pdx1*-lacZ embryos (G-K) from E8.0 to E9.5. Embryos in A,B,G,H face forward. Embryos in C-E and I-K face left. *Ngn3* and *Pdx1* initiate in the dorsal pancreas at relatively similar time points shortly after turning, between E8.25 and E8.5 (A-C *Ngn3*, G-I *Pdx1*). *Ngn3* initiates in the dorsal pancreas at 9s (inset in B). *Pdx1* is expressed in two ventral pancreas domains, as early as E8.0 (5s) (arrowheads in G). These ventral domains fuse as the embryo turns (arrowheads in H,I). While *Pdx1* marks the ventral pancreas from early stages (G-K), *Ngn3* is not expressed in the ventral pancreas (arrows in C-E) at any time during early development (prior to E10.0). See insets in (A-C) for close-ups on early dorsal and ventral domains for onset of *Ngn3* expression, and insets in (G-I) for close-ups of *Pdx1* initiation. Note also that *Ngn3* marks anterior neurectoderm in the forebrain (head staining in D,E), ventral to Rathke's pouch. dp, dorsal pancreatic bud; h, heart; hd, head; nf, neural folds; rp, Rathke's pouch; vp, ventral pancreatic bud

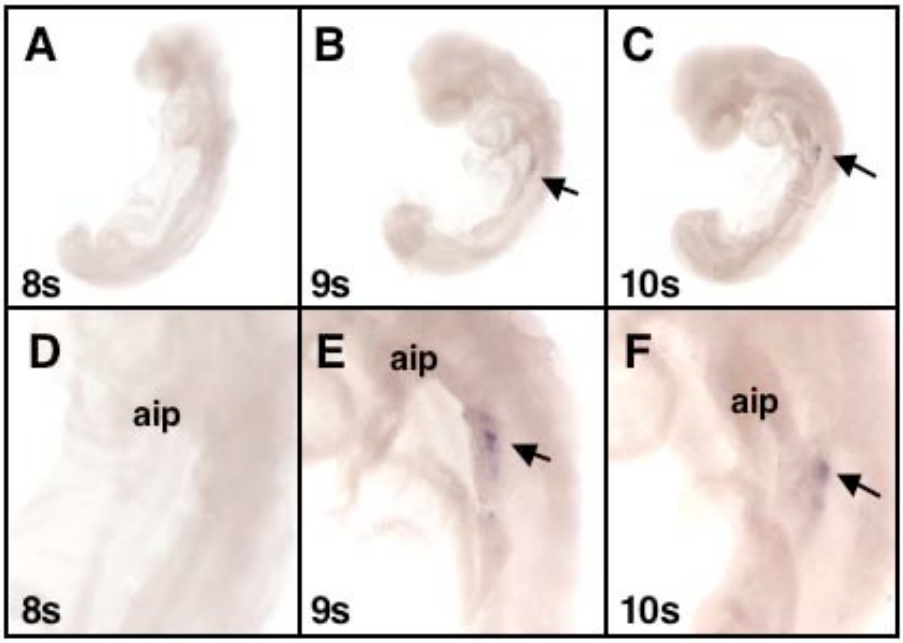

Figure 3.2. Initiation of *Ngn3* expression at E8.25. In situ hybridization for *Ngn3* expression. A-C) Whole stained embryos. D-F) Close-up of pre-pancreatic endoderm. A,D) At the 8-somite stage, *Ngn3* expression is never detected. B,E) At the 9-somite stage, low levels of *Ngn3* expression are observed in a few cells of the dorsal pre-pancreatic endoderm (arrows in B,E) (in 1 out of 3 embryos assayed). C,F) At the 10-somite stage, *Ngn3* expression is readily detected in scattered cells of the dorsal pancreas in all embryos assayed (arrows in C,F). aip, anterior intestinal portal.

3.2.3 Biphasic expression of Ngn3

In order to elucidate whether *Ngn3* is regulated throughout pancreatic growth, *Ngn3* expression was examined during dorsal pancreatic bud growth and branching (Fig. 3.3). Surprisingly, *Ngn3* was expressed in a biphasic manner and each wave of expression precedes the first and the secondary transitions of pancreas development. In the dorsal pancreatic epithelium, high *Ngn3* expression was detected from E10.0 to E10.5 (28s-35s) (Fig.3-3A-C). Shortly after E10.5, a dramatic and precipitous decrease in *Ngn3* transcript

was detected in the dorsal pancreas. Careful examination revealed that the downregulation of *Ngn3* expression started to occur about E10.75 (36s-38s) (Fig. 3.3D) and continued to decrease until about E11.25 (41-42s), when it was found a distinct downregulation, as assayed by *in situ* hybridization (Fig. 3.3F).

Afterwards, levels of *Ngn3* mRNA started to recuperate and before the onset of the secondary transition, around E12.5, higher *Ngn3* transcript levels were observed (Fig. 3.3G-K). This high level of expression was maintained as the dorsal bud began to oblate and extend along the flank of the stomach. After approximately E13.5, expression of *Ngn3* became restricted to axial, endodermally-derived epithelial cells that undergo extensive branching (Fig. 3.3M-O). This region is known to generate endocrine and duct cells, while the more peripheral regions consisting of the tips of lobules/branches are known to generate acinar cells (Zhou et al., 2007).

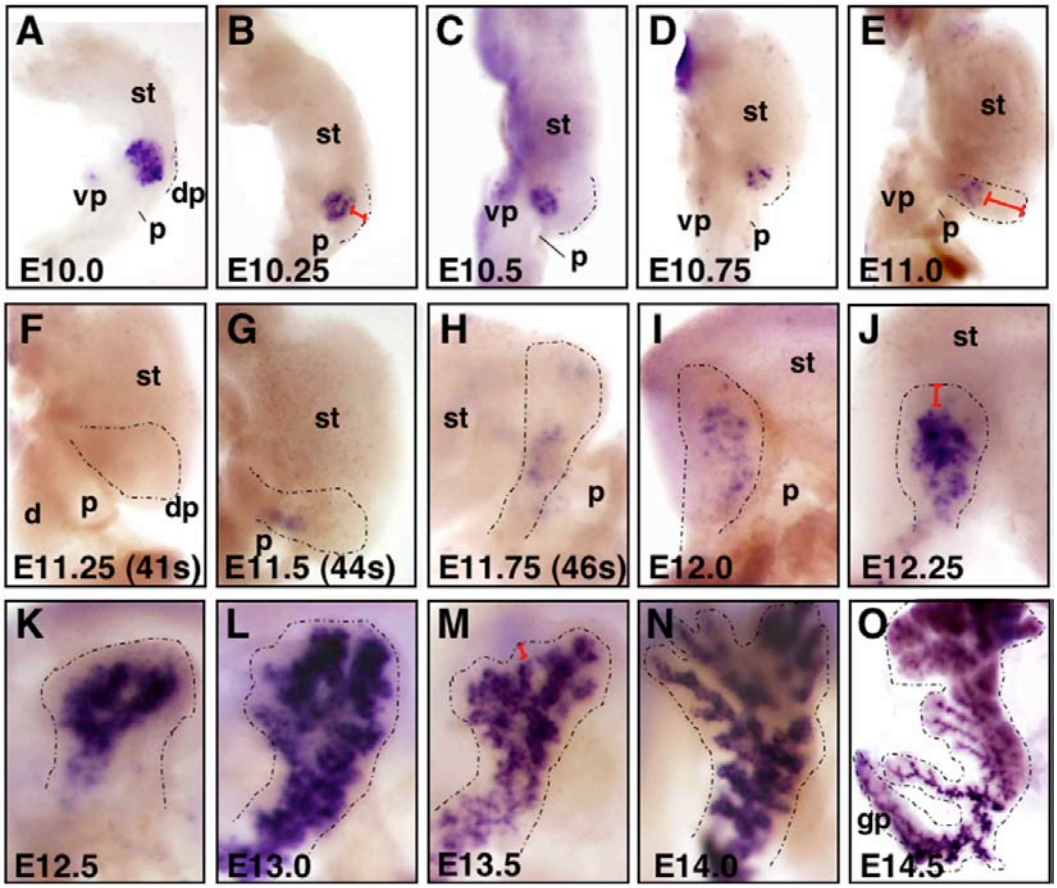

Figure 3.3. Biphasic transcription of *Ngn3* in the developing pancreas. Whole mount in situ hybridization of *Ngn3* in wildtype embryos from E10.0 to E14.5. **A-G)** Dissected gut tubes, anterior is up, dorsal is to the right; **H)** gut tube in process of turning, anterior is up, but pancreas is shifting relative to stomach, and focus is on pancreas near portal vein; **I-O)** Dorsal pancreatic bud, with stomach seen in background, except in O where pancreas is isolated. Dorsal pancreas in all panels is outlined with a black dotted line. **A-C)** Note robust expression of *Ngn3* in dorsal pancreatic bud at E10.0 to E10.5. **D,E)** Decline of *Ngn3* expression begins at E10.75, and **F)** is undetectable at E11.25. **G-K)** Expression then begins to increase from E11.5-12.5, after which expression is strong in cells of the branching epithelium **(L-O)**. **A-E)** Note that *Ngn3* expression in ventral pancreas is low at all stages shown. Ventral pancreas is not shown in **(F-O)**. After E11.0, the ventral pancreas grows posteriorly, along the mesentery of the duodenum, and is not visible in images as presented. Note also that distal pancreatic mesenchyme (or 'cap') is thickest around E11.0, but becomes progressively thinner as development proceeds (compare red brackets in **B,E,J,M)**. Precise staging of embryos was accomplished by counting somites (see Table 3.1). dp, dorsal pancreatic bud; d, duodenum; gp, gastric pancreas; p, portal vein; st, stomach; vp, ventral pancreatic bud.

Embryonic Stage	No. of Somites	Embryonic Stage	No. of somites
E7.5	1-2	E10.5	33-35
E7.75	3-4	E10.75	36-38
E8.0	5-7	E11.0	39-40
E8.25	8-10	E11.25	41-42
E8.5	11-13	E11.5	43-44
E8.75	14-16	E11.75	45-46
E9.0	17-19	E12.0	47-48
E9.25	20-22	E12.25	49-50
E9.5	23-25	E12.5	51-52
E9.75	26-27	E12.75	53-55
E10.0	28-30	E13.0	56-60
E10.25	31-32	E13.5	~61-63

Table 3.1. Staging of embryos. To establish a developmental profile of Ngn3 expression, precise staging of embryos is accomplished by counting somite number. This table is based on staging by M.H.Kaufman (Kaufman, 1992), but provides increased resolution within each stage. Staging shown in figures is based on somite counts as presented here.

Of interest, it was noted the temporal coincidence of *Ngn3* downregulation with two anatomical phenomena. First, *Ngn3* transcription decreased precipitously at precisely the time when the midgut undergoes dramatic remodeling. Before this, from E9.5-E10.5, the pancreatic buds are bilaterally symmetric along the midline. However, between E10.75 to E12.0, the stomach and duodenum fold relative to each other and rotate. During this turning, the pancreas swings left and comes to lie against the left flank of the stomach (Fig. 3.3D-I). It was precisely during this rotation that *Ngn3* expression ceased. *Ngn3* cessation also correlated with a change in the thickness of the distal pancreatic mesoderm or ‘cap’. Initially, this ‘cap’ is of moderate thickness, but during gut turning it

expands dramatically, more than doubling in thickness (compare red brackets in Fig. 3-3B and 3.3-E). Subsequently, as the pancreas branches, this mesoderm progressively thins again, until it is a rather minor component enveloping the pancreas (compare brackets in Fig. 3.3E with Fig. 3.3J,M). Given that mesenchyme is known to repress or delay *Ngn3* induction (Duvillie et al., 2006), it is possible that when the mesenchyme is at maximal thickness, *Ngn3* is repressed by mesenchymal factors. Alternatively, the mesenchyme may change molecularly during this time and affect the underlying endoderm differently. Although tight correlation of *Ngn3* transcription cessation with both gut turning and changes in mesenchymal thickness is intriguing, it remains unclear what is causative, what might regulate this transcriptional activity and what purpose it may serve.

The observed biphasic expression of Ngn3 was highly reproducible, and restricted to a narrow developmental window. To ensure that this was not an experimental artifact, a large numbers of systematically staged embryos (n=142 pancreases assayed between E9.5-E14.5; n=23 at E11.0-11.5) (Fig. 3.4A,B and Table 3.1). At E11.25, a significant decrease of *Ngn3* transcripts was consistently detected by *in situ* hybridization and *Ngn3* expression was low shortly before and after this time point (Fig. 3.5G,H). Close examination of sections revealed that this downregulation in developmental *Ngn3* expression was due to both a decrease in the number of cells expressing high levels of *Ngn3* and to an overall decrease of transcript levels in individual cells (Fig.3.5, and data not shown). In addition, these observations were confirmed using semi-quantitative RT-PCR (Fig. 3.4C). While *Ngn3* transcript by PCR at E10.5 and E13.5 was detected, little *Ngn3* expression was detected at E11.5.

A *Ngn3* relative expression levels (# embryos)

	E10.5	E11.5	E12.5	E13.5
No Expression	0	10	2	0
Low Expression	4	9	9	0
Medium Expression	3	4	11	0
High Expression	14	0	17	28

B Percentage (%) of embryos assayed

	E10.5	E11.5	E12.5	E13.5
No Expression	0	43	5	0
Low Expression	19	39	23	0
Medium Expression	14	17	28	0
High Expression	67	0	44	100

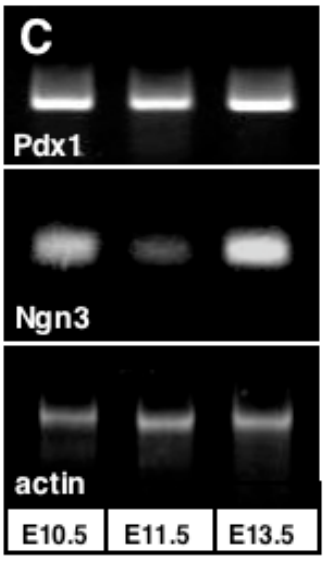

Figure 3.4. Biphasic of *Ngn3* transcripts. Semi-quantitative analysis of *Ngn3* and *Pdx1* expression during early pancreas development. A) Total numbers of embryos displaying relative intensities of expression by in situ hybridization analysis (arbitrary thresholds). Stages shown represent a small range of closely staged embryos. B) Percentage of embryos in (A) showing different expression levels, relative to total numbers. C) RT-PCR for *Pdx1* (top), *Ngn3* (middle) and *actin* (bottom) expression in isolated pancreata at E10.5, 11.5 and E13.5.

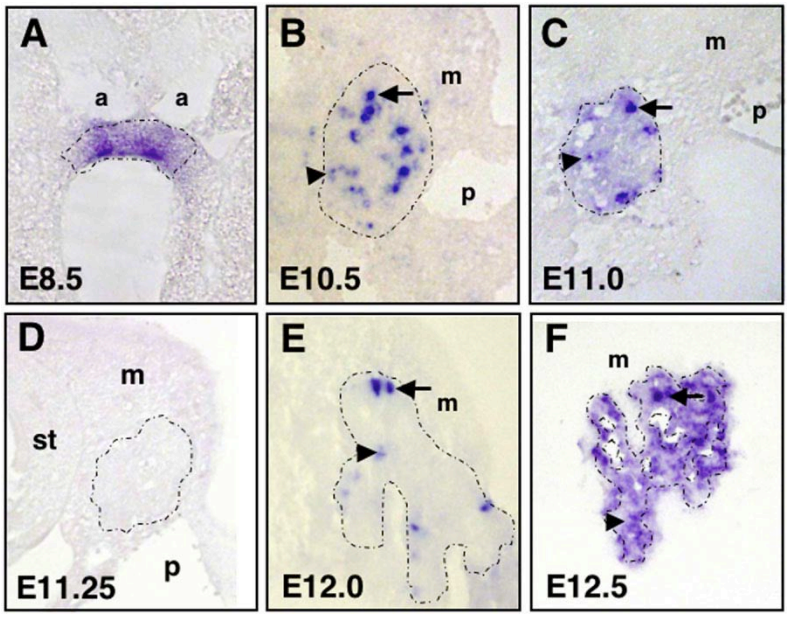

Figure 3.5. *Ngn3* expression in pancreatic epithelium. Sections showing in situ hybridization of *Ngn3* in wildtype embryos from E8.5 to E12.5. A) Note more homogeneous expression in early endoderm (E8.5). At this stage, the endoderm has not yet thickened or stratified and is still a cuboidal epithelium. B) At E10.5, expression becomes heterogeneous with 'high' (arrow) and 'low' (arrowhead) expressing cells. C) By E11.0, fewer scattered cells still express higher levels of *Ngn3* (arrow), while expression levels decline in the rest of the epithelium (arrowhead). D) *Ngn3* expression is undetectable at E11.25. E) Cells expressing *Ngn3* can be easily detected at E12.0. F) Expression then increases, both at higher levels in scattered cells and at lower levels throughout the epithelium (E12.5 shown). Pancreatic epithelium is outlined with a dotted line. a, aortae; m, mesenchyme; p, portal vein; st, stomach.

3.2.4 Biphasic expression of NGN3 protein

In order to determine whether the observed biphasic transcriptional profile of *Ngn3* translates into differences in protein levels at different stages, NGN3 protein was assayed using immunofluorescence (Fig. 3.6). Previous reports had identified small numbers of NGN3 protein expressing cells at approximately E11.5 (Schwitzgebel et al., 2000), so an expression profile of NGN3 protein was examined during the timeframe

encompassing the observed *Ngn3* transcriptional cessation (n=24 pancreases between E10.5-E14.5; n=7 at E11.25-E11.5). Again, using carefully staged embryos from E10.5 to E14.5, it was found that protein levels did indeed experience a similar downregulation (Fig.3.6 and data not shown).

At E10.5 NGN3 protein was clearly detected in many cells within the stratified pancreatic epithelium (Fig. 3.6A). These levels started to decrease by E10.75-E11.0 (data not shown), were very low at E11.25-11.5 (Fig. 3.6B,C), and started to increase by E12.0 (Fig. 3.6D), in accordance with observed mRNA levels. By E13.5 and thereafter, there was a dramatic increase in NGN3 protein that correlated with increasing *Ngn3* transcript levels (Fig. 3.6F). In contrast to *in situ* hybridization analysis, a total absence of NGN3 protein was not observed during the E11.25-11.5 window, although protein levels were significantly lower at these stages (Fig. 3.6G).

3.2.5 Expression of Ngn3 transcripts is more widespread than NGN3 protein

The expression patterns of *Ngn3* transcripts and NGN3 protein were distinctly different. Although rather extensive expression of *Ngn3* throughout the branching epithelium was observed by *in situ* hybridization (Fig. 3.3L-O), NGN3 protein was clearly restricted to individual scattered cells (Fig. 3.6). To assess the extent of epithelial expression, *Ngn3* expression was compared to *Sox9* expression, which marks the entire early pancreatic epithelium (Fig. 3-.7A,B). Results showed that although not all cells of the epithelium expressed *Ngn3*, many more than expected did, when compared to

published reports (Apelqvist et al., 1999; Schwitzgebel et al., 2000) and to our own protein analyses (Fig. 3.7C).

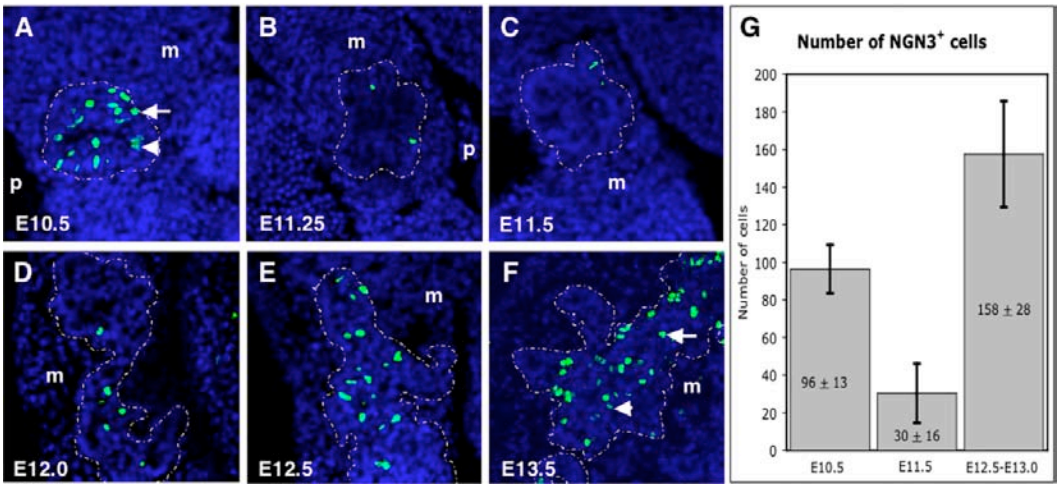

Figure 3.6. Biphasic NGN3 protein expression in pancreatic epithelium. NGN3 protein detected by immunofluorescence on sectioned pancreas, from E10.5 to E13.5. A) NGN3 protein is readily detected in the stratified epithelium of the E10.5 bud. B,C) From E11.25 to E11.5, few if any cells show NGN3 staining in single sections. D-F) At E12.0, we start to detect a steady increase in the number of cells expressing NGN3 that continues to E13.5. Pancreatic epithelium is outlined with a white dotted line. High (arrows) and low (arrowheads) levels of NGN3 protein can be observed in individual cells. m, mesenchyme; p, portal vein. G) Quantification of the number of cells showing NGN3 protein expression at E10.5, E11.5 and E12.5-E13.0 (n=3 for each stage). average number of cells showing protein expression at E11.5 is approximately 30, while at E10.5 it is 96 and between E12.5-E13.5 it is 158. Note the statistically significant reduction of $NGN3^+$ cells at E11.5 ($p \leq 0.02$).

Thus, *Ngn3* transcripts were unexpectedly more widespread in the pancreatic epithelium than NGN3 protein. While it is possible that *in situ* hybridization is simply more sensitive than immunostainings at detecting low levels of Ngn3, these observations may alternatively suggest that post-transcriptional regulation is likely to be important during endocrine differentiation. In addition, *Ngn3*-expressing cells did not all express

equal levels of either transcript or protein. Sections revealed clear ‘high’ and ‘low’ *Ngn3*-expressing cells, presented within the dorsal pancreatic endoderm, both by RNA (Fig. 3.5B,E,F) and protein (Fig.3.6A,F). Moreover, the appearance of ‘high expressors’ at E10.5 (Fig.3.5B) seemed to correlate with the first differentiated endocrine cells, which are detected as early as E10.0 (Jorgensen et al., 2007). These results suggest that certain threshold levels of total *Ngn3* mRNA are required for NGN3 protein accumulation. In addition, it is possible that only $Ngn3^{high}$ cells ultimately express enough NGN3 protein to give rise to endocrine cells.

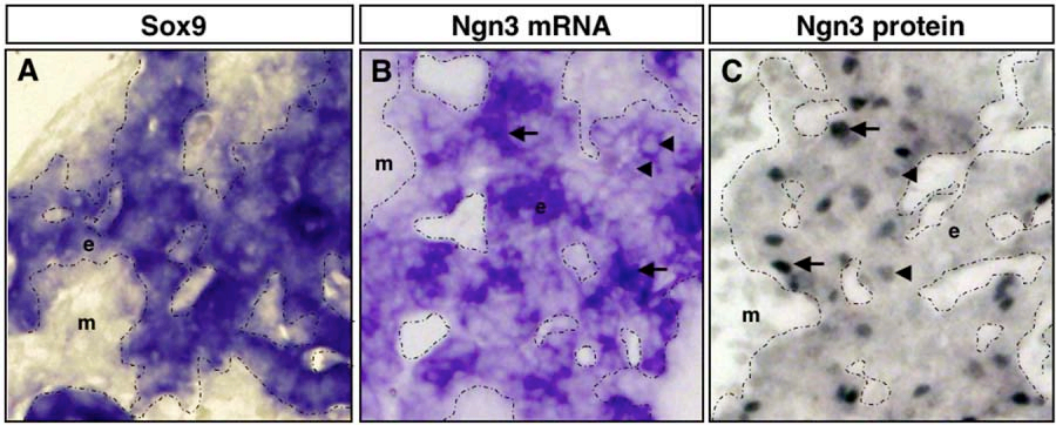

Figure 3.7. *Ngn3* transcripts are more widespread in pancreatic epithelium than NGN3 protein. Sections through E13.0 dorsal pancreas. A,B) In situ hybridization. C) Immunohistochemistry for NGN3. A-C) High magnification of the pancreatic epithelium (20X). A) Sox9 is expressed throughout the pancreatic epithelium. B) *Ngn3* is expressed in many cells within the pancreatic epithelium, displaying both high (arrows) and low (arrowheads) expressing cells. C) NGN3 protein is concentrated in scattered cells of the pancreatic epithelium. In addition, cells are observed that express either high (arrows) or low (arrowheads) levels of NGN3 protein. Note that there are significantly more cells that express the *Ngn3* transcript (B), than cells that express NGN3 protein (C). Pancreatic epithelium is outlined with a dotted line. e, epithelium; m, mesenchyme.

This may be similar to reported 'high' and 'low' *Pdx1* expressing cells, where the *Pdx1*^{high} cells are thought to give rise to β cells (Fujitani et al., 2006; Nishimura et al., 2006). Finally, it is possible that *Ngn3* is initially expressed in a broader domain of the pancreatic epithelium than the future endocrine compartment. This is supported by lineage analysis using Cre-mediated recombination, which demonstrates that at least some proportion of both ductal and acinar progenitors express *Ngn3* at some point during their development (Schonhoff et al., 2004).

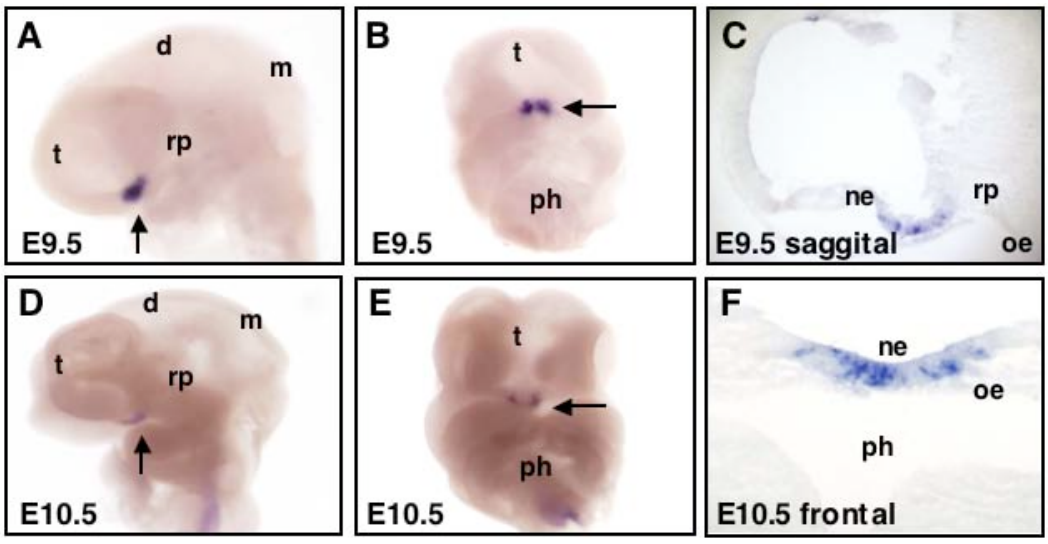

Figure 3.8. Expression of *Ngn3* in embryonic neural tissues. In situ hybridization for *Ngn3* transcripts in the head. A,D) Lateral views of heads, facing left, anterior is up. B,E) Frontal view of same heads as in A,D, facing forward and up. C,F) Sections of heads in A,D respectively. A) *Ngn3* is expressed in a small region in the anterior neural folds, specifically the ventral telencephalon, near Rathke's pouch (arrow). B) This expression is in two patches flanking the midline (arrow). C) Saggital section showing that Ngn3 expression is restricted to the neuroectoderm. D,E) *Ngn3* expression in this region declines at E10.5 (arrows). F) Frontal section through the neurectoderm at E10.5. d, diencephalon; ne, neuroectoderm; m, mesencephalon; oe, oral ectoderm; ph, pharynx; rp, Rathke's pouch; t, telencephalon.

3.2.6 Neural expression of Ngn3

Separately, during the analysis of early *Ngn3* expression, prominent expression was detected in a region of the ventral telencephalon/anterior neuroepithelium (Fig. 3.1D,E). In this region, early and strong *Ngn3* expression was observed in two small patches flanking the midline (Figure 3.8). Although this domain is close to the pre-pituitary oral ectoderm and Rathke's pouch, it is slightly more ventral and is likely to represent pre-hypothalamus ectoderm. Indeed, expression of *Ngn3* in the later hypothalamus has been previously noted in different species, including mouse (Huang et al., 2000; Wang et al., 2001) (www.genepaint.org).

3.3 DISCUSSION

This chapter reports the novel observation that *Ngn3* expression is biphasic during early pancreatic development. This is one of few demonstrations of a molecular correlation with the first and the secondary transitions of pancreatic endocrine differentiation. The first period of *Ngn3* expression is temporally correlated with the primary transition endocrine lineage, while the reactivation of *Ngn3* expression initiates just prior to the secondary transition. Given that very little is known regarding the regulation of these two separate waves of endocrine differentiation, it is a step towards identifying similarities and differences between 'early' versus 'late' embryonic endocrine cells.

Recent data from Grapin-Botton and colleagues demonstrate that these two populations of endocrine cells have different developmental potentials (Johansson et al.,

2007), with early *Ngn3*-expressing precursors giving rise mostly to α-cells and later precursors giving rise to a full range of endocrine cell types, including insulin-expressing β-cells. It is likely that these different pools of *Ngn3*-expressing endocrine precursors experience different molecular contexts, which change over time and result in different differentiation outcomes. It is therefore important for pancreatic studies to identify and recognize whether similar fluctuations occur in the expression of other essential endocrine differentiation factors and to better understand the profile of factors expressed in endocrine cells, 'early' versus 'late'. Studies support the hypothesis that pancreatic progenitors are inherently different during the first and secondary waves. Melton and colleagues, for instance, have recently identified pancreatic multipotent progenitor cells (MPCs) that give rise to three pancreatic lineages, including endocrine, exocrine and ductal, however these are only maintained until E12.5 (Zhou et al., 2007). After E12.5, their potential becomes restricted and they give rise solely to acinar cells. How and why these precursors undergo an abrupt restriction in cell fate during the secondary transition remains unclear, but the answer is likely to lie in the complex interplay of molecular cascades that change as the pancreas develops. Clarifying the role of the first and the secondary transition endocrine cells and elucidating whether they emerge as a result of distinct genetic programs will undoubtedly forward the field of pancreatic islet studies, ES cell differentiation to β cells and regenerative therapies for diabetes.

Chapter 4. RGS PROTEINS ARE EXPRESSED IN PANCREATIC ENDOCRINE CELLS AND IN MODELS OF β-CELL REGENERATION.

NB: This chapter is in revision under the title: "Rgs8 and Rgs16 gene expression in embryonic endocrine pancreas and regenerating adult islets". Text has been modified to suit the purposes of this thesis. Thomas Wilkie and Ozhan Ocal provide the animals, did the genotyping and glucose measurements. Zhao V. Wang provided figure 4.9.

4.1. INTRODUCTION

Diabetes affects over 246 million people worldwide and accounts for about 6% of annual global mortality (www.idf.org). This disease is characterized by defective glucose metabolism and hyperglycemia resulting from the destruction of insulin-producing β−cells within the pancreas (type 1), or defects in the insulin signaling pathway (type 2). Diabetes has no cure, although there are palliative treatments to control its symptoms. There is great need to understand the cellular and molecular basis for islet cell proliferation and differentiation in an effort to generate regenerative therapies for diabetic patients. While groundbreaking work has advanced our ability to drive stem cells towards the pancreatic endocrine cell fate in culture (D'Amour et al., 2005; D'Amour et al., 2006; Kroon et al., 2008), much remains unknown about the molecular pathways regulating the differentiation of islet cell lineages (Collombat et al., 2006; Lammert et al., 2001; Lammert et al., 2003; Oliver-Krasinski and Stoffers, 2008) or the mechanisms underlying islet regeneration (Bonner-Weir et al., 2008; Dor et al., 2004; Xu et al., 2008)

It is well established that the pancreas under metabolic stress is capable of β-cell proliferation and/or differentiation. For example, during pregnancy, maternal β−cell expansion compensates for increased metabolic demands of the developing fetus (Karnik et al., 2007). In type 2 diabetes, β−cell expansion transiently controls elevated glycemic levels before β−cell failure (Chua et al., 2002). In type 1 diabetes, β−cells continually replenish in a futile effort to manage hyperglycemia resulting from β−cell destruction by the immune system (von Herrath and Homann, 2004).

The cellular origin of the new endocrine cells remains controversial. Studies from Melton and others suggest that new β−cells derive from replication of pre-existing β−cells(Dor et al., 2004; Teta et al., 2007). However, work from Bonner-Weir supports the existence of “foci of regeneration” located in the pancreatic ducts (Bonner-Weir et al., 2004). Bonner-Weir suggests that ductal cells can regress to a less differentiated stage and function as a progenitor pool. Recent work by Heimberg and colleagues has shown that the adult pancreas has the ability to reactivate expression of Ngn3 (a pro-endocrine gene) during β−cell formation in response to extreme pancreatic injury (Gradwohl et al., 2000; Xu et al., 2008). An important goal in the field of pancreatic studies is to identify the signaling pathways that control pancreatic β−cell expansion via replication of preexisting β−cells or neogenesis.

Recently, it has been found that Glp-1 (Exendin-4) and other G protein-coupled receptor (GPCR) agonists stimulate β−cell replication and neogenesis and improve glucose tolerance in mouse models of type-1 diabetes (Chu et al., 2007; Kodama et al., 2005; Sherry et al., 2007; Tourrel et al., 2001; Xu et al., 1999) suggesting an implication for GPCR signaling in β-cell expansion. Regulators of G protein signaling (RGS)

proteins are GTPase activating proteins (GAPs) that regulate the frequency and duration of GPCR signaling(Berman et al., 1996; Ross and Wilkie, 2000). RGS expression correlates with GPCR signaling making them good indicators of active GPCR signaling (Dohlman et al., 1996). Therefore, we decide to investigate GPCR signaling in the pancreatic endoderm by characterizing RGS gene expression during pancreatic endocrine cell development and proliferation. Understanding how RGS genes regulate GPCR signaling in pancreatic endocrine cells is likely to further the development of novel therapies for treatment of diabetes.

Here, Rgs8::GFP and Rgs16::GFP expression was characterized during pancreatic endocrine cell development and proliferation. Pancreatic progenitor cells expressed Rgs8 and Rgs16, beginning in the dorsal pancreatic anlagen and continuing throughout embryogenesis. In the perinatal pancreas, Rgs-expressing cells aggregated into islets in tight association with pancreatic blood vessels and initiated hormone production. In adults, pancreatic expression of Rgs8 and Rgs16 became quiescent. However, it was found that Rgs8 and Rgs16 expression was induced in adult pancreatic islets in two models of glucose stress: i) PANIC-ATTAC mice, a model of type 1 diabetes (Wang et al., 2008), and ii) hyperglycemic ob/ob mice, a model of type 2 diabetes (Chua et al., 2002; Prentki and Nolan, 2006). In addition, *Rgs16* was also expressed in peculiar population of scattered cells and small cell clusters (2-10 cells) in postnatal stages. These clusters were termed these vessel- and ductal-associated Rgs16::GFP positive cells (VDAC). VDACs disappeared in adult pancreas but re-appeared in midgestation pregnant females a model of β-cell expansion.

4.2 RESULTS

4.2.1 Rgs gene expression during pancreas development

Rgs16 and the tandemly duplicated *Rgs8* are both induced during hepatic gluconeogenesis (Huang et al., 2006); Wilkie, unpublished data). Two separate lines of GFP-expressing BAC transgenic mice (Fig. 4.1A,B) were used to determine if these genes are expressed during development or maintenance of the pancreas, another organ known to regulate glucose homeostasis (Gong et al., 2003). These transgenic lines have previously been shown to faithfully reproduce endogenous Rgs8 and Rgs16 mRNA expression in mice and primary hepatocytes (Gong et al., 2003; Huang et al., 2006; Morales and Hatten, 2006); Johnson and Wilkie, unpublished data). Indeed, both Rgs8::GFP and Rgs16::GFP expression began early in the pancreas and continued throughout embryonic and neonatal development (Fig. 4.1C,D and Table 4.1).

Rgs16::GFP was expressed throughout the early gut tube endoderm (E8.5) from the foregut to the tip of the open hindgut (Fig. 4.2A and data not shown). However, as the embryo turns at E8.75 and the pancreas begins to evaginate, *Rgs16* expression in the gut became restricted to the early liver and dorsal pancreatic bud epithelium (E9.5-E10.5) (Fig. 4.2B,C). During dorsal bud outgrowth, *Rgs16* expression was observed in a punctate pattern within the pancreatic epithelium, suggesting that expression was restricted to a subpopulation of cells (Fig. 4.2C). Around E12.5, bud elongation and branching begins, and *Rgs16* expression was seen along the axis of the developing pancreatic buds, both dorsal and ventral, in a central region known to contain mostly epithelial and endocrine cell types (Fig. 4.2D,E). The location of *Rgs16* expressing cell

clusters, scattered within the core of pancreatic branches, suggest that they are endocrine precursors.

By postnatal stages, when islets are forming via aggregation of endocrine cells, Rgs16 expression became restricted to aggregates that appear to be forming Islets of Langerhans (Fig. 4.2F). In contrast to the broad distribution of early Rgs16::GFP expression in the endoderm, Rgs8::GFP expression in posterior foregut was initially localized to a distinct dorsal patch in a region fated to give rise to the pancreatic endoderm (E8.5) (Fig. 4.2G) (Wells and Melton, 1999). This striking expression initiated prior to any cellular or molecular evidence of pancreas specification, such as expression of *Pdx1/Ipf1* or *Ngn3* (Villasenor et al., 2008). By E9.5, *Rgs8* expression, like *Rgs16*, became restricted to the forming pancreatic bud and dorsal endoderm slightly anterior and posterior to the bud (Fig. 4.2H-I). From E10.5 to E12.5 stages, *Rgs8* was expressed in a pattern almost identical to that of *Rgs16*, in scattered clusters of cells within pancreatic epithelium in the central region of the developing bud (Fig. 4.2J). This expression continued in a pattern consistent with endocrine cell distribution until postnatal stages (Fig. 4.2K-L). In contrast to Rgs16::GFP, weak Rgs8::GFP expression was also evident in the exocrine pancreas (Fig. 4.2K,L).

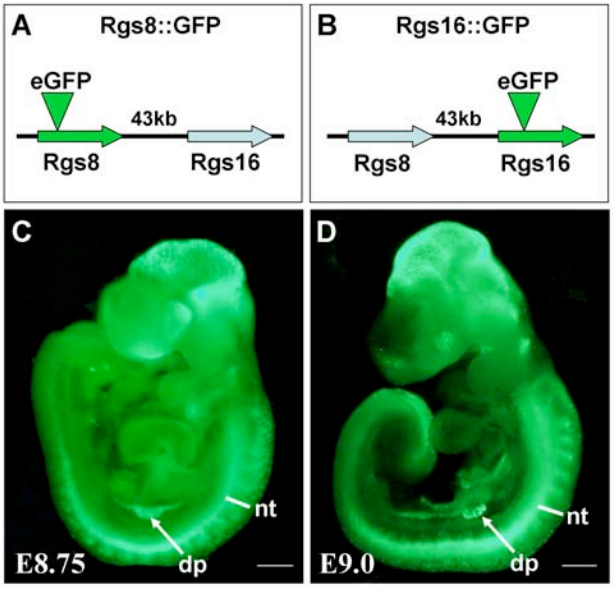

Figure 4.1. Rgs8::GFP and Rgs16::GFP are expressed in the pancreatic bud. Rgs8 and Rgs16 are tandemly duplicated genes separated by 42 kb of intragenic DNA Transgenic mice containing either a BAC with eGFP inserted at the translation initiation site of (A) Rgs8::GFP BAC id: RP23-184B11) or (B) Rgs16::GFP BAC id: RP23-101N8) display eGFP expression in progenitor cells of the endocrine dorsal pancreas at e9.5 (arrows). Other sites of expression include neural tube and brain (arrowheads).

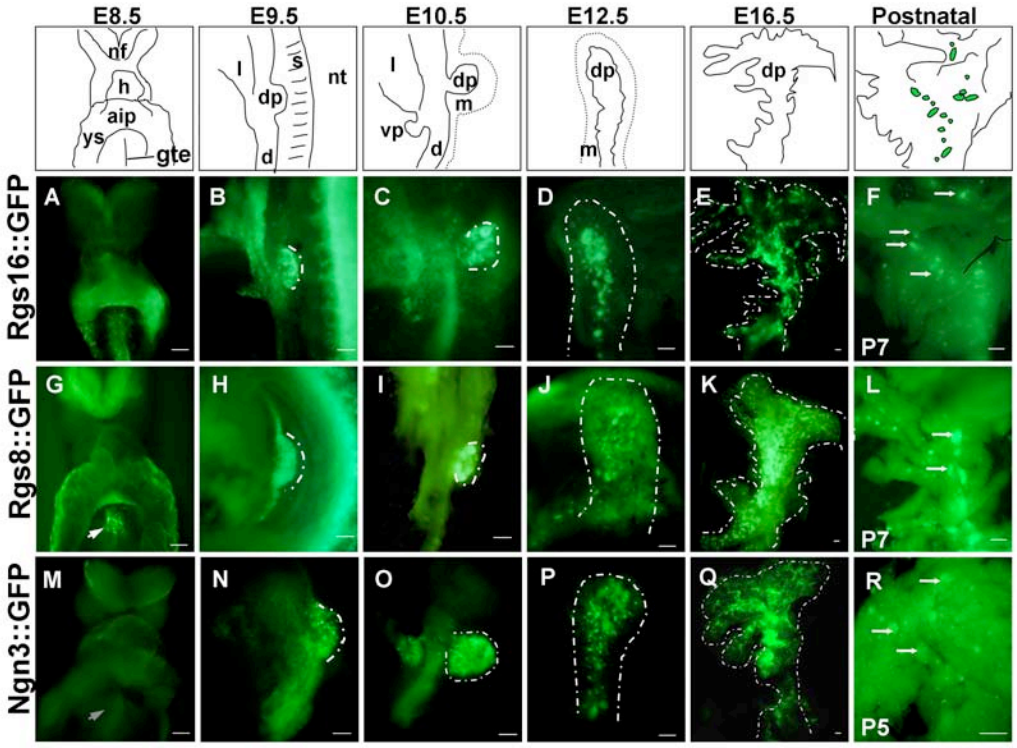

Figure 4.2. Rgs16::GFP, Rgs8::GFP, and Ngn3::GFP expression in the developing pancreatic bud. Rgs16::GFP (A-F) is initially broadly expressed in endoderm at e8.5, but resolves into the dorsal pancreas by e9.5. Expression then continues in groups of cells along the central axis of the pancreatic tree. By contrast, Rgs8::GFP (G-L) is first expressed within the foregut specifically in the pre-dorsal pancreas at e8.5. Similar to Rgs16, expression of Rgs8 continues in scattered cells, in the central region of the pancreatic bud. Note that Rgs8 is expressed in the dorsal pancreas prior to Ngn3::GFP, which is first detected in the dorsal pancreas at about e9.5 (compare G-H and N). All three genes are subsequently expressed in endocrine pancreas throughout embryogenesis, in a very similar pattern (C-F,I-L,O-R) (arrows mark coalescing islets during postnatal development). Expression of Ngn3 is extinguished during the first week after birth, while Rgs8 and Rgs16 persists in islets. Rgs8 and Rgs16 are expressed in the neural tube (nt) throughout development. Dotted lines define the limit of the developing pancreas at each stage. Aip, anterior intestinal portal; dp, dorsal pancreatic bud; nt, neural tube; vp, ventral pancreatic bud.

Because the spatiotemporal distribution of *Rgs16* and *Rgs8* expressing cells is reminiscent of endocrine precursors, their expression was compared to that of *Ngn3*, a well-characterized endocrine progenitor marker (Gradwohl et al., 2000). The Ngn3::GFP transgenic model developed by Kaestner and colleagues was used for these experiments (White et al., 2008). It was observed that the expression patterns of all three genes were highly similar throughout embryogenesis (Fig. 4.2). However, both Rgs::GFP genes were expressed extremely early in the dorsal pancreatic endoderm (E8.5), whereas Ngn3::GFP was not expressed in this area until after the embryo has turned at E8.75 (Fig. 4.2A,G,M; see also (Villasenor et al., 2008). At E9.5, all three genes displayed similar expression patterns within the dorsal bud, with all three transgenic lines exhibiting strong punctate expression in the dorsal bud endoderm. Outside the pancreatic bud, however, endodermal *Rgs8/16* and *Ngn3* expression diverged from each other, with Rgs16::GFP in the budding liver (Fig. 4.2B), Rgs8::GFP in the adjacent dorsal endoderm (Fig. 4.2H) and Ngn3::GFP faint in the posterior duodenal endoderm (Fig. 4.2N,O). Within the pancreas, Rgs16::GFP, Rgs8::GFP and Ngn3::GFP were similarly expressed throughout pancreatic development and islet formation (Fig. 4.2), until about 2 weeks after birth, when all three genes were extinguished in islets. By contrast, only Rgs16::GFP remained strong in scattered cells along veins, ducts and arteries for the first 3-4 weeks of post-natal development (see below). Throughout embryonic pancreatic development, Rgs16::GFP expression was generally stronger than that of Rgs8::GFP (photographic exposure time of Rgs8::GFP was on average about 2-fold that of Rgs16::GFP). Consistent with GFP transgene expression, endogenous Rgs16 is about 2-fold more abundant than Rgs8 in E14.5 pancreas mRNA assayed by qPCR (data not shown). Therefore, further

investigation focused on Rgs16::GFP expression during development and adult models of islet regeneration/expansion.

PANCREATIC STAGE	ISLET (Rgs16::GFP Expression)	VDACs (Rgs16::GFP Expression)
E8.5	+/-	NA
E8.75-E9.0	++	NA
E9.5-E16.5	+++	NA
P0	+++	NA
P1	+++	NA
P3	+++	NA
P7	+++	NA
P10	+++	+
P11	+	++
P14	-	++
P15	-	++
P16-P30	-	+
P69	-	-
Adult (2 months)	-	-
Adult (3 months)	-	-

Table 4.1. Expression of Rgs16::GFP in post-natal pancreas. Arbitrary expression levels were assigned by independent visual analysis of relative intensity of fluorescence (2 observers). Live dissected pancreatic tissue was examined in PBS, under fluorescence microscopy. Pancreas stage (E) embryonic stage and (P) postnatal day. Expression could be detected either in forming islets (middle column) or within scattered cells along ducts and blood vessels (VDACs, right column). (NA) not determined because of extensive expression in islets at these stages; (-) absent; (+) present; (++) medium; (+++) strong.

4.2.2 Rgs16::GFP expression in pancreatic endocrine cells

To determine whether endocrine cells within the pancreas expressed *Rgs16*, co-expression of Rgs16::GFP and different endocrine cell markers was assessed by immunofluorescence (Fig. 4.3). *Rgs16* expression was examined at E15.5 because at this stage there is a rapid wave of endocrine expansion and differentiation. Rgs16::GFP was not expressed in DBA^+ tissue (Fig. 4.3A). Thus, Rgs16 expressing cells are not pre-duct cells or pro-endocrine cells within the epithelium at this stage, but are nonetheless closely associated. This is in contrast to early Rgs16::GFP expression at E9.5, which is clearly in cells integrated within the budding pancreatic epithelium (Fig. 4.1,2). Overlap of *Ngn3* and Rgs16::GFP expression was also examined, since their expression appeared similar in transgenic tissue. Surprisingly, Rgs16::GFP was never co-expressed with *Ngn3* (Fig. 4.3B). Consistent with this expression pattern, greater than 98% of Rgs16::GFP-positive cells were Ki67-negative, indicating that the vast majority of Rgs16::GFP expressing cells were non-replicating at E15.5 (Fig. 4.4 and data not shown). Since the delaminating cells that transiently express *Ngn3* are considered committed to the endocrine cell fate, and have been shown to be non-replicating, this suggests that Rgs16::GFP expression at this stage marked differentiating endocrine precursors. Rgs16 expression is thus observed early, in progenitor cells prior to endocrine commitment (pancreatic bud), and again later, during their differentiation (post-secondary transition). These two waves of Rgs16::GFP expression during pancreatic development are similar to the ‘biphasic’ expression of pancreatic genes before and after the secondary transition, such as *Hlxb9* and *Ngn3* (Li and Edlund, 2001; Pictet et al., 1972; Villasenor et al., 2008)

In contrast to *Ngn3,* Rgs16::GFP co-localized with Pdx1 (Fig. 4.3C), a pancreatic progenitor marker that is partly co-expressed with insulin at E15.5 (Offield et al., 1996). Rgs16::GFP was also partially co-localized with markers of endocrine cell fate, such as Nkx6.1 (Fig. 4.3D), supporting the idea that Rgs16 expressing cells belong to the group of endocrine cells that are in the process of differentiation. Indeed, robust co-immunoreactivity for Rgs16::GFP and terminal endocrine differentiation markers (such as glucagon and insulin hormones) was found (Fig. 4.3E,F), indicating that *Rgs16* was expressed in islet lineages. Together, these co-labeling data suggest that Rgs16::GFP expression is likely to represent endocrine cells post-delamination, once they have escaped from the epithelium and are aggregating into pre-islet clusters

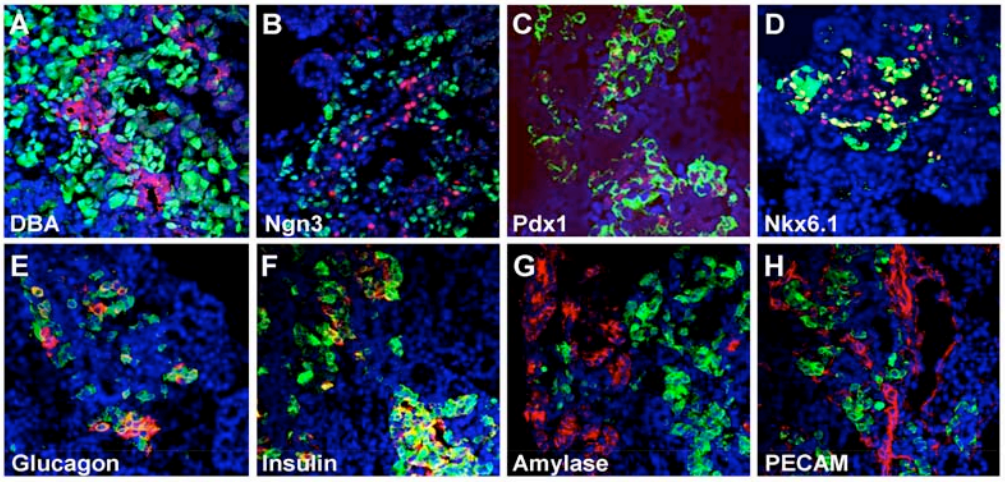

Figure 4.3. Rgs16::GFP is co-expressed with genes of the developing endocrine pancreas at e15.5. Rgs16::GFP is co-expressed with Pdx1 (column A), Insulin (column B), and Glucagon (column C). Note that Pdx1 is nuclear while Rgs16 expression is cytoplasmic (A). Rgs16::GFP is not expressed with markers of the exocrine (Amylase; column D), or vascular lineages (PECAM; column E). Nuclei identified by DAPI staining of DNA (blue).

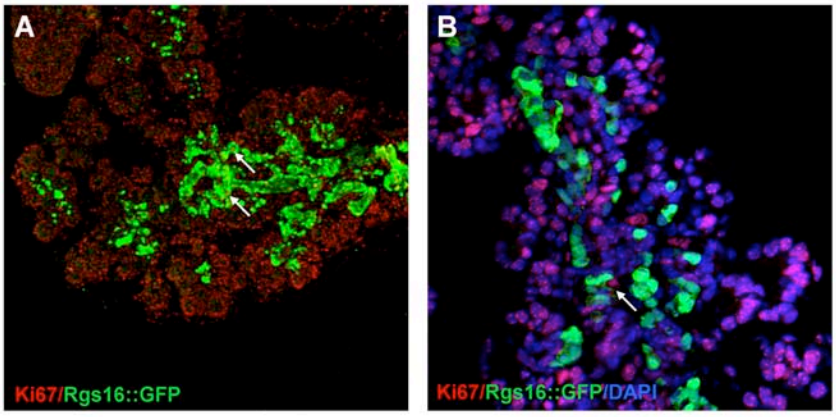

Figure 4.4. The majority of Rgs16::GFP+ cells are non-replicating at E15.5. Ki67 and Rgs16::GFP immunolocalization in E15.5 embryonic pancreas. (A) Low magnification view of centrally located *Rgs16* expressing cells. Quantification of Ki67 and Ki67 co-expressing cells reveals that less than 2% of *Rgs16* expressing cells are proliferating. Confocal micrograph, 10X. (B) High magnification view of *Rgs16* expressing cells, showing that most Rgs16+ cells do not stain for Ki67. White arrows point to rare costaining cells. Confocal micrograph, 40X.

As expected, *Rgs16* expression did not localize to amylase-positive cells (Fig. 4.3G), indicating that *Rgs16* is not in acinar tissue. There was also a close association of *Rgs16* expressing cells with blood vessels (marked by PECAM, Fig. 4.3H; and data not shown), reflecting the known close association of endocrine and vascular tissues. Together, these results revealed that pancreatic cells committed to an endocrine fate expressed *Rgs16* during embryonic and perinatal development. These results established *Rgs16* as a new marker for both pancreatic progenitors and differentiating cells of the endocrine lineage.

4.2.3 Rgs16::GFP expression in endocrine cells in postnatal pancreas

From E18.5 until a few weeks after birth, endocrine cells aggregate in the core of pancreatic branches to form islets (Cleaver and Melton, 2004). During the early stages of this process, strong *Rgs16* expression was detected within the forming islets (Fig. 4.5A) and always in close association with blood vessels (Fig. 4.5B). Indeed, its expression within islets remained strong in large numbers of endocrine cells after birth. However, Rgs16::GFP expression declined gradually over the first two weeks after birth (compare Figs 4.5A-B with 4.5C-E). While GFP expression continued in both large and small islets as late as P11 (Fig. 4.5C) it significantly declined by this stage. These studies demonstrate that the Rgs16::GFP transgenic mouse can be used as a model to study islet formation, since it is possible to clearly track and observe the entire process of isletogenesis, from endocrine cells shortly after delamination to their aggregation into mature islets.

Interestingly, during our studies in post-natal stages (weaning-P11 and beyond), we were able to discern another aspect of *Rgs16* expression in scattered cells and small cell clusters (2-10 cells). These clusters were located along the central axis of distinct pancreatic branches (Fig. 4.5D-F). They were termed these vessel- and ductal-associated Rgs16::GFP positive cells (VDAC) (Fig. 4.5H). Relatively strong VDAC expression could be observed throughout early postnatal stages up to p30 (approximately 12 days following weaning) (Table 4.1), when expression was extinguished (Fig. 4.5G). VDAC were not observed in quiescent adult pancreas (data not shown).

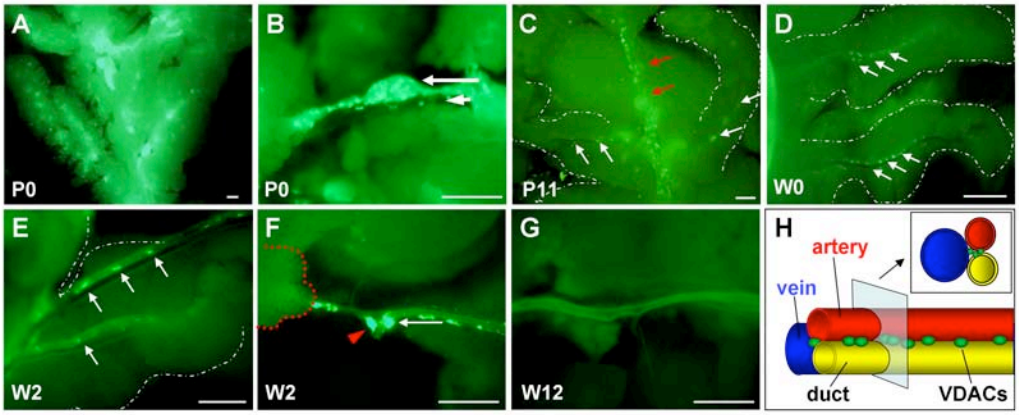

Figure 4.5. Rgs16::GFP+ cells are associated with blood vessels during neonatal islet formation. Neonatal Rgs16::GFP expression is observed in coalescing islets throughout the postnatal pancreas. (A) *Rgs* expression is evident in endocrine cells as they aggregate into clusters along blood vessels at P0. (B) Forming islet (thick white arrow) can be seen overlying blood vessel (white arrowhead). (C) Expression continues in islets until approximately P11 (short red arrows), but expression remains in scattered cells, or VDACs, along the axes of lateral branches (short white arrows). (D) At weaning (P16,W0), islet expression of Rgs16::GFP is no longer detectable in islets, however (E,F) expression continues in VDACs lining axial blood vessels at the center of lateral pancreatic branches (short white arrows). (F) GFP+ cells (long thin arrow) are tightly associated with tracts of blood vessels and associated pancreatic ducts, and are especially enriched at vascular branch points (red arrowhead; red dotted line delineates a mature islet). (G) Expression vanishes by day 12 of weaning (P28,W12). (C-E) Dotted white lines depict margins of lateral pancreatic branches in postnatal pancreas. (H) Schematic of VDACs location along the 'triad' composed of artery (red), vein (blue) and duct (yellow). Cross section shows approximate location of VDACs at the interface between ducts and blood vessels. Scale bars, 100μm.

All VDACs without exception were located in the central region of branches, along "triads" composed of a pancreatic duct, an artery and a vein (Fig. 4.5E,F,H). VDACs were frequently clustered around triad branch points, where vessels and ducts branch coordinately (Fig. 4.5F). The arteries and veins in these triads are distinguishable by PECAM staining in fixed tissue (Fig. 4.6A; data not shown), and by the presence of blood or the differing thickness of the vessel walls in live pancreas tissue (thick in

arteries, thin in veins) (Fig. 4.5B,E). VDACs were easily detected lining these triads, often at the interface between vessels, however it was difficult to identify the nature of the vessel most closely associated with VDACs. From visual observation of fresh, intact Rgs16::GFP pancreas, it appeared that VDACs were most tightly associated with pancreatic ducts, since the tubular structures closest to VDACs never contained blood and appeared thinner and more tortuous than blood vessels.

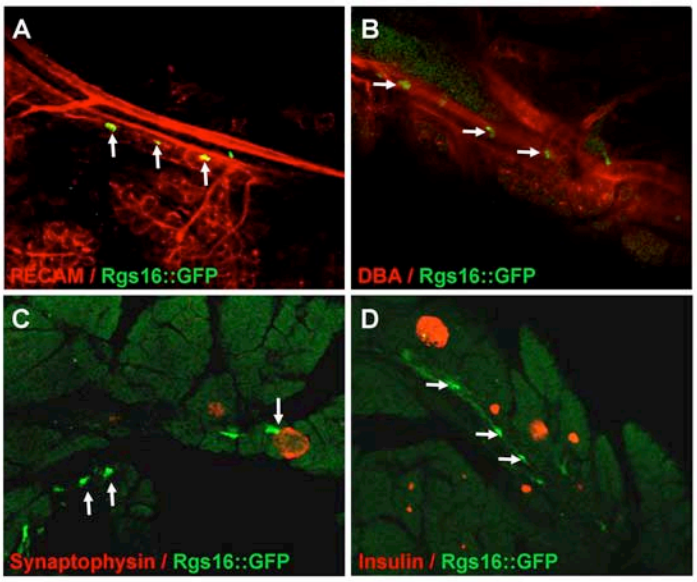

Figure 4.6. Rgs16::GFP+ cells are associated with ducts during postnatal islet formation. (A) Whole mount staining for GFP in the BAC transgenics demonstrates close association of *Rgs16*-expressing VDACs with blood vessels (PECAM) and (B) ducts (DBA lectin). (C) Rgs16::GFP+ VDACs do not appear in endocrine clusters as shown by co-stains with synaptophysin, a marker of all early endocrine cells and (D) insulin in β−cells of the islets. Confocal micrographs, 10X.

To precisely identify the type of vessel associated with VDACs, immunofluorescence was performed to distinguish blood vessels from pancreatic ducts (Fig. 4.6A-B). Confirming our expectations, *Rgs16* expressing cells were closely

associated with blood vessels (PECAM, Fig. 4.6A), ducts (DBA, Fig. 4.6B) and lymphatics (LYVE-1, Fig. 4.7). In addition, VDACs were often in close proximity to developing islets. Co-staining for GFP and for markers of the various pancreatic lineages revealed that VDACs were located along ducts, sometimes near endocrine cell clusters or their progenitors, such as those expressing synaptophysin (Fig. 4.6C) or later differentiation markers, such as insulin (Fig. 4.6D). The expression of *Rgs16* within VDACs differed from the expression of embryonic *Rgs16*, where *Rgs16* is co-expressed with endocrine differentiation markers (see Fig. 4.3CF). This difference may reflect different populations of Rgs16 expressing cells.

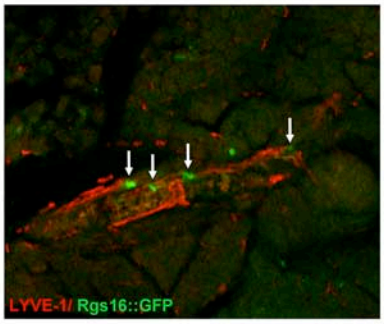

Figure 4.7. Rgs16::GFP VDACs are associated with lymphatic vessels, but do not co-express the lymphatic marker LYVE-1. LYVE-1 and Rgs16::GFP immunolocalization in post-natal, weanling embryonic pancreas. VDACs are closely associated with, but not within, the lymphatic vessel, nor do VDACs express lymphatic markers. White arrows point to Rgs16::GFP expressing cells. Confocal micrograph, 20X.

4.2.4 Rgs16::GFP re-expression in pancreas of pregnant females

To determine whether *Rgs16* expressing cells might re-emerge in the pancreas of metabolically stressed mice, the pancreas of pregnant females was first examined at different times during gestation. Islets within the pancreas of a pregnant female are

known to expand dramatically in mass during pregnancy (Van Assche et al., 1978). While it was never observed Rgs16::GFP expression in normal adult pancreas, either within islets or as VDACs, re-expression of *Rgs16* was noted along vessel and duct tracts in mid to late gestation female pancreas (Fig. 4.8). Indeed, starting at approximately 8 days of gestation, rare GFP+ cells could be readily observed along the central axes of lateral pancreatic branches (Fig. 4.8A). Later, between E10.5-E15.5 days of gestation, increasing numbers of VDACs were present along many different branches (Fig. 4.8B-E).

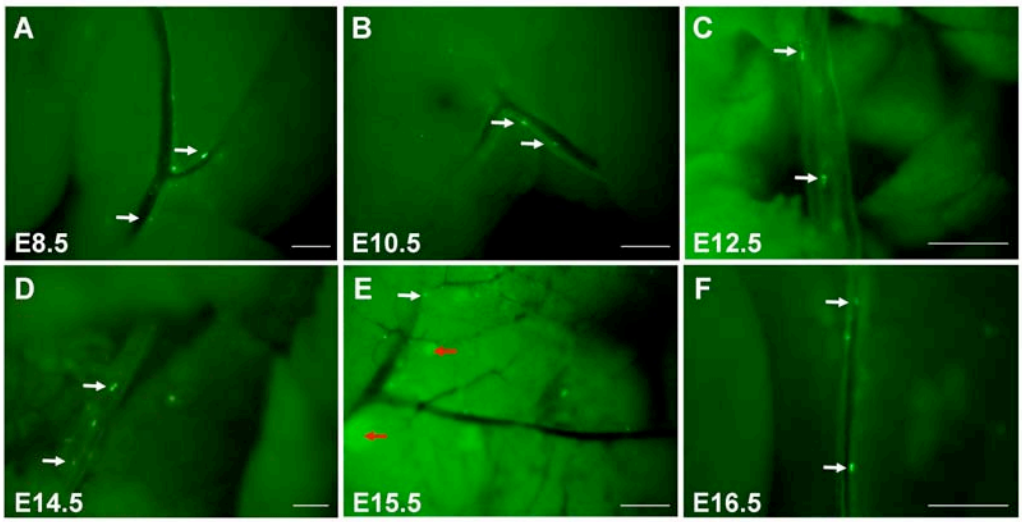

Figure 4.8 Rgs16::GFP is expressed in the pancreas of pregnant females. Rgs16::GFP expression, in single GFP+ cells or vessel-ductal associated cells (VDACs), is detected along blood vessels of the pancreas of pregnant females during mid to late gestation. (A) Starting at E8.5, VDACs were observed scattered along the vessel/duct tracts, at the center of lateral pancreatic branches. (B-E) Increasing numbers of GFP+ cells could be identified at E10.5 through E15.5 (D) In one female, we observed islet expression (red arrows). (F) The number of blood vessel associated GFP+ cells declined from E16.5 to birth. VDACs were extremely rare in adult male pancreas or in adult non-pregnant female pancreas. White arrows point to Rgs16::GFP expressing VDACs. Scale bar, 100μm.

Rgs16::GFP expression was coincident with the initiation of a known phase of β−cell expansion in pregnant females (Gupta et al., 2007), but then faded between E16.5-E18.5 (Fig. 4.8F; data not shown). Lactating females did not express Rgs16::GFP in pancreas (data not shown). Rgs16::GFP expression in pregnant females suggests that increased maternal metabolic demands might be conveyed by GPCR signaling and regulated by RGS proteins in expanding islets.

4.2.5 Rgs16::GFP re-expression in regenerating β−cells

Given the correlation of *Rgs16* expression with β−cell proliferation, we asked whether Rgs16::GFP might also be re-expressed in islets during β−cell regeneration. Several groups have recently reported that the majority of new β−cells that emerge within regenerating islets come from division of pre-existing β−cells (Dor et al., 2004; Teta et al., 2007). Recently, Scherer and colleagues also demonstrated islet regeneration following ablation in PANIC-ATTAC mice (Wang et al., 2008). In this new model of type 1 diabetes, pancreatic β−cells are targeted for cell death by the regulated expression of a FKBP-caspase 8 fusion protein. Upon induction, β−cells are destroyed and hyperglycemia ensues. To assess expression of *Rgs16* during islet regeneration, Rgs16::GFP transgene was crossed into the background of the PANIC-ATTAC mice. Following β−cell apoptosis, we observed that Rgs16::GFP was co-expressed with insulin in a subset of pancreatic β−cells during the first two weeks of islet regeneration (Fig. 4.9). The percentage of Rgs16::GFP+ cells was higher in hyperglycemic mice with more severe hyperglycemia and islet destruction, than in mice with moderate glucose levels

(Fig. 4.9A,B), indicating that *Rgs16* expression correlates with the extent of the necessity of the pancreas to replenish β−cells. GFP^+ cells were not detected in the pancreas of either PANIC-ATTAC (Fig. 4.9C) or normoglycemic (vehicle treated) Rgs16::GFP;PANIC-ATTAC mice (Fig. 4.9D).

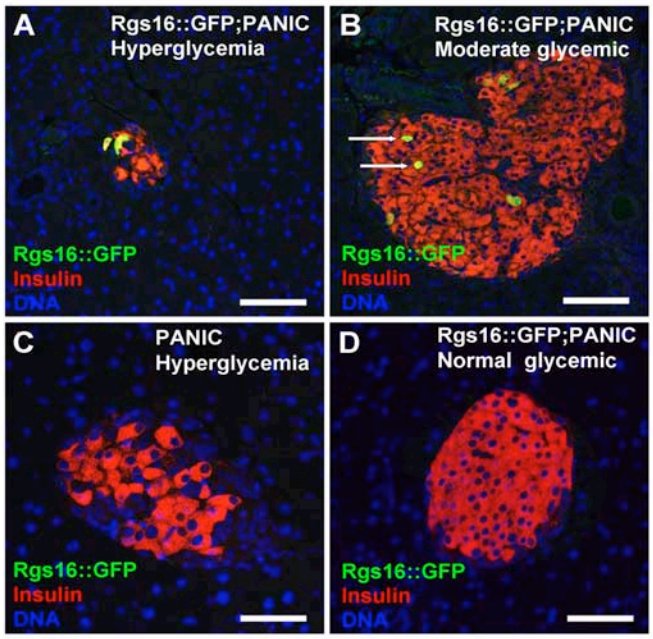

Figure 4.9. Rgs16::GFP is expressed in regenerating islets of hyperglycemic *PANICATTAC* mice. Rgs16::GFP and insulin are co-expressed in a few cells within islets of hyperglycemic PANIC-ATTAC;Rgs16::GFP transgenic mice during pancreatic β−cell proliferation (recovery) following ablation. (A) Expression is high in severely hyperglycemic or (B) moderate glycemic mice (arrows mark Rgs16::GFP+;insulin+ double positive cells). (C) No background GFP expression is detected in hyperglycemic PANIC-ATTAC mice. (D) Rgs16::GFP is never detected in normoglycemic (vehicle treated) PANIC-ATTAC;Rgs16::GFP mice. Scale bars, 50μm. Figure courtesy of Z. Wang

4.2.6 Rgs16::GFP re-expression in pancreas of *ob/ob* hyperglycemic mice

β−cell proliferation also occurs in obese, diabetic *ob/ob* mice, a model of type 2 diabetes(Chua et al., 2002; Prentki and Nolan, 2006). Therefore, Rgs16::GFP expression was assessed in normo- and hyperglycemic *ob/ob* mice (Fig. 4.10). Although GFP+ cells were never found in the pancreas of double heterozygous (Rgs16::GFP/+;*ob*/+) (Fig. 4.10A) or normoglycemic Rgs16::GFP;*ob/ob* mice (Fig. 4.10B), *ob/ob* mice had elevated GFP transgene expression that correlated with increases in both blood glucose and insulin (Fig. 4.10C-E; and data not shown). In these animals, Rgs16::GFP expression in a subset of islets was very intense, with more than half of the endocrine cells within these islets expressing Rgs16::GFP. Of note, the majority of Rgs16::GFP+ islets were found along the central region of the main axis of the pancreas. Indeed, Rgs16::GFP expression appeared to be restricted to large islets near ducts (Fig. 4.10H), while absent from smaller peripheral islets.

Interestingly, *Rgs16* was not expressed in Ki67+ cells, suggesting that Rgs16::GFP+ cells in *ob/ob* islets are not actively proliferating (Fig. 4.10F). Many Rgs16::GFP+ cells co-expressed insulin, indicating *Rgs16* is indeed expressed in β−cells, most likely initiating expression following their expansion (Fig. 4.10G-I). Expression declined in the *ob/ob* mice more than 20 weeks of age, as normoglycemia was restored following β−cell expansion (data not shown). Rgs8::GFP was similarly induced specifically in islets of hyperglycemic and hyperinsulinemic *ob/ob* mice.

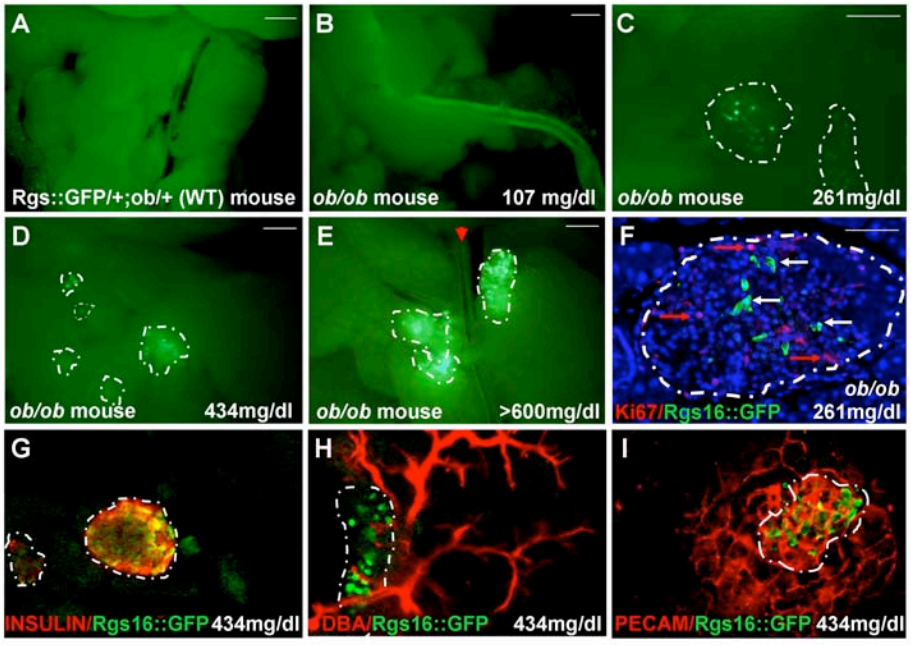

Figure 4.10. Rgs16::GFP is expressed in expanding islets of hyperglycemic *ob/ob* mice. Rgs16::GFP is expressed in expanding islets of hyperglycemic *ob/ob* adult mice, but not (A) in wild type or (B) normoglycemic Rgs16::GFP;*ob/ob* adults. (C-E) The number of cells expressing Rgs16::GFP generally increases with increasing glucose levels in Rgs16::GFP;*ob/ob* mice. (E) Note the close association of Rgs16::GFP+ islets with large blood vessels (vessel, red arrowhead). (F) Rgs16::GFP (white arrows) is not in proliferating BrdU+ cells (red arrows). (G) Double immunostaining for Rgs16::GFP and Insulin, (H), DBA, or (I) PECAM demonstrates that *Rgs16* positive cells are found within islets, co-express endocrine markers, and are closely associated with ducts and blood vessels. Scale bars, (A-E) 100µm; (F) 50µm. (G-I) Confocal micrographs, 10X.

4.3 **DISCUSSION**

In this report, we identify Regulators of G protein Signaling (*Rgs*) *Rgs16* and *Rgs8* as genes expressed in endocrine cells within the developing pancreas, as well as in models of both type 1 and type 2 diabetes. Both genes appeared to be expressed in a similar manner in the endocrine lineage, with slight differences in intensity and timing. Both Rgs8::GFP and Rgs16::GFP were expressed in the earliest endocrine progenitor cells within the budding pancreatic epithelium, in differentiating endocrine cells which have escaped the pancreatic epithelium and in perinatal endocrine β−cells as they undergo isletogenesis. This report showed that Rgs8::GFP and Rgs16::GFP transgenic mice are unique tools for the study of the endocrine pancreas because they allowed visualization of the endocrine lineage spanning a wide developmental window. In addition, we found that Rgs8 and Rgs16 expression becomes quiescent during adulthood and is only re-activated under models of islet regeneration and pancreatic stress suggesting that the actions of both *Rgs* might be required to compensate pancreatic metabolic stress.

4.3.1 Rgs8/16::GFP expression in embryonic pancreas

Rgs8 and *Rgs 16* are early expressed in the pre-pancreatic endoderm and as many other molecular regulators in endocrine development (Zaret, 2008; Zaret and Grompe, 2008), they showed differential expression during the first and the secondary transition of pancreatic development. During the first transition, Rgs16::GFP and Rgs8::GFP were expressed through out the pancreatic epithelium, while following the secondary transition

their expression became restricted to islets. The expression of *Rgs16* following the secondary transition was specific to the endocrine lineage. Expression is likely to represent delaminated post-mitotic endocrine cells as Rgs16:GFP expressing cells were not observed within the epithelium and did not co-express *Ngn3* during this second phase of expression. Expression appeared in delaminated endocrine cells that co-expressed Pdx1, Nkx6.1, and/or the islet hormones insulin and glucagon. In addition, fewer than 2.5% of Rgs16::GFP^{+} cells are Ki67^{+}. These results suggest that following the secondary transition, *Rgs16* expression, and hence GPCR signaling activation was restricted to endocrine cells that have started cytodifferentiation. Of notice, there was lack of expression of both *Rgs* genes in the ventral pancreas during the first stages of pancreatic development. It has long been recognized that the ventral and dorsal pancreas develop via different molecular cascades and our results suggest the involvement of G-protein signaling in the initiation steps of these cascades, as well as in dorsal pancreatic specification and in differentiating endocrine cells.

Finally, it is important to mention the fact that *Rgs8* and *Rgs16* were similarly expressed in the pancreas, which raises the concern that both genes are likely to be co-expressed in endocrine cells and have redundant functions in these cells. Future studies are required to establish whether indeed the same population of cells express *Rgs8* and *Rgs16.* In addition, it will be interesting to generate mice allowing lineage tracing of these cells to determine whether early *Rgs8/16*-expressing cells within the bud give rise to all pancreatic lineages or to specific the endocrine lineages.

4.3.2 Rgs8/16::GFP expression in models of diabetes

Rgs8 and *Rgs16* were not expressed in adult endocrine or exocrine pancreas under normal conditions. Interestingly, however, these genes were re-expressed in models of diabetes and pancreatic metabolic stress. The absence of expression in normal pancreatic endocrine cells suggests RGS did not directly regulate daily glucose homeostasis or release of pancreatic digestive enzymes. However, *Rgs8* and/or *Rgs16* re-expression in islets of hyperglycemic type 1 and type 2 diabetic mice, suggests that *Rgs8/16* play a role in regulation of glucose stress or β-cell expansion.

Recent work showed that the GPCR ligand Glp-1 augments β−cell replication in models of type 1 diabetes (Kodama et al., 2005; Lee et al., 2006; Sherry et al., 2007; Tourrel et al., 2001; Xu et al., 1999); suggesting a potential role for *Rgs* genes in β-cell expansion. To our surprise, Rgs16::GFP was not expressed in replicating ($Ki67^{+}$) β−cells in hyperglycemic *ob/ob* mice. Similar results by Keller et al. showed that endogenous *Rgs8/16* genes are induced in 10-week old BTBR *ob/ob* mice, in which β−cell expansion is known not to occur (Keller et al., 2008). These results suggest a role for *Rgs8* and *Rgs16* regulating GPCR signaling in glucose stressed β-cells rather than a role in β-cell expansion.

4.3.3 Rgs16::GFP expression - VDACs

A distinct population of *Rgs16* expressing cells was discovered and termed VDACs (vessel- and ductal-associated Rgs16::GFP positive cells; VDAC). These cells are of great interest because of their appearance during weaning and pregnancy and their

location along the ducts. Bonner-Weir has long supported the existence of a “foci of regeneration”, or progenitor cells, located in the pancreatic ducts (Bonner-Weir et al., 2004). The findings that Rgs expressing VDACs reside in ducts and are expressed in two models of β−cell expansion: early weanlings and pregnant female raised the possibility that VDACs constitute an endocrine progenitor cell-type. The conundrum that VDACs are not observed in PANIC-ATTAC or *ob/ob* mice, where β−cells are also known to expand by replication, can be explained by either: 1) the possibility that Rgs gene expression in VDACs was transient and our studies did not capture that expression or 2) the possibility that the molecular mechanisms for β−cell expansion were different under physiological conditions (pregnancy) than during disease conditions (type1/ type 2 diabetes). Future analyses are required to determine the identity of these cells and their role in β−cell expansion.

4.3.4 Summary *Rgs8* and *Rgs16* in pancreas

The work presented here indicates that induction of *Rgs8* and *Rgs16* occurs throughout pancreatic development and in models of metabolic stress and disease. We have identified some GCPRs that are specifically expressed in endocrine cells, for example the Gq-coupled receptor Gpr56 (Gu et al., 2004)www.genepaint.org) and Gpr120 (collaboration with Melton and Sherwood, unpublished). It will be interesting to determine whether, *Rgs8* and/or *Rgs16* regulate the signaling of these GCPR receptors during pancreatic development. In addition, future work will identify the ligands and receptor-signaling pathways regulated by these two *Rgs* in the embryo as well as in

hyperglycemic type 1 and type 2 diabetic mice. These GPCRs, regulatory RGS proteins and as yet unknown ligands, are likely to be important signaling molecules in pancreatic development the progression towards diabetes, and in therapeutic approaches for a cure.

Chapter 5: EPH/EPHRIN B SIGNALING MODULATES PANCREATIC DEVELOPMENT.

5.1. INTRODUCTION

Ephs receptors are the largest subfamily of receptor tyrosine kinase (RTKs) and they have recently been shown to be expressed on the developing pancreatic endoderm (van Eyll et al., 2006). The Eph receptor extracellular domain compromises an N-terminal ligand binding domain, cysteine rich domains, and fibronectin-III repeats, while their intracellular domain contains a kinase domain, a SAM domain and a PDZ-binding motif (Egea and Klein, 2007). Following ligand binding, the Eph receptors become autophosphorylated and their domains are then able to interact with other signaling proteins in a process known as forward signaling. The Eph receptors are divided in two subclasses: the EphAs and EphBs. In mouse, there are 13 receptors that bind a total of 8 ligands. There are two classes of ligands: the ephrinAs and the ephrinBs that bind preferentially to either EphA or EphB receptors respectively. The only known exceptions are ephrinA5, which is able to bind to the EphB2 receptor and the EphA4 receptor, which can bind promiscuously to either class of ligands. Unlike other RTKs that bind soluble ligands *Eph/ephrin* signaling requires of cell- to cell contact. Its signaling is bidirectional since it implicates both cells in contact: the Eph-receptor-expressing cells (produce forward singalling) and the ephrin-ligand-expressing cells (reverse signaling).

Our understanding of *Eph/ephrin* signaling is largely based on studies of the central nervous system. Eph signaling has been shown to regulate growth cone collapse,

axon guidance, synapse formation, synaptic plasticity, dendritic spine morphogenesis, and coordination of migration and proliferation of intestinal cells (Cheng et al., 1995; Drescher et al., 1995; Frisen et al., 1998; Henkemeyer et al., 1996; Orioli et al., 1996; Park et al., 1997) In addition, Eph and ephrins are involved in cellular repulsion and formation of boundaries, axon guidance, formation of topographic axonal projections. Specifically, Eph signaling has been shown to control a variety of cell movements by regulating cell-cell repulsion and adhesion (Cowan and Henkemeyer, 2002; Frisen et al., 1999; Gale and Yancopoulos, 1999; Holmberg and Frisen, 2002; Kullander and Klein, 2002; Wilkinson, 2001). They accomplish this by transducing bidirectional signaling in both receptor- and ligand-bearing cells. Interestingly, however, recent work has identified the importance of Eph-ephrin signaling in other developmental processes such as intestinal cell positioning in intestinal crypts (Batlle et al., 2002) and urorectal development (Dravis et al., 2004).

Here, the role of *Eph/ephrinB* signaling during pancreatic development was examined. It was found that *EphB2* is expressed in the pancreatic epithelium and *EphB3* is found in potential 'delaminating' cells. This chapter also shows that *ephrin* ligands were expressed in mesenchyme (*ephrinB1*); in arterial endothelium (e*phrinB2*); and in pancreatic epithelium (*ephrinA5*). Disruption of *Eph/ephrinB* signaling impaired pancreatic development. $EphB2^{LacZ/LacZ}/EphB3^{-/-}$ showed gross pancreatic morphology, reduced total endocrine cell mass; produced defects in vascular remodeling; caused mislocalization of mesenchymal domains, and disrupted epithelial organization and cell polarity. Our data suggests a previously unnoticed role for *Eph/ephrinB* signaling in

regulating proper pancreatic morphogenesis and physiology by regulating cellular organization within the embryonic epithelium**.**

5.2 RESULTS

5.2.1 *EphB* receptors and *ephrinB* ligands are expressed in the pancreas

Studies by Van Eyell et al. showed that Ephs and ephrins are expressed at the burgeoning structures of the pancreatic epithelium (van Eyll et al., 2006). Whole mount *in situ* hybridization, immunofluorescence studies, and β-galactosidase staining of mouse embryos were done in order to confirm their data and extend Eph/ephrin characterization in the pancreas. The expression of all 5 *EphB* receptors and their ligands at different developmental time points during both the first and the secondary transition were analyzed and the results are described below.

EphrinB ligands

EprhinB1 was expressed in the mesoderm surrounding the pancreatic epithelium starting at around E10.5 (Fig. 5.1 A-A'). At this stage, *ephrinB1* was highly expressed in the pancreatic mesoderm in a dorsal-ventral gradient fashion as observed by *in situ* hybridization (Fig. 5.1 A'); it was absent from the pancreatic epithelium and it was modestly expressed throughout the mesenchyme of the gut tube. Of note, *ephrinB1* was the only ligand found to be expressed anterior to the dorsal bud (compare Fig. 5.1 A',B' and Fig. 5.2 D', white arrow). By E13.5 *ephrinB1* expression remained strong in the mesenchyme with enrichment in the pancreatic 'ridge' (Fig. 5.1A'', white arrow). *EphrinB2* (*EB2*) expression was detected in the pancreas throughout all embryonic

developmental stages. Its expression was mesodermal during early stages of development (E9.5-E10.5)(Fig. 5.1B-B'), but later it became restricted to blood vessels as observed by *in situ* hybridization (Fig. 5.1B'', black arrow) and LacZ staining (Fig. 5.1E). Expression of *ephrinB2* in the pancreatic mesenchyme appeared to be mutually exclusive to expression of *eprhinB1*. Contrary to *ephrinB1*, *ephrinB2* was absent anterior to the dorsal bud, but it was strongly expressed posterior to the bud. *EphrinB3* expression was very transient during pancreatic development. We were only able to detect a weak signal at E9.5 in the pancreatic epithelium (Fig. 5.2D-D'').

EphrinA5, which is the only ligand from the A-subclass known to cross-activate *EphB2* (Gale et al., 1996; Himanen et al., 1998) was expressed in the pancreatic epithelium (Fig. 5.2-E-E'').

EphB receptors

From the array of EphB receptors assayed, *EphB1* receptor was not expressed in the pancreas at any developmental stage examined (Fig. 5.2 column A); *EphB2* and *EphB3* were expressed in the pancreatic epithelium (Fig. 5.1 columns C and D); and *EphB4* and *EphB6* were expressed in the pancreatic mesenchyme (Fig. 5.2 column B-D). Specifically, at early developmental stages (E9.5-E10.5), both *EphB2* and *EphB3* expression was nearly excluded from much of the gut tube but it was clearly detectable in the pancreatic epithelium (Fig. 5.1C-D'). At later developmental stages, whole mount β-galactosidase (β-gal) staining of *EphB2*-LacZ reporter embryos showed that *EphB2* was expressed at the tips of the growing pancreatic epithelium (Fig. 3.1C''). Transverse sections of E13.5 and saggital sections E15.5 pancreata revealed that *EphB2* expression

was restricted to the exocrine tissue, specifically to the apical side of acini clusters (Fig. 5.1F,G, arrows). At 10.5 and E13.5, *EphB3* expression was observed in a punctate pattern within the pancreatic epithelium, suggesting that expression was restricted to a subpopulation of cells (Fig. 5.1 D',D''). Later, the identity of this population of *EphB3*$^{+}$ cells is analyzed in detail. At E9.5, *EphB4* was excluded from the mesenchyme surrounding the pancreatic epithelium, but it was strongly expressed by the mesenchyme posterior to the pancreatic bud (Fig. 5.2B). By E10.5, however, *EphB4* expression was strong throughout all the pancreatic bud mesenchyme. *EphB4* expression appeared to be distributed in a gradient: its expression was at its highest in the outer mesothelium and sequentially decreased ventrally towards the gut tube (Fig. 5.2B). At E13.5, *EphB4* expression became restricted to blood vessels (Fig. 5.2B'', white arrow) in accordance with previous studies that showed *EphB4* expressed by veins (Swift and Weinstein, 2009). *EphB6* was faintly found throughout the pancreatic and gut mesenchyme (Fig. 5.2C-C'').

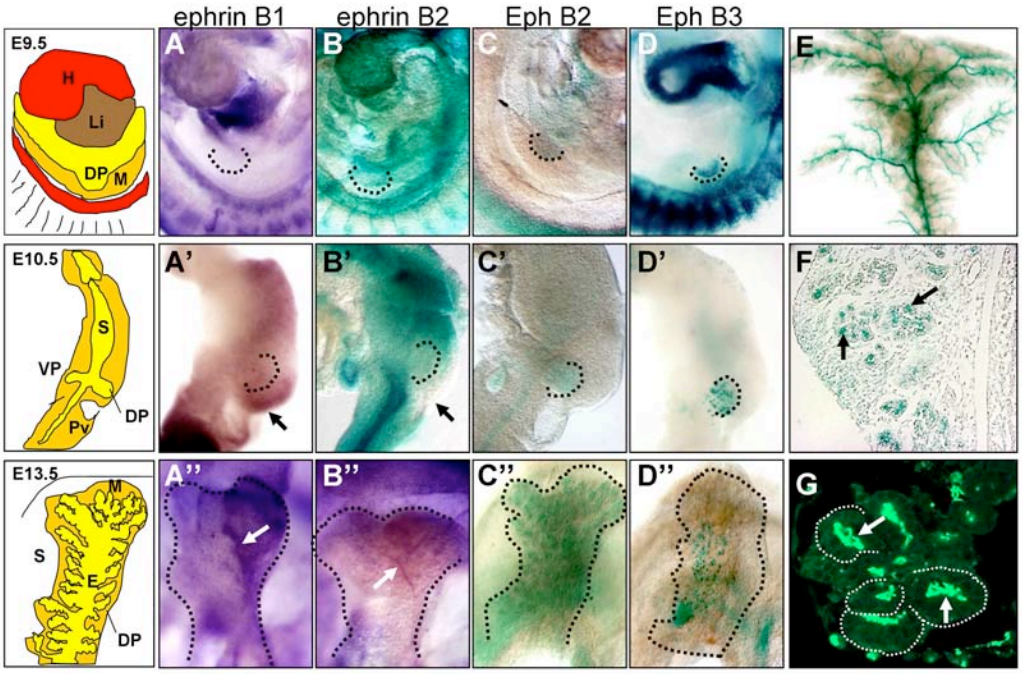

Figure 5.1. Expression of ephrin ligands and Eph receptors during pancreatic development. Whole mount in situ hybridization and whole mount β-galactosidase staining of ephrinB ligands and EphB receptors. *In situ* hybridization of *ephrinB1* **(column A)** and whole mount β-galactosidase staining using *ephrinB2*-lacZ **(column B)**; *EphB2*-LacZ **(column C**); *EphB3*-LacZ **(column D)** at stages indicated. E9.5 embryos in A-D are facing forward. E10.5 dissected gut tubes in **A'-D'** have anterior up and dorsal to the right. E13.5 Dorsal pancreatic buds in **A''-D''** have stomach in the background and are facing forward. The pancreatic endoderm is delineated by dotted lines **A-D''**. Cartoons in the right column represent the different developmental stages studied. *EphrinB1* is expressed in the mesenchyme **(A-A'')** while *ephrinB2* is expressed in blood vessels **(B-B'')**. *EphB2* and *EphB3* are expressed in the pancreatic epithelium **(C-D'')**. E18.5 isolated pancreas showing specific expression of *ephrinB2* to blood vessels **(E)**. Transverse sections of whole mount β-galactosidase showing that *EphB2* accumulates apically in the acini floret **(F)**. Immunofluorescence in pancreatic sections E15.5 showing *EphB2* expression located apically in the acini florets (delaminated by white dot lines) **(G)**. Arrow in **A''** points to pancreatic 'ridge'. Arrow in **B''** points to blood vessel. Arrows in **F** and **G** show *EphB2* expression. H, heart; Li, liver; DP, dorsal pancreas; E, epithelium; M, mesenchyme; Pv, portal vein; S, stomach; VP, ventral pancreas.

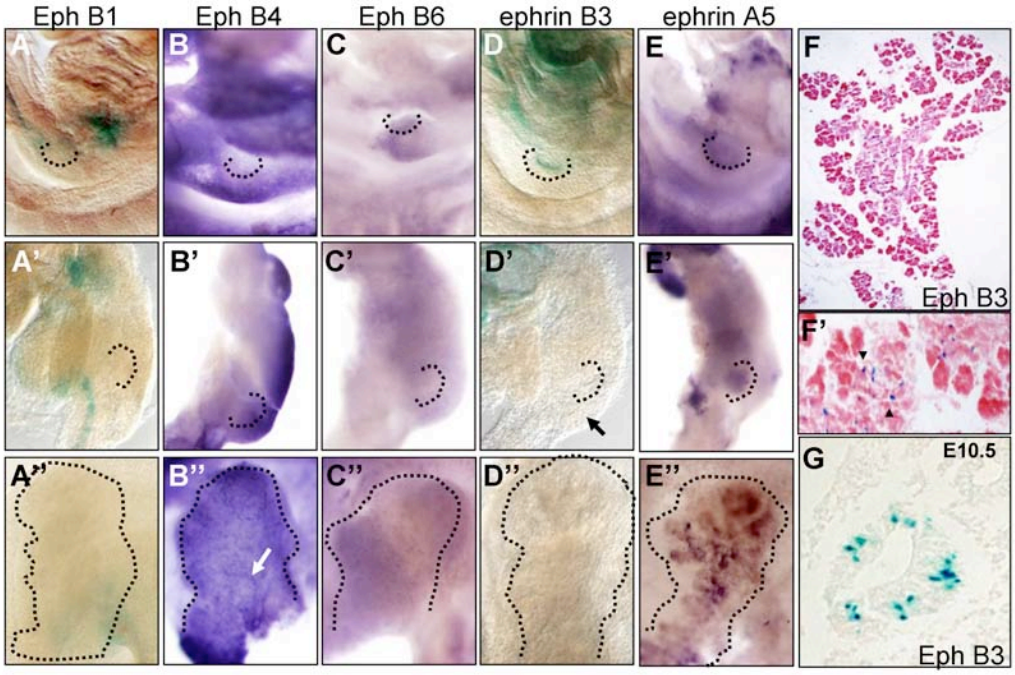

Figure 5.2. Expression of Eph receptors and ephrin ligands during pancreatic development. Whole mount in situ hybridization and whole mount β-galactosidase staining of *ephrinB3* ligand and *Eph* receptors. Whole mount β-galactosidase staining using EphB1-lacZ **(column A)** and ephrinB3-LacZ **(column D)**. In situ hybridization of *EphB4* **(column B)**, *EphB6* **(column C)**, **and** *ephrinA5* **(column E)** at stages indicated. E9.5 embryos in **A-E** are facing forward. E10.5 dissected gut tubes in **A'-E'** have anterior up and dorsal to the right. E13.5 Dorsal pancreatic buds in **A''-E''** have stomach in the background and are facing forward. The pancreatic endoderm is delineated by dotted lines **A-D''**. *EphB1* and *ephrinB3* are not expressed in the pancreas **(A-A''; D-D'')**. *EphB4* is expressed in the mesenchyme **(B-B'')** while *EphB6* is weakly expressed in the mesenchyme **(C-C'')** and *ephrinA5* is expressed in the pancreatic epithelium **(E-E'')**. H & E of E16.5 pancreatic sections of whole mount β-galactosidase of *EphB3*-LacZ showing that *EphB3* is localized in along the proximo-distal axis of the pancreas **(F)** and close up of same section **(F')** arrowheads indicate EphB3^{+} cells. Section of E10.5 *EphB3*-LacZ pancreatic bud showing expression of *EphB3* in a sub-population of cells in the pancreatic epithelium **(G)**. H, heart; Li, liver; DP, dorsal pancreas; E, epithelium; M, mesenchyme; Pv, portal vein; S, stomach; VP, ventral pancreas.

5.2.2 *EphB3* is expressed in pro-endocrine delaminating cells

Sections of *EphB3*-LacZ reporter pancreas showed that EphB3 was expressed in a subpopulation of pancreatic epithelial cells at E10.5 (Fig. 5.2G). At E15.5 these cells were scattered throughout the endoderm and were localized in the center of the pancreas along the major duct, where most endocrine cells reside (Fig. 5.2F). Mucin-1 and amylase stainings revealed that indeed EphB3^{+} cells clustered along the ducts (Fig. 5.3G), like endocrine cells and they did not express exocrine markers (Fig. 5.3F). This data suggested that EphB3 was expressed in pro-endocrine or endocrine cells.

In order to test this idea immunostainings with Pdx1 were performed. Pdx1 is a transcription factor that marks all cells of the primitive epithelium and later becomes restricted to insulin-expressing cells (Guz et al., 1995). About 72% of EphB3^{+} cells co-expressed Pdx1 (Fig. 5.3A arrowheads). From this population, 52% of these cells co-stained with low expressing Pdx-1^{+} cells and 20% with high Pdx1^{+} cells. In addition, not all Pdx1 expressing cells expressed EphB3. In actuality, EphB3 marked a subpopulation of Pdx1^{+} cells with only about one tenth of Pdx-1 co-expressing EphB3.

Afterwards, the transcription factor Sox9 was examined. Sox9 is used as a marker of the epithelial cords, since by E15.5 its expression becomes restricted to undifferentiated epithelial cells (Seymour et al., 2007). About 95% of EphB3^{+} cells expressed low to no levels of Sox9 (Fig. 5.3B). Furthermore, EphB3^{+} appeared to detach from the epithelium, suggesting that EphB3^{+} cells are potential ‘delaminating’ cells that have already acquired an endocrine fate.

Ngn3^{+} co-expression was then assayed. *Ngn3* is a transcription factor that determines endocrine cytodifferentiation. Any cell in the primitive epithelium that is destined to become an endocrine cell will transiently express *Ngn3* and as this progenitor cell delaminates it will down-regulate *Ngn3* expression, which allows its differentiation into an endocrine cell (Gradwohl et al., 2000) (Johansson et al., 2007). Cells that expressed EphB3^{low} levels co-expressed high levels Ngn3^{+}; while EphB3^{high} cells did not. These results suggest that as *Ngn3* expression declines, EphB3 levels increase (Fig. 5.3C). In order to test whether the remaining EphB3 $^{+}$ cells represented newly formed endocrine cells synaptophysin stainings were performed (Fig. 5.3D). Around 74% of

EphB3^{+} cells co-expressed synaptophysin, an endocrine marker that appears as soon as the endocrine cells differentiated, indicating that most of EphB3^{+} cells are pro-endocrine cells. Insulin, glucagon, somatostatin, and ghrelin stainings showed that EphB3^{+} cells did not co-express mature hormones (Fig. 5.3E, H and data not shown). Together, these results suggest that EphB3 expression is transient and confined to committed endocrine cells. EphB3 was expressed in cells ready to delaminate, cells that are in the process of delaminating, or cells that have started cytodifferentiation (model, Fig. 5.3I).

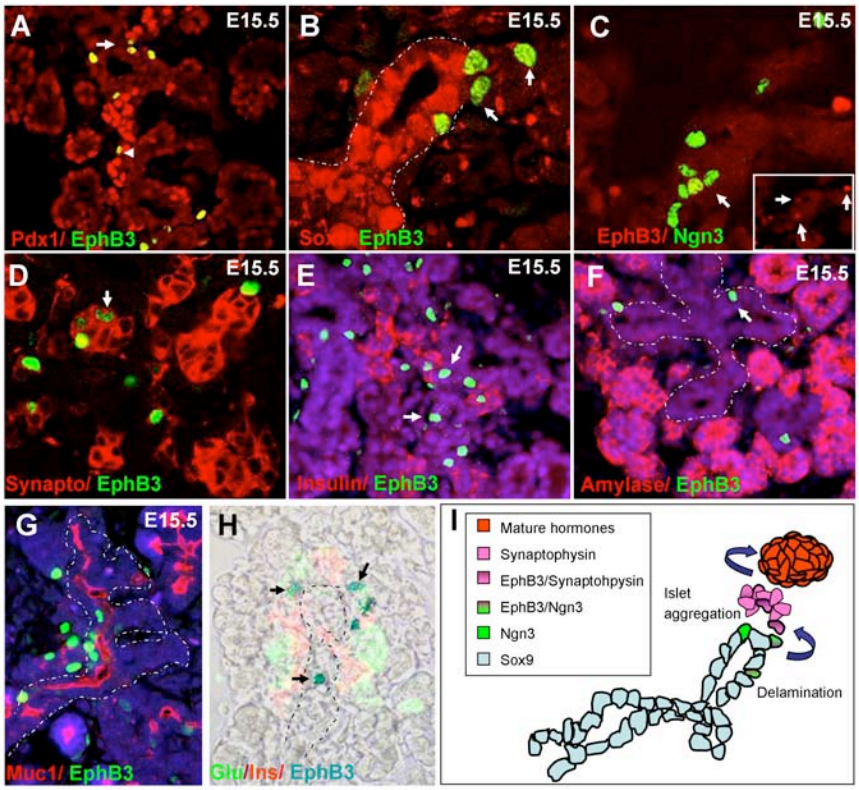

Figure 5.3. *EphB3* receptos are expressed in delaminating cells. *EphB3* protein detected by β-galactosidase immunofluorescence on cross-sections of E15.5 pancreas. *EphB3* protein co-expresses with Pdx1 **(A)** ; Ngn3 **(C)** and Synaptophysin **(D)** ; but it does not co-stain with Sox9 **(B)** and Insulin **(E,H)** ; glucagon **(H)** ; amylase **(F)** . *EphB3* receptors are found along ducts **(G)**. Model of *EphB3* expression during islet formation **(I)**. Pancreatic epithelium is delaminated by white broken line.

5.2.3 Eph/ephrin B signaling is required for proper pancreatic branching and development.

In order to determine the function of the Eph/ephrin B molecules, *EphB2*$^{LacZ/LacZ}$/ *EphB3*$^{-/-}$ mice was analyzed. These mice were generated by Henkemeyer and colleagues (Henkemeyer et al., 1996) and are null for the *EphB3* receptor and dominant negative for *EphB2*. In this mouse model, the cytoplasmic domain of *EphB2* has been replaced with a β-galactosidase cassette blocking any forward signaling through this receptor but still allows reverse signaling through its ligand binding.

To examine the overall morphology of these mutants, *in situ* hybridization on E13.5-E14.5 isolated gut tubes was performed on *EphB2*$^{LacZ/LacZ}$/ *EphB3*$^{-/-}$; *EphB2*$^{LacZ/+}$/ *EphB3*$^{-/-}$; and CD1 embryos. The expression of two epithelial markers, *Ngn3* and *Sox9* was performed since both genes have previously been shown to be widely expressed throughout the pancreatic epithelium at these developmental stages (Seymour et al., 2007; Villasenor et al., 2008). About 54% of *EphB2*$^{LacZ/LacZ}$/ *EphB3*$^{-/-}$ and 41% of *EphB2*$^{LacZ/+}$/ *EphB3*$^{-/-}$ pancreata showed defects in their overall morphology and branching. However, these defects varied significantly in intensity, some were more severe than others (data not shown) (Fig. 5.4). At both stages it was observed that the pancreas had a smaller tail (Fig. 5.5C) and a loss of the characteristic ‘anvil-shaped’ tail (Fig. 5.4 A-F). In addition, the right lateral branches in the tail were truncated causing a decrease in the thickness of the tail, and consequently the distinctive ‘ridge’ did not form properly (Fig. 5.4D-F), as measured by height of the apex of the ‘anvil-shaped’ tail (Fig. 5.4 H-J; Fig. 5.5D). Mutant pancreata also showed a decrease in lateral branching (Fig. 5.4K-L, white arrows). In adults, mutant pancreata were recognizable from wildtype

because of their smaller size, their reduced tail, fewer and shorter branches, and their overall condensed/tighter consistency (Fig. 5.5A-B).

Both *EphB2*$^{LacZ/+}$/*EphB3*$^{-/-}$ and *EphB2*$^{LacZ/LacZ}$/*EphB3*$^{-/-}$ showed defects in pancreatic morphology suggesting three possible alternatives. The first is that the abnormal shape of the pancreas was only due to the lack of *EphB3* receptor; the second is that it merely depended on the *EphB2* receptor and its haploinsufficiency was sufficient for the phenotype; and the third is that both receptors were required for proper pancreatic development. In order to test whether single mutants would recapitulate the observed phenotype and discern the functionality of each receptor, E14.5 pancreas of mutants lacking single *EphB* receptors: *EphB3*$^{-/-}$ nulls and *EphB2*$^{LacZ/LacZ}$ were assayed. We observed that none of the single mutants exhibited defects in pancreatic morphology or branching (Fig. 5.6 and data not shown), suggesting that both *EphB2* and *EphB3* receptors may act in concert and be functionally redundant during pancreatic development.

5.2.4 Dysregulated expression of mesenchymal genes and vascular remodeling defects in *EphB2*$^{LacZ/LacZ}$/ *EphB3*$^{-/-}$ animals.

Eph/eprhinB signaling has the unique characteristic of bi-directionality, where both cells in contact respond accordingly to receptor (forward signaling) as well as to the ligand (reverse signaling) (Murai and Pasquale, 2003; Pasquale, 2005).

To address the question whether disruption of *EphB2* receptor and lack of *EphB3* in the pancreatic epithelium will implicate also non-cell autonomous changes in the

tissues expressing the ligands outside the epithelium (*ephrinB1* for mesenchyme and *ephrinB2* for blood vessels), the mesenchymal expression of *Barx1*, *Hox11* and *ephrinB1* was analayzed in *EphB2*$^{LacZ/LacZ}$/ *EphB3*$^{-/-}$ mice. *Barx1* and *ephrinB1* expression was dispersed and not restricted to the left and right side of the pancreas as in wildtype (Fig. 5.7A,E) but was widespread throughout the whole pancreatic tail (Fig. 5.7 B,F) and *Hox11* expression was almost negligible in the EphB mutants (Fig. 5.7C,D). In addition, *in situ* hybridization of PECAM was performed in mutant pancreata in order to analyze vascular remodeling. Interestingly, *EphB2*$^{LacZ/LacZ}$/ *EphB3*$^{-/-}$ mice failed to remodel the major pancreatic vessels (Fig. 5.7 G-J, black arrows) implying that *EphB2* forward signaling is required for vascular remodeling.

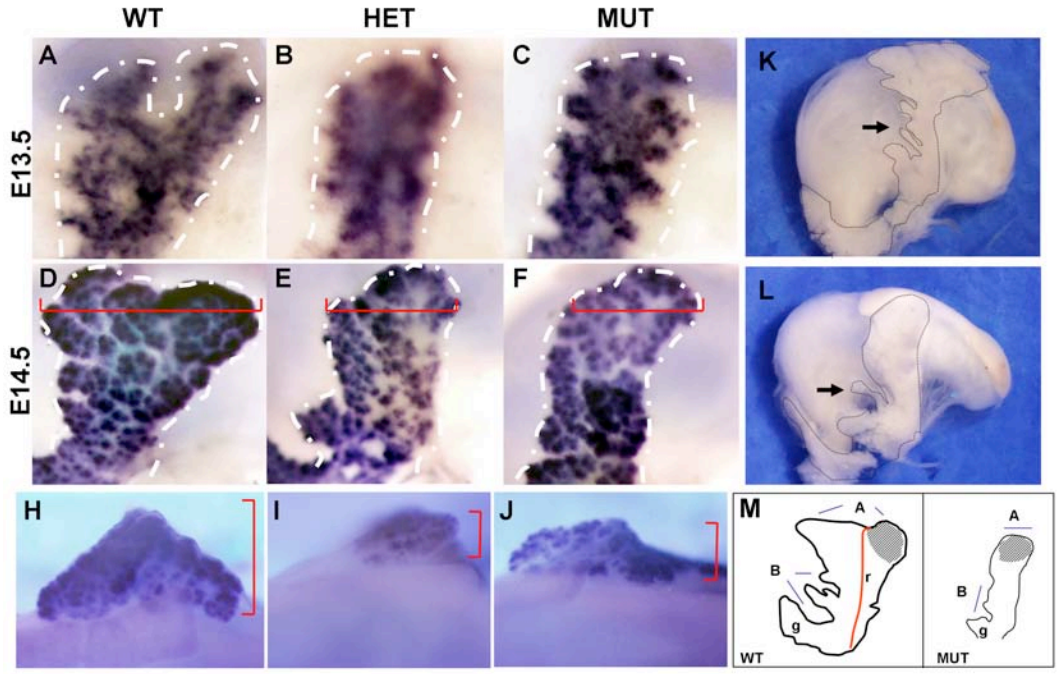

Figure 5.4. EphB signaling is required for proper pancreatic morphology and branching. (A-C) *In situ* hybridization of *Ngn3* in isolated E13.5 dorsal pancreata. (**D-F).** *In situ* hybridization of Sox9 in dissected E14.5 dorsal pancreata **(H- J)** Top views of pancreatic tails. **(K-L)** E16.5 Dorsal pancreatic bud, with stomach seen in the background. **(M)** Cartoon representing the major morphological defects observed in mutant. The pancreatic epithelium is delaminated by a broken line. Red lines in D-F measure width of pancreatic tail while lines in H-J measure its height. **(A,D,H,K)** are WT, wildtype; **(B, E, I)** are HET, *EphB2*$^{LacZ/+}$/*EphB3*$^{-/-}$; and **(C,F,J, L)** are MUT, *EphB2*$^{LacZ/LacZ}$/*EphB3*$^{-/-}$. A, 'anvil-shaped' tail; B, left pancreatic branches; g, gastric branch; r, 'ridge'.

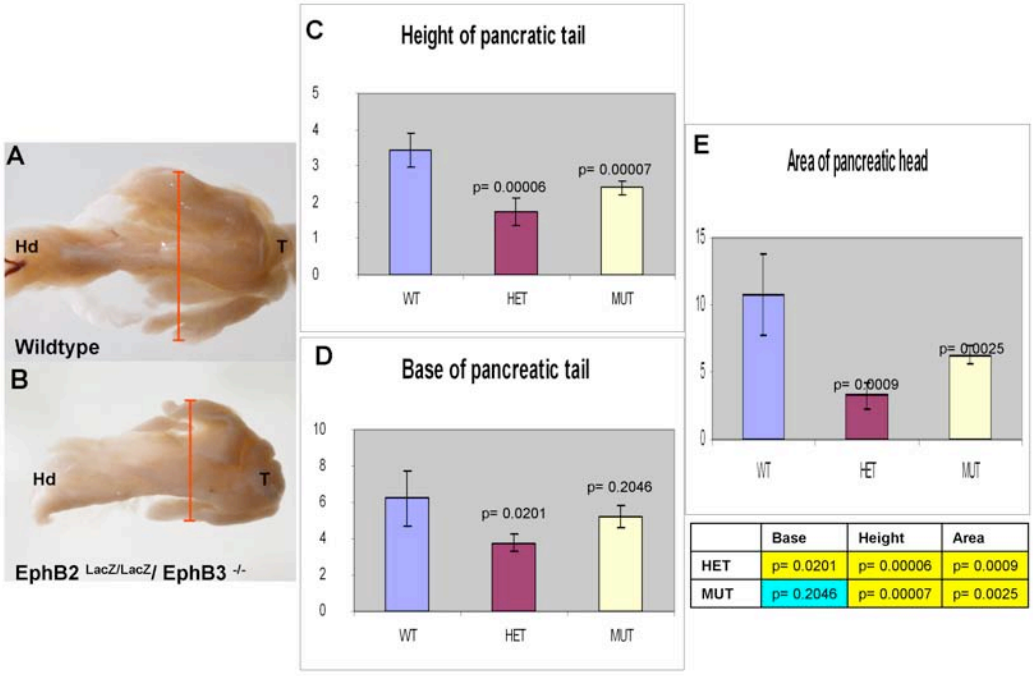

	Base	Height	Area
HET	p= 0.0201	p= 0.00006	p= 0.0009
MUT	p= 0.2046	p= 0.00007	p= 0.0025

Figure 5.5. Quantification of pancreatic tail size and thickness and morphology of adult mutant pancreas. (A-B) Bright field pictures of adult whole dorsal pancreas **(A)** is wildtype and **(B)** is *EphB2*$^{LacZ/LacZ}$/*EphB3*$^{-/-}$. **(C-E)** Graphs showing difference in E14.5 pancreatic tail height **(C)**; length **(D)**;and area **(E)**. Bottom of E graph there is the table with p values. On yellow are statistically significant and on blue are not statiscally significant. WT=Wildtype. HET= *EphB2*$^{LacZ/+}$/*EphB3*$^{-/-}$ and MUT *EphB2*$^{LacZ/LacZ}$/*EphB3*$^{-/-}$ Hd, pancreatic head; T, pancreatic tail.

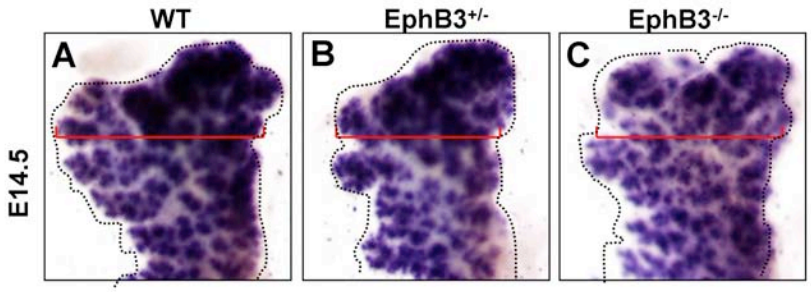

Figure 5.6. *EphB2*$^{LacZ/LacZ}$ show normal pancreatic morphology. (A-C) *In situ* hybridization of *Sox9* in E14.5 isolated dorsal pancreata, wildtype **(A)** *EphB3*$^{-/+}$ **(B)** and *EphB3*$^{-/-}$. The pancreatic epithelium is outlined by a dotted line.

5.2.5 *EphB2*$^{LacZ/LacZ}$/*EphB3*$^{-/-}$ display disrupted epithelial organization, cellular polarity and lack of proper lumen formation.

B-class *Eph/ephrinB* signaling is required for proper epithelium patterning in the intestine (Batlle et al., 2002), and recent work has implicated a role for *ephrinB1* in cell-cell junctions in epithelial cells (Lee et al., 2008). Because *ephrinA5* and *EphB2* are both highly expressed in the pancreatic epithelium, and *ephrinB*1 is in surrounding mesenchyme, Eph/ephrinB signaling might be required for pancreatic epithelium organization and formation. In order to address this question, pancreatic epithelium of E12.0 *EphB2*$^{LacZ/LacZ}$/*EphB3*$^{-/-}$ pancreata was examined. The mutant epithelium was disorganized (Fig. 5.8 A-B, E-F). Epithelial cells showed a decrease in expression of β-catenin (Fig. 5.8B,F) and E-cadherin was reduced in clusters of epithelial cells in the bud (Fig. 5.9 A-C, white arrows). In addition, there were disorganized β-catenin rich

aggregates localized within the stratified bud (Fig. 5.8B,F, white arrows). Overall the uniform and delineated peripheral expression of E-cadherin and β-catenin at the cell surface in epithelial cells was lost in *EphB2*$^{LacZ/LacZ}$ / *EphB3*$^{-/-}$ cells (Fig. 5.8 A-B, E-F).

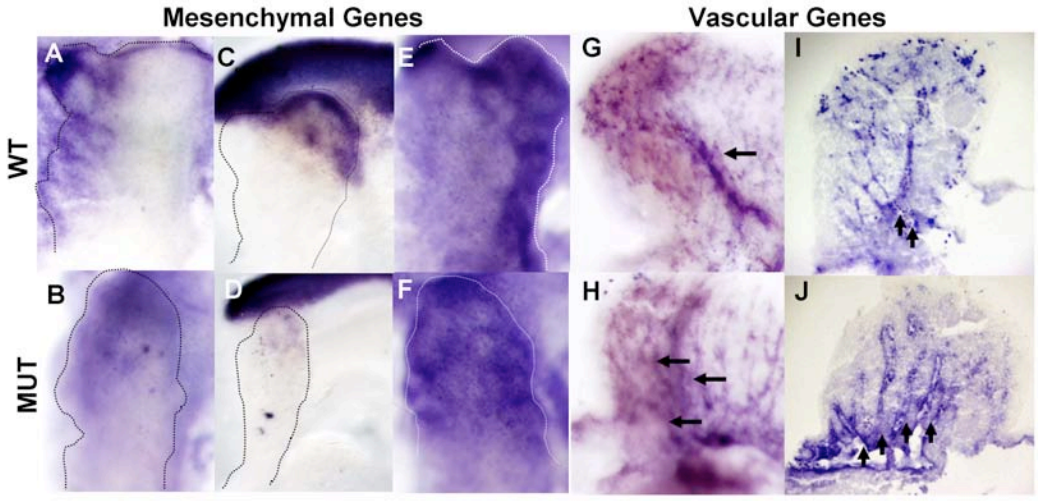

Figure 5.7. Dysregulated expression of mesenchymal genes and vascular remodeling defects in *EphB2*$^{LacZ/LacZ}$/*EphB3*$^{-/-}$ mice. (A-H) Whole mount *in situ* hybridization of **(A-B)** *Barx1* in E14.0 pancreata; **(C-D)** *Hox11* in E13.0 pancreata; **(E-F)** *ephrinB1* in E14.0 pancreata; and **(G-H)** *PECAM* in E11.5 pancreata. **(I-J)** Saggital sections of whole *in situs* showing that mutants fail to remodel the major pancreatic vessels. Black arrows point to blod vessels. WT=wildtype, MUT= *EphB2*$^{LacZ/LacZ}$ / *EphB3*$^{-/-}$.

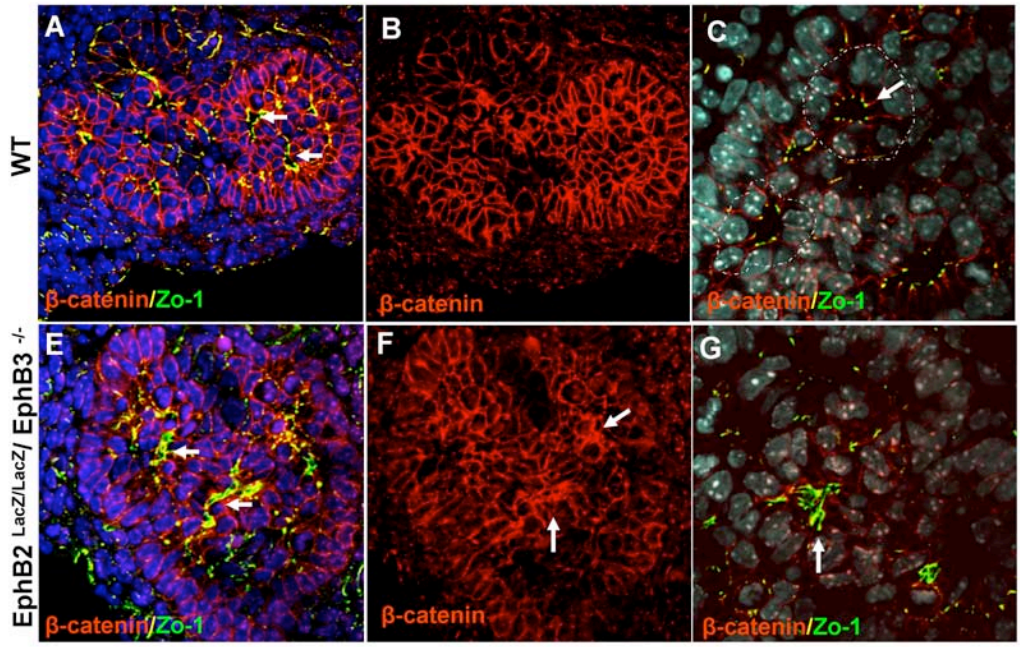

Figure 5.8. *EphB2*$^{LacZ/LacZ}$/*EphB3*$^{-/-}$ pancreata exhibit a disorganized epithelium and shows a defect in lumen formation. Immunostainings in E12.0 dorsal pancreata of **(A,E)** ZO-1 (green) and β-catenin (red) 40X **(B,F)** β-catenin (red) and **(C,G)** ZO-1(green), β-catenin (red), and DAPI (teal) 63X. Arrows in **A,E** show microlumens, in **F** point to β-catenin accumulation and **C,G** show to ZO-1 staining. Acini rosettes are indicated by dotted white line.

Interestingly, the polarity of *EphB2*$^{LacZ/LacZ}$/*EphB3*$^{-/-}$ epithelial cells was also abnormal. Mutant cells within the bud exhibit apical polarity even though they were not in direct contact with a lumen (Fig. 5.8 A,E). These cells did not orient properly into rosettes (Fig. 5.8C) and they expressed higher levels of the tight junction protein ZO-1 (Fig. 5.8 C,G white arrows) possibly preventing the proper formation of microlumens as many collapsed lumens were observed (Fig. 5.8A,E,C,G). In addition, *EphB2*$^{LacZ/LacZ}$/*EphB3*$^{-/-}$ epithelial cells also displayed increased levels of laminin (Fig. 5.9 A'-C', white arrows).

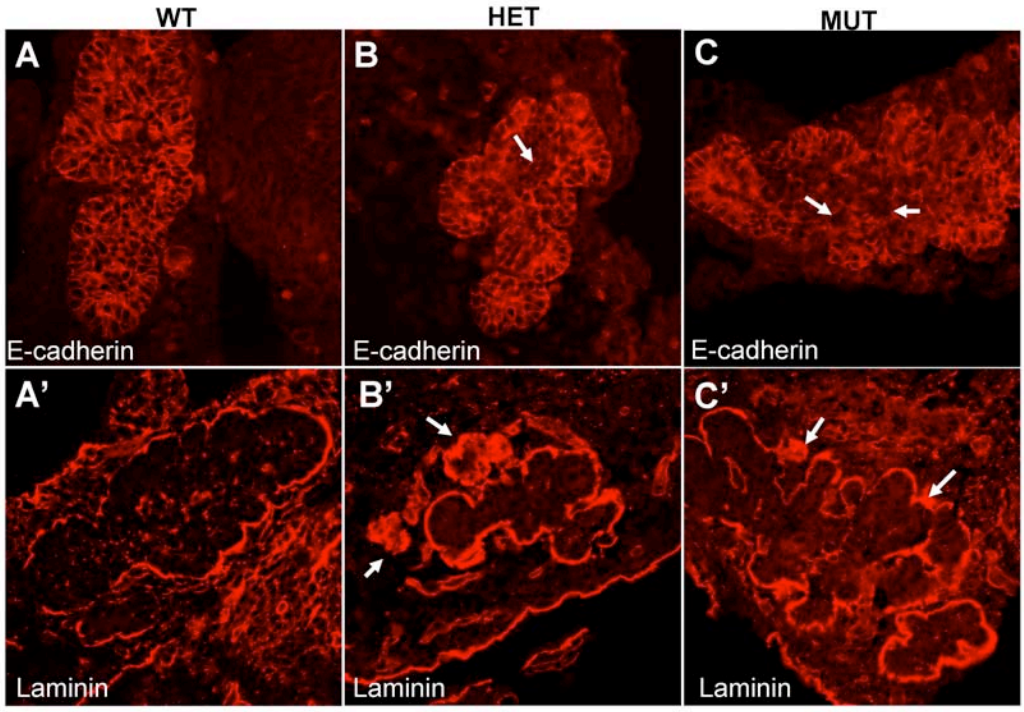

Figure 5.9. *EphB2*$^{LacZ/LacZ}$/*EphB3*$^{-/-}$ exhibit a decrease in E-cadherin expression but an increase in laminin expression. E12.0 saggital sections of dorsal pancreas **(A-C)** E-cadherin staining. Arrows point to regions in mutant pancreas lacking E-cadherin expression and **(A'-C')** Laminin staining. White arrows point to laminin aggregates. WT=wildtype, HET= *EphB2*$^{LacZ/+}$/ *EphB3*$^{-/-}$ and MUT= *EphB2*$^{LacZ/LacZ}$ / *EphB3*$^{-/-}$.

5.2.6 *EphB2*$^{LacZ/LacZ}$/*EphB3*$^{-/-}$ mutant have fewer endocrine cells and show disrupted islet morphology.

Because the *EphB3* receptor marks pro-endocrine cells, the disruption of *Eph/ephrinB* signaling was tested to see whether its action affected proper formation of the endocrine compartment. Immunofluorescence stainings on paraffin sections of E12.0

(primary wave endocrine cells) and E16.5 (secondary wave endocrine cells) were performed on *EphB2*$^{LacZ/LacZ}$/*EphB3*$^{-/-}$ and wildtype dorsal pancreata. At E12, α-cells were loosely associated in the endocrine aggregates (Fig. 5.10A-B, white arrows) and there was an overall decrease in total number of these cells of about 33% (Table 5.1). At E16.5, the decrease was found in both α and β-cells in the dorsal pancreas (Table 5.1). There was about 48% fewer glucagon cells (α) and about 44% fewer insulin cells (β). This decrease was more prominent in the distal portion of the tail of the pancreas as oppose to proximally (Fig. 5.10 E-H and Table 5.1).

To elucidate whether this decrease in number of endocrine cells was due to reduced cell proliferation, Ki67 stainings were performed on E16.5 dorsal pancreas sections from *EphB2*$^{LacZ/LacZ}$/*EphB3*$^{-/-}$ and wildtype mice. Similar numbers of proliferating cells in wildtype and mutant pancreas were found either distally or proximally (Fig. 5.11, and Table 5.2) in both the endocrine and the exocrine compartment. This indicates that cell proliferation was not affected in our mutants and hence was not likely to be the cause for the decrease number of endocrine cells observed in our mutants.

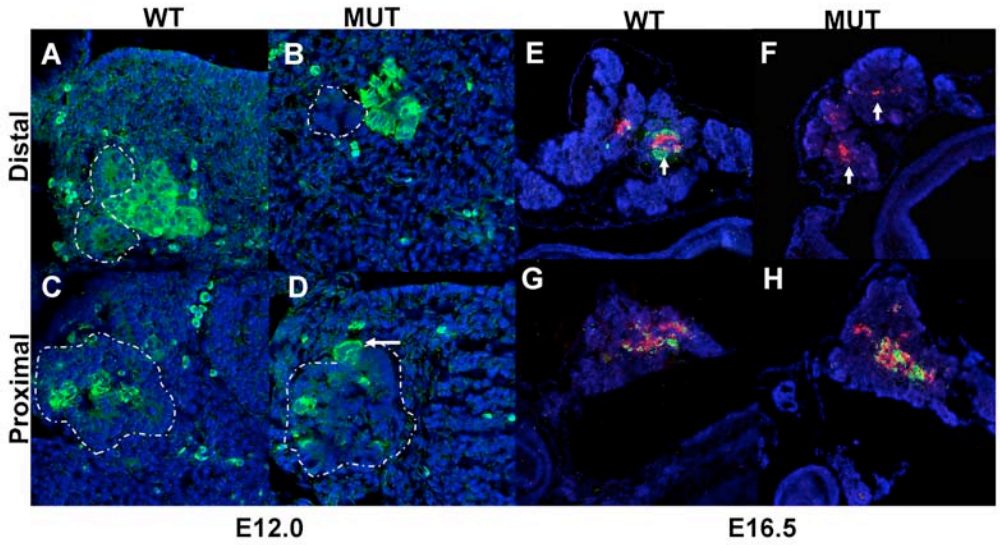

Figure 5.10. EphB signaling is required for proper islet mass. Immunofluorescence staining of paraffin sections of E12.0 (A-D) and E16.5 (E-H) dorsal pancreas. Top row show sections from distal pancreas and bottom row show representative images of proximal pancreas. **(A-D)** Glucagon (green) and DAPI (blue). Pancreatic epithelium is outlined by white dotted line. **(E-H)** Glucagon(green), Insulin (Red) and DAPI (blue). Notice how distally there is very few endocrine cells.

Developmental stage	Wildtype	$EphB2^{LacZ/LacZ};EphB3^{-/-}$
E12.0 Dorsal pancreas Total number of glucagon cells	269	179
E16.5 Distal Pancreas Number of glucagon/ /insulin cells	40 / 78	10 / 36
E16.5 Proximal Pancreas Number of glucagon/ insulin cells	31 / 70	24 / 46

Table 5.1. Quantification of endocrine cells. For E12.0 total number of glucagon positive cells was quantified (n=3 wildtype and n=3 mut). For E16.5 four representative sections that spanned the entire proximo-distal area of the pancreas were quantified (n=3 wildtype and n=3 mut)

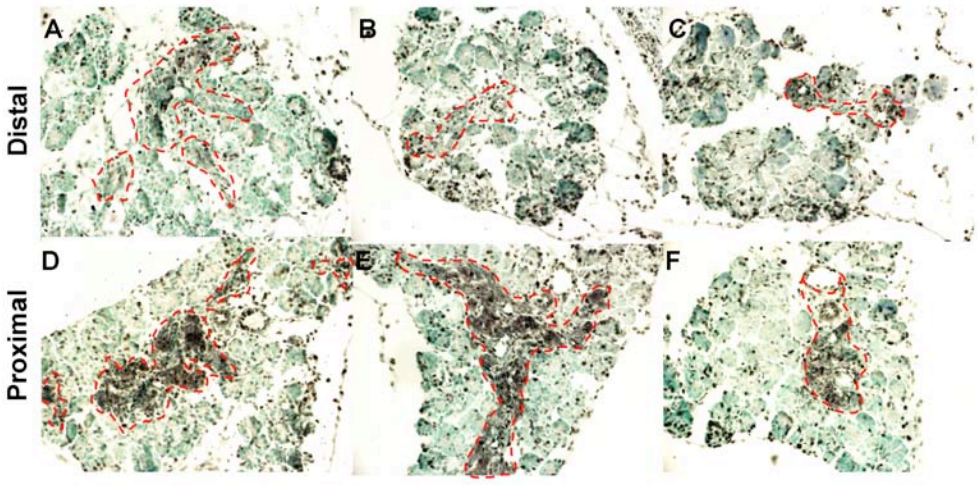

Figure 5.11. *EphB2*$^{LacZ/LacZ}$ / *EphB3*$^{-/-}$ mice display normal rates of cellular proliferation. Immunohistochemistry staining of Ki67 in E16.5 pancreatic sections. Endocrine compartment is delineated by red dotted line. Top row shows from distal pancreas, bottom row shows sections from proximal pancreas. **(A,D)** Wildtype. **(B,F)** *EphB2*$^{LacZ/LacZ}$/*EphB3*$^{-/-}$ mice**.**

Distal

Percentage of Ki67^{+}	WT	Mutant #1	Mutant #2
Endocrine	(75/167) 45%	(27/46) 59%	(27/40) 67%
Exocrine	(184/526) 35%	(195/349) 55%	(200/427) 47%

Proximal

Percentage of Ki67^{+}	WT	Mutant #1	Mutant #2
Endocrine	(155/209) 74%	(210/302) 69%	(61/92) 66%
Exocrine	(210/523) 40%	(292/593) 49%	(272/598) 45%

Table 5.2. Quantification of cell proliferation in wildtype and *EphB2*$^{LacZ/LacZ}$ / *EphB3*$^{-/-}$ mice Four representative sections of E16.5 pancreas were quantified. Percentage of proliferation is given by number of Ki67 positive cells / total number of cells.

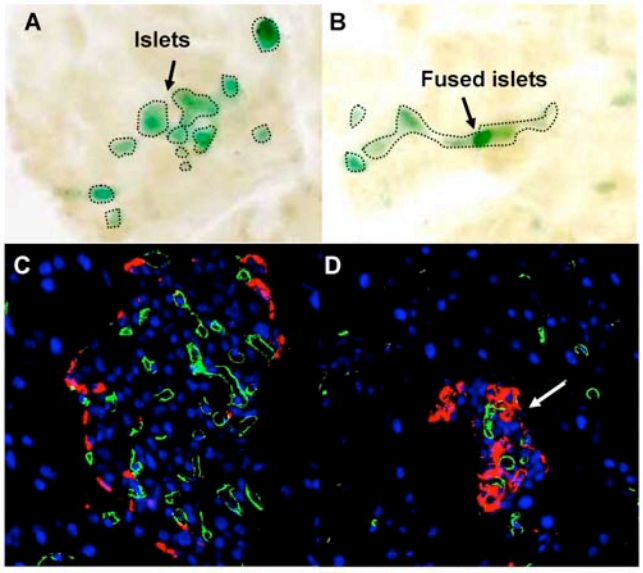

Figure 5.12. *Eph/ephrinB* signaling is required for proper islet morphology. Whole mount β-galactosidase staining of adult islets in wildtype **(A)** or *EphB2*$^{LacZ/LacZ}$/*EphB3*$^{-/-}$ (B) mice. Arrow is pointing to 'fused' shaped islets. **(C-D)** PECAM(green) and Glucagon (red) immunostaining of adult pancreatic sections. Arrow in D is pointing to glucagon aggregate.

Whole mount islet β-galactosidase staining was performed in adult pancreas of *EphB2*$^{LacZ/LacZ}$/*EphB3*$^{-/-}$ and wildtype mice. Islets stained green due to their intrinsic endogenous β-galactosidase activity (Inada et al., 2006) and whole pancreas were studied. *EphB2*$^{LacZ/LacZ}$/*EphB3*$^{-/-}$ mice displayed abnormal istle morphology, as islets appeared aggregated into elongated 'ribbon-like' amorphous structures (Fig. 5.11 A-B). Immunostainings with endocrine markers (insulin and glucagon) revealed the amorphous shape of many islets that did not exhibit the typical distribution of endocrine cells found in islets (β-cell mantle and α-cells in the periphery) (Fig. 5.11 C-D and data not shown). These results suggest that *Eph/ephrin*B signaling is required for proper endocrine development and islet formation.

5.2.7 *EphB2*$^{LacZ/LacZ}$/*EphB3*$^{-/-}$ mice display defects in pancreatic function.

Since *EphB2*$^{LacZ/LacZ}$/*EphB3*$^{-/-}$ showed defects in pancreas morphogenesis and a decrease in the number of endocrine cells, it was examined whether disruption of *Eph/ephrinB* signaling also produced defects in pancreatic function. *EphB2*$^{LacZ/LacZ}$/*EphB3*$^{-/-}$ animals did not develop diabetes and their plasma glucose levels were not statistically different from the wildtype (Fig. 5.13A and data not shown). To our surprise, when *EphB2*$^{LacZ/LacZ}$/*EphB3*$^{-/-}$ animals were glucose challenged by an intraperitoneal (ip) glucose tolerance test, an improved glucose tolerance was observed (Fig. 5.13B). This enhancement of glucose tolerance was only observed in the double *EphB2*$^{LacZ/LacZ}$/*EphB3*$^{-/-}$ animals, as single mutants *EphB2*$^{LacZ/LacZ}$ or *EphB3*$^{-/-}$ did not show abnormal pancreatic function.

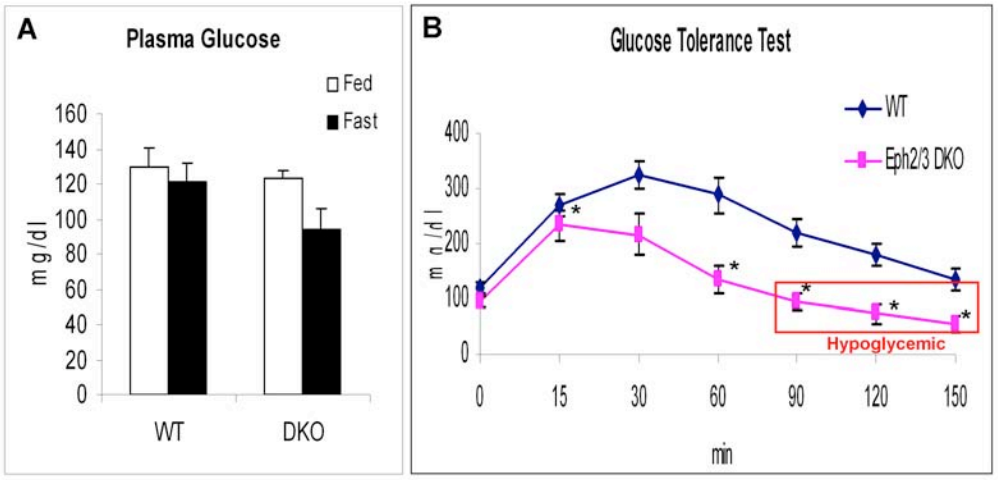

Figure 5.13. ***EphB2*$^{LacZ/LacZ}$*/EphB3*$^{-/-}$ **mice show improved glucose tolerance. (A)** Plasma glucose levels at fed (white columns) and fast conditions (black columns) in WT= Wildtype and DKO= *EphB2*$^{LacZ/LacZ}$*/EphB3*$^{-/-}$ **(B)** Blood glucose concentrations at the indicated time points after ip injection of glucose in WT=Wildtype (n=6) and *EphB2*$^{LacZ/LacZ}$*/EphB3*$^{-/-}$ (n=4).

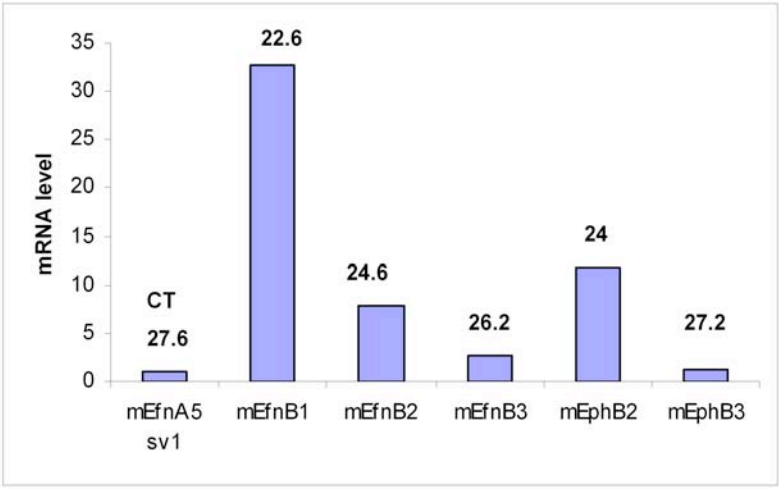

Figure 5.14. Eph/ephrinB are expressed in adult islets expression. Q-PCR from mRNA isolated from mice islets. Primers were validated with brain mRNA. CT was calculated utilizing cyclophilin expression as baseline. Efn=ephrin.

5.3 DISCUSSION

Pancreas development is a complex process that requires branching morphogenesis and tubulogenesis concomitant with cellular differentiation of progenitor cells into three main tissues: the exocrine, the endocrine, and the ductal. Many molecular regulators have been shown to be involved in these processes, including a large number of transcription factors (Oliver-Krasinski and Stoffers, 2008; Sander and German, 1997; Wilson et al., 2003). However, little is known about the role that cell-surface Eph/ephrins play in pancreatic development. Here, we have identified a novel role for *Eph/ephrin*B signaling during pancreas organogenesis in regulating endocrine differentiation as well as branching morphogenesis. Specifically we found that *Eph/ephrinB* signaling is required for proper cell polarity and subsequent allocation of progenitors during early epithelial development. Disruption of *Eph/ephrin*B signaling in the pancreas produced less endocrine cells and a disorganized pancreatic epithelium that consequently created an amorphous gross pancreas. Our results implicated, for the first time, the involvement of *Eph/ephrinB* signaling in modulating pancreatic development.

A comprehensive characterization of the expression of the B-subclass of Eph receptor and their respective ligands in the developing pancreas was carried out. E*phrinA5*, *EphB2* and *EphB3* were expressed in the pancreatic endoderm; *ephrinB2* and *EphB4* were expressed in the vascular endothelium; and *ephrinB1*, *EphB4*, and *EphB6* were expressed in the surrounding mesenchyme. The widespread expression of *Eph/ephrin*B subclass throughout the tissues that make up the pancreas (epithelium, endothelium, mesenchyme) suggests that cell-to-cell communication via *Eph/ephrin*B signaling might be required for proper pancreatic development. It is known that

pancreatic branching morphogenesis, ductal formation, and endocrine differentiation all require the communication of epithelium, endothelium and mesenchyme. For example, blood vessels are known to send active signals to the pancreatic epithelium to promote endocrine differentiation (Lammert et al., 2001; Lammert et al., 2003) while mesenchyme is known to inhibit endocrine differentiation (Attali et al., 2007; Duvillie et al., 2006). The proper balance and interchange of signals between these tissues allows proper pancreatic development. Furthermore, recent work has shown that the *EphB2* and *EphB3* receptors are required for the normal development of several organs such as the midbrain (Altick et al., 2005), cleft palate (Risley et al., 2009), genitourinary/anorectal formation (Yucel et al., 2007) and retina neuronal mapping (Hindges et al., 2002) . Therefore we ask whether *Eph/ephrinB* signaling may be required for pancreatic morphogenesis.

Indeed we found that mice that are null for *EphB3* receptor and dominant negative for *EphB2* (*EphB2*$^{LacZ/LacZ}$/*EphB3*$^{-/-}$) displayed defects in pancreatic formation. The pancreata of these mutants exhibited distinct morphological abnormalities, including reduced left lateral branching and aberrant tail formation (see Chapter 2). We assayed single mutants for each receptor (either *EphB2*$^{LacZ/LacZ}$ or *EphB3*$^{-/-}$) and found that none showed defects in pancreatic morphology indicating that the function of both receptors in pancreatic development are likely to be required for pancreas formation. These observations are not altogether surprising, given that previous studies have shown that *EphB2* and *EphB3* receptors can be functionally redundant in other organs (Orioli et al., 1996). What is perplexing is that in pancreas these receptors are expressed in different pancreatic tissues: *EphB2* is expressed in the exocrine tissue while *EphB3* marks pro-

endocrine cells. This conundrum may be explained by the different developmental windows of expression of these receptors: at early pancreatic stages *EphB2*, like *EphB3*, is widely expressed in the pancreatic epithelium and it is only after the secondary transition, that each receptor becomes restricted to different cell types: *EphB2* in the apical side of acinar cells and *EphB3* in delaminating endocrine cells. It is then possible that at early developmental stages *EphB2* and *EphB3* function is redundant, and their early signaling in pancreatic proto-differentiated cells is required for the proper formation of the pancreas. Alternatively, it is possible that these receptors are never redundant and they carry on individual functions in pancreatic development: *EphB2* in exocrine development and *EphB3* in endocrine development and that only a disruption of either is not sufficient to produce pancreatic malformations. Future studies will help clarify these aspects.

In addition, mutants had a disorganized epithelium and abnormal cellular polarity. Their epithelium showed an increase in laminin and in the amount of tight junctions presented in the foci inside the cells. Foci appeared to merge with one another, however, epithelial cells did not orient in a rosette fashion around the ZO-1 clusters, but appeared as disorganized aggregates. In addition, epithelial cells did not show uniform distribution of β-catenin and showed lower levels of E-cadherin suggesting a loss of adherence between cells and possible disruption of cell-to-cell communication. Our results suggest *Eph/ephrin*B signaling between epithelial cells is required for proper microlumen formation and pancreatic branching.

EphB2$^{LacZ/LacZ}$/*EphB3*$^{-/-}$ mutants showed a decrease number of endocrine cells of about 30-48% depending on the stage assayed. It has been shown that *EphB2* and *EphB3*

signaling promotes cell proliferation in the intestine (Holmberg et al., 2006). Therefore, in order to test whether this decrease in endocrine numbers was due to a decrease in cell proliferation, we assayed cell proliferation by Ki67 staining. There was no difference between the rates of proliferation of the mutant pancreatic tissues. Future studies in apoptosis need to be done to exclude the possibility of an increase in cell death in mutant endocrine cells. However, it is likely that the reduction in endocrine cells is a consequence of the defects in epithelium. As mentioned before, *EphB2*$^{LacZ/LacZ}$/*EphB3*$^{-/-}$ epithelium was disorganized and lost adherence (i.e. reduction of E-cadherin) making it difficult for cells to communicate. It is then possible that in order to differentiate there is need of this cellular contact with neighboring epithelial cells.

Ephs are known to regulate processes through cell –to-cell contact by the binding to their ligands. Therefore we also speculated that ligand-expressing tissues might also be affected non-cell autonomously by disruption of EphB receptor function. Indeed we find that mesenchyme, blood vessels and epithelium are disrupted in our mutants. *EphB2*$^{LacZ/LacZ}$/*EphB3*$^{-/-}$ mice showed misexpression of mesenchymal genes and problems in vascular remodeling indicated that reverse signaling by both ligands, *ephrinB1* (mesenchyme) and *ephrinB2* (blood vessels), is likely to be activated by these receptors. In addition, the epithelial defects observed proposed a communication between *ephrinA5* and *EphB2* for cell to-cell adhesion in pancreatic epithelial cells.

In order to test whether signaling through *ephrinB1* (mesenchyme) was playing a role in pancreatic morphogenesis, the E14.5 pancreata of *ephrinB1* null mice was analyzed. It was found that pancreas development was normal (data not shown). These results postulate *ephrinB2* or *ephrinA5* as the main candidate ligands for *EphB2* and

EphB3 receptors in pancreatic development. It is provocative to think that establishment of the vasculature network is co-dependant to branching morphogenesis of the pancreas and vice versa. Future experiments utilizing the *ephrinB2*$^{lacZ/lacZ}$ (mice lacking all *ephrinB2* reverse signaling) (Cowan et al., 2004; Dravis et al., 2004) will help resolve this question.

Finally, adult *EphB2*$^{LacZ/LacZ}$/*EphB3*$^{-/-}$ showed enhanced glucose tolerance. In order to interpret these results, insulin and glucagon measurements are necessary. Recent work, however, has shown that Eph/ephrinA signaling is involved in insulin secretion by a rigorous balance between forward and reverse signaling: EphA inhibits insulin secretion while ephrinA stimulates it. Their studies also showed that *ephrinA5* was the ligand required for glucose-stimulated insulin secretion. Analysis by Q-PCR in adult islets shows expression of *EphB2* and *EphB3* (Fig. 5.14) (Konstantinova et al., 2007) It is known that *ephrinA5* can interact with *EphB2*, thus it is possible that *EphB2*/*ephrinA5* interaction functions in a similar way in insulin secretion, as described previously for EphA/ephrin A signaling. All in all, the results of this chapter suggest that during development Eph receptor and their ephrin B ligands have a function in patterning and morphogenesis of the pancreas, but that during adulthood they are involved in endocrine hormone secretion functions. Future experiments will address these questions.

Chapter 6: SUMMARY, FUTURE DIRECTIONS, AND CONCLUSIONS

The research in this dissertation covers a wide array of topics all related to pancreatic developmental biology: from the basic characterization of embryonic organ morphology, to the more complex analysis of different signaling cascades involved in pancreatic development and function. Each chapter provides new insights and strengthens the understanding of pancreatic development, opening new avenues of research. In this summary the potential future directions for each individual chapter are discussed.

Chapter 2: Pancreatic Organogenesis: Epithelial polarity, lumen formation and branching morphogenesis.

SUMMARY: In this chapter, we performed an in depth macro and microscopic description of the morphogenesis of the pancreatic anlagen during midgestation (E8.5-E15.5). Microscopic analysis of the pancreas showed that formation of the mature pancreatic tubular network occurs in a non-conventional manner. The process started from a single polarized epithelial layer, which first adquired a columnarized shape and then evaginated from the gut tube. During the primary pancreatic transition, the pancreatic epithelium underwent active epithelial stratification and reorganization, only later re-organizing into a single-layered polarized epithelium following the secondary transition. Pancreatic lumens initially formed during the primary transition by cellular arrangements, rather than either apoptosis or epithelial bulging. Of particular importance is the relationship between pancreatic epithelium and endocrine cells. We observe that

endocrine cells lose connectivity with the epithelium by decreasing baso-lateral adhesion proteins and losing their polarity. These molecular changes in the endocrine cells allow their physical separation from the pancreatic epithelium either by budding (during the first transition) or by delamination (following the secondary transition). In addition, a detailed analysis of the gross morphology of the pancreas is provided, establishing an anatomical model of pancreatic development that demonstrates predictable trends in overall branching patterns. This model will serve as a framework for future studies of the organ, both wildtype and mutant. Together, these studies showed that the pancreatic organ forms via dramatic pancreatic epithelial remodeling and our characterization of normal pancreatic branching patterns will aid in the analysis of mutant phenotypes.

FUTURE DIRECTIONS:

In this chapter, we have described the gross branching patterns of the developing pancreas. However, a possibility for future studies would be to categorize length and position of individual branches and label orientation of branching events, in a detailed study analogous to the one carried out in the developing lung by the Krasnow group (Metzger et al., 2008). For this study, mucin-1 immunostaining in whole pancreata would prove valuable since it allows for complete visualization of all branches.

In addition, further characterization of the endocrine compartment would provide a better understanding of endocrine delamination. We observe that individual endocrine cells do not show peripheral laminin staining while budding endocrine aggregates do. It would be interesting to determine whether this difference in endocrine polarity is due to different types of endocrine cells (first versus second wave) or whether endocrine polarity

is only acquired as endocrine cells aggregate. This is a possibility, given observations by the Dor group (personal communication) that suggest blood vessels act as organizing foci for rosettes of endocrine cells. Immunostaining of endocrine cells at early versus late stages of pancreatic development, as well as the analysis of mutant mice that only show first wave of endocrine cells (*Pdx1* null) would help clarify these interesting questions.

Given that a decrease in β-catenin in endocrine cells was also observed, it would be interesting to test whether a decrease in β-catenin is necessary for delamination of endocrine cells from the pancreatic epithelium. We could address this question by creating compound heterozygous mice utilizing the $Catnb^{lox(ex3)}$ mice (Harada et al., 1999), mice in which the regulatory exon of β-catenin is sandwiched by two floxP sequences allowing for the production of stable β-catenin, and *Pdx1*-Cre, mice, which express Cre recombinase specifically in pancreatic cells. Generation of these mice would allow us to express constitutively active β-catenin levels in the pancreatic epithelium. The question would be whether this genetic manipulation would impair endocrine delamination.

Another interesting direction would be to study specific deletion of mNumb in pancreatic cells. mNumb is expressed in pancreatic endocrine cells (Yoshida et al., 2003) and it is an ortholog of *Drosophila* Numb which during neuronal precursor asymmetric cell division, functions by inhibiting Notch signaling in one of the daughter cells (Frise et al., 1996). Notch signaling is known to determine endocrine fate in the pancreas by repressing the expression of the endocrine transcription factor *Ngn3* (Apelqvist et al., 1999). Generating mice utilizing the $Numb^{flox/flox}$ and crossing them out with *Pdx1*-cre line would let us test whether numb function is required for endocrine differentiation.

Chapter 3: Analysis of Ngn3 expression in pancreatic development.

SUMMARY: In this chapter, we reported the unexpectedly dynamic embryonic expression of the endocrine master regulator *Ngn3* in the pancreatic anlagen. We characterized the expression of *Ngn3* transcripts and protein throughout pancreatic development and we identified and defined a dramatic and previously unnoticed gap in developmental *Ngn3* expression. We showed that both *Ngn3* transcript and protein expression occur in two distinct temporal waves, the first occurring early from approximately E8.75 to E11.0, and the second initiating at approximately E12.0. This observed biphasic expression correlates with the 'first' and the 'second' transitions, which encompass two distinct waves of embryonic endocrine differentiation. In addition, our studies demonstrated that *Ngn3* transcripts are markedly more widespread in the pancreatic epithelium than NGN3 protein, indicating that post-transcriptional regulation is likely to play a critical role during endocrine differentiation.

FUTURE DIRECTIONS:

Our work demonstrated the temporal biphasic expression of *Ngn3* during pancreatic development. Clearly, as the molecular underpinnings of this changing expression remain unknown, it would be interesting to identify the molecular regulators of *Ngn3* during this developmental window. It is known that *Ngn3* is activated by the coordinated action of many transcription factors such as *HNF-6*, *HNF-1*, and *HNF-3* (Lee et al., 2001) and possible *Sox9* (Maike Sander, BCBC meeting). In addition, its expression is known to be inhibited by Hes1. It would be easy and interesting to assay the

expression of these known regulatory factors during this timeframe, to test whether the correlate with the Ngn3 expression cessation, suggesting they might regulate Ngn3.

Other studies in our laboratory (carried out by Diana Chong) utilizing *Flk*-lacZ mice have shown that vascular remodeling in the pancreas correlates with the *Ngn3* transcriptional dip. At E10.5, the pancreatic bud is covered by an immature vascular plexus and this plexus undergoes dramatic remodeling into larger blood vessels exactly during the developmental window in which we observe *Ngn3* transcriptional repression. The questions arise: Is *Ngn3* repression a consequence of vascular remodeling? Or are $Ngn3^{+}$ cells directly communicating with blood vessels? Or alternatively, is this observed correlation merely a coincidence? In order to address these questions the *Ngn3* null pancreas anlagen can be assayed for defects in vascular remodeling. Indeed, we have started these experiments in our laboratory and noticed that *Ngn3* null pancreata have defects in their vasculature, supporting the idea that vasculature development occurs in a coordinated manner with endocrine differentiation.

Chapter 4: Rgs proteins are expressed in pancreatic endocrine cells and in models of β-cell regeneration.

SUMMARY:

Here we have assessed expression of *Rgs* genes during pancreatic development and in models of pancreatic disease. First, we surveyed expression of two tandemly duplicated *Rgs* genes (*Rgs8* and *Rgs16*) in embryonic and adult pancreas using GFP reporter lines. During mouse embryonic development, Rgs8::GFP and Rg16::GFP were first expressed in the pre-pancreatic endoderm, and then become restricted to pancreatic endocrine cells. Expression in the endocrine pancreas continued in neonates, but in

weanlings became restricted to individual cells associated with pancreatic ducts and blood vessels (VDACs), and it was extinguished in the adult pancreas. Because of their physical location, VDACs are attractive candidates for the long sought group of ductal progenitors. In adults, we found that Rgs16 expression was reactivated in three models of pancreatic endocrine proliferation: i) in pregnant females at midgestation, ii) during islet regeneration in PANIC-ATTAC mice, a model of type 1 diabetes, and, together with Rgs8::GFP, iii) in obese, hyperglycemic *ob/ob* mice, a model of type 2 diabetes. Our results suggest a role for *Rgs8* and *Rgs16* as regulators of G-protein signaling in pancreatic development and in models of metabolic stress and disease.

FUTURE DIRECTIONS:

Our studies characterized the expression of *Rgs8* and *Rgs16* throughout pancreatic development and in models of pancreatic endocrine proliferation. At early developmental stages, both genes are expressed in the pancreatic epithelium, while at later stages their expression becomes restricted to islets. Although we characterize in detail Rgs16 expression in E15.5 pancreata, future characterization of Rgs8 and Rgs16 is important in order to determine whether these genes are expressed by the same cell-type. At early stages (E9.5-E11.5) co-stainings with Pdx1, Sox9, E-cadherin, TCF2/HNF1β will help to test whether both Rgs genes are expressed through all pancreatic epithelial cells, or whether their expression is restricted to a subpopulation of cells. In addition, analysis of possible co-expression of Rgs genes with a variety of transcription factors can be assayed at later developmental stages to help reveal which endocrine lineage expresses either Rgs16 or Rgs8. For example, co-stainings with MafA (for β-cells produced after

E13.5), MafB (for α cells), Pax4 (β- and δ-cell lineage) Pax6 (α- cell lineage), and GLUT2 would refine our understanding of which cell types express Rgs8/16.

It is important to note that we assayed Rgs expression utilizing Rgs16::GFP and Rgs8::GFP transgenic mouse lines, and performed antibody stainings against GFP. Since GFP is a long-lived protein, these experiments may in fact represent a de facto lineage tracing of Rgs expression. Our studies cannot exclude the possibility that Rgs expression is more transient and short lived than it appears. In order to exclude this possibility, it will be important to correlate our expression patterns with the expression of antibodies directly targeted to Rgs proteins.

The discovery of VDACs was intriguing. For a long time there has been controversy regarding the origin of new β-cells in the adult. Do β-cells arise from pre-existing β-cells? Or do they arise from ductal progenitors? The identification of VDACs within ducts and the observation that they are seen in weanlings and pregnancy models suggests the possibility that VDACs constitute the long sought ductal progenitor. Future studies will help elucidate the identity and lineage of VDACs. One way to answer this question would be to create a mouse line with Rgs16-CreER. This construct indelibly label VDAC descendents when induced by a pulse of tamoxifen, turning on Cre expression in this cell population. The idea would be to induce pregnant females or late weanlings and in this way exclusively label VDACs (as Rgs16 is restricted to VDACs in the pancreas at these postnatal stages). Subsequently, co-immunostainings for Cre and for a variety of pancreatic markers would help identify this population of cells. Another idea would be to isolate VDACs from Rgs16::GFP transgenic mice (either by FACs or manually) and re-implant them in pancreatic explants in which β-cells have been ablated.

Stainings utilizing GFP and other pancreatic markers would help lineage trace and identify this particular population of cells, and assess whether they contribute to regeneration of new islets.

One of the most fascinating results of our study was the observation that Rgs expression was re-activated in models of pancreatic disease. There is an enormous need for the development of therapeutic agents and the identification of regulatory proteins that function in the adult during pancreatic stress conditions may help further these aims. Future studies to elucidate the role that Rgs proteins play in these disease models are necessary. Are Rgs proteins involved in glucose homeostasis? Or are they involved in β-cell expansion/neogenesis? Our results tend to favor a function in glucose metabolism rather than β-cell neogenesis since we do not observe co-expression of Rgs16::GFP with any proliferation markers. However, it has been shown that GPCR agonists stimulate β-cell replication and neogenesis in mouse models of diabetes, strongly suggesting a role for Rgs proteins in β-cell expansion. One explanation for the lack Rgs16::GFP expression in proliferating cells is that the *ob/ob* animals we assessed were hyperglycemic and β-cell expansion is known to occur before hyperglycemia is reached (Nolan et al., 2006). Thus, further experiments should be aimed at assessing β-cell replication during the early phases of endocrine failure in this model system. In addition, to better understand the function of Rgs16 in β-cell expansion, it would be interesting to assay other models of β-cell ablation where β-cell replication is more prominent such as Yuval Dor's mice model of β-cell ablation, where transgenic mice expresses diphtheria toxin specifically in β-cells after doxycline induction; or Pedro Herrera's transgenic mice, where β-cells express

diphtheria toxin receptor, promoter, therefore after diphtheria toxin administration β-cells are selectively destroyed ((Nir et al., 2007) and BCBC meeting). Interestingly, not all islets in the *ob/ob* mice showed Rgs16::GFP re-activation. It would be interesting to isolate Rgs16::GFP^{+} and Rgs16::GFP^{-} β-cells and assay their metabolic properties. These would help us distinguish whether Rgs16 re-expression plays a role in islet function.

Finally, it is important to mention, that we analyzed the pancreas of *Rgs16* null mice (results are not included in this thesis) and we find no defects in pancreatic development or function. Since *Rgs8* and *Rgs16* have overlapping expression patterns, our results strongly suggest functional redundancy between these genes, explaining why the single null shows no defects. The development of the double-targeted knockout for *Rgs8* and *Rgs16* will help elucidate the function of these genes.

Chapter 5: *Eph/ephrin* signaling modulates pancreatic development.

SUMMARY:

In these last studies, we demonstrated the requirement for EphB signaling during pancreatic development. We showed that EphB receptors are expressed within the pancreatic epithelium, while ephrinB ligands are expressed in embryonic blood vessels, pancreatic epithelium, and mesenchyme. These observations suggest that *Eph/ephrinB* tissue cross-talk may be involved in pancreas organogenesis. Indeed, we showed that disruption of the *Eph/ephrinB* signaling has severe effects on pancreatic formation and growth. *EphB2*$^{LacZ/LacZ}$ *EphB3*$^{-/-}$ mutant mice displayed defects in pancreatic branching, a

reduced number of endocrine cells, mislocalization of mesenchymal domains, defects in vascular remodeling and impaired pancreatic function. In addition, these mutants exhibited disrupted epithelial organization and cell polarity. Our data suggests a previously unnoticed role for *Eph/ephrinB* signaling in regulating proper pancreatic morphogenesis and physiology, by regulating cellular organization within the embryonic epithelium**.**

FUTURE DIRECTIONS:

We have shown that *EphB2*$^{LacZ/LacZ}$*EphB3*$^{-/-}$ mutant mice have disrupted epithelial organization and microlumen formation at E12.0, which in turn is likely to lead to the observed defects in both branching and endocrine differentiation. However, it would be extremely interesting to determine exactly when do these defects arise? *EphB2* and *EphB3* are first expressed throughout the pancreatic epithelium and later their expression becomes restricted to either the apical part of acinar cells (*EphB2*) or to delaminating endocrine cells (*EphB3*). Do the epithelial defects arise because of a primary disorganization of the stratified epithelium at early developmental stages? Or do they arise after *EphB2* and *EphB3* expression becomes restricted to different pancreatic compartments? Immunofluorescence studies of early pancreata (E10.5) utilizing polarity markers would determine whether pancreatic epithelium is disrupted at early stages and would help clarify these questions.

Additionally, it would interesting to determine the reason for the apical localization of *EphB2*? Are these receptors directly regulating apical complexes and tight junctions, as suggested by other studies (Lee et al., 2008)? Recent work by Lee et al.

shows that reverse signaling via *ephrinB1* regulates cell-to-cell tight junctions. They show that *ephrinB1* competes with cdc42 for association with Par6 complex. This competition causes inactivation of the Par complex and as a consequence loss of tight junction. In addition, it was shown that phosphorylation of *ephrinB1* (i.e. through Eph binding) blocks the interaction of *ephrinB1* with Par6 restoring tight junction formation (Lee et al., 2008). Recently, it was presented in the Beta Cell Biology Consortium meeting that *cdc42* null mice displayed defects in lumen formation (Henrik Semb, unpublished data). The lumens of these animals were collapsed and resembled the ones observed in $EphB2^{LacZ/LacZ}EphB3^{-/-}$ mutant. It will be interesting to test whether forward Eph signaling also plays a role in tight junction formation. To address these questions, the whole array of apical markers (Par3, Par6, cdc42) should be assayed in mutant pancreata. In addition, measurements of mRNA and protein of components of apical complexes should be compared between mutant and wildtype to check whether deregulation of forward *EphB2* signaling directly affects the expression of these proteins. *In vivo* pancreatic explants assays where we assay lumen formation after blockage of EphB signaling by use of soluble ephrinB-Fc ligands would also help elucidate the fundamental molecular mechanism. Another possibility to explain the purpose of *EphB2* apical localization is that it is necessary for endocrine rosette formation (which precedes microlumen formation). We have shown that *EphB2* and *ephrinA5* are co-expressed in pancreatic epithelial cells. Therefore, it is possible that during epithelial remodeling, *EphB2* localizes apically and repulses cells when in contact with *ephrinA5* ligand (we speculate should be expressed basally). This repulsion may re-organize epithelial cells inside the stratified epithelium into a rosette shape. Once cells are aligned, the middle of

the rosette then consolidate their polarity, and the ultimate result is microlumen formation.

Our studies also demonstrated the novel expression of *EphB3* in delaminating endocrine cells. *EphB3* expression is transient, so it is provocative to speculate that as cells start expressing *EphB3*, they interact with adjacent *ephrinB2*-expressing blood vessels and this interaction facilitates delamination. It has been shown that blood vessels and endocrine cells are always in close association (Konstantinova and Lammert, 2004; Nikolova et al., 2006). Immunofluorescence studies showing both receptor and ligand interacting in adjacent cells would support this hypothesis. In addition, analysis of endocrine delamination in animals with disrupted *ephrinB2* (Cowan et al., 2004; Dravis et al., 2004) would help clarify these issues.

Finally, our studies proposed a role of *Eph/ephrinB* signaling in β-cell function. We observed that as *Eph/eprhinA* subclass, *Eph/ephrinB* are expressed in pancreatic islets. Furthermore, we observe that disregulation of *Eph/ephrinB* enhances glucose tolerance, indicating that *Eph/ephrinB* might also play a role in insulin secretion. It was shown by Konstantinova and colleagues that Eph/ephrinA signaling is required for insulin secretion in pancreatic cells. They showed that *EphA* forward signaling inhibited insulin secretion while *ephrin-A* reverse signaling stimulated it (Konstantinova et al., 2007). *EphB2* is known to interact with ephrin-A5 and both are expressed in β-cells in the adult suggesting that *EphB2*/*ephrinA5* might also be involved in insulin secretion in a similar fashion as the one described by Konstantinova, et. al. Further studies will help resolve this possibility.

CONCLUSIONS

Overall, the work presented in this thesis provides a thorough analysis of different aspects of the biology of pancreatic development. We studied and described basic aspects of pancreatic growth such as branching, epithelium remodeling, and cellular polarity. In addition we established an anatomical model that summarizes the features of pancreatic growth. We believe our work is invaluable since it provides both novel observations and the framework for future analysis of pancreatic mutants at both levels: the gross and the cellular. In addition we presented an analysis of previously uncharacterized signaling molecules: the Rgs and the *Eph/ephrinB* in pancreatic development. Our work highlights the importance of both signaling pathways in the pancreas and opens new avenues of research. Future studies of these pathways will provide a better understanding of the organ and will aid in the development of therapies for pancreatic disease.

APPENDIX A

MATERIALS AND METHODS

COMMON METHODS

Mouse embryos

Embryos were collected from pregnant CD1 female mice. Plugging date was designated as embryonic day 0. Embryos were fixed in 4% paraformaldehyde (PFA) in PBS solution overnight at 4°C with gentle rocking. The amnion and body wall were removed during dissection for better probe penetration to the pancreatic anlagen, or alternatively, the entire gut tube of older embryos (E10.5-E14.5) were isolated prior to analysis. Embryos or isolated gut tubes were washed twice in PBS for 10 min at 4°C, and dehydrated using an ethanol series, and stored in 70% ethanol at –20°C.

Sectioning and histology

For paraplast sectioning embryos were dehydrated to 100% ethanol, transferred to xylene and then carried through a series of rinses in 100% Paraplast Plus tissue embedding medium (McCormick) at 60°C. The embryos were then embedded and sectioned with a 2030 Reichert-Jung microtome and mounted on SuperfrostPlus glass slides (Fisher). For examination, sections were deparaffinized in xylene twice for 5 min each and mounted with glass coverslips using Permount (Fisher).

Pdx1-lacZ embryo generation and β-Galactosidase reaction

Pdx1-lacZ embryos were generated by mating *Pdx1*-lacZ heterozygous males (generously provided by Chris Wright, Vanderbilt) and CD1 females. Embryos were collected from pregnant females (E9.5 through E18.5) by dissection and fixed in 4% paraformaldehyde (PFA) in PBS solution for 15 min at room temperature. After fixation, the embryos were rinsed 3 times in PBS for 5 min each. After rinsing the embryos were incubated with lacZ staining solution (20 mM $K_4Fe(CN)_6 \cdot 3H_2O$; 20 mM $K_3Fe(CN)_6$; 2 mM $MgCl_2$; 0.02% NP-40; 400μg X-Gal) overnight, shielded from light, to allow the color reaction to develop. Then, the embryos were washed 3 times with PBS for 5 min each, and transferred to 40% glycerol. Pancreas were photograph using NeoLumar stereomicroscope (Zeiss) and a DP70 camera (Olympus).

Whole mount in situ hybridization and RNA probes

Whole mount in situ hybridization was carried out using a protocol adapted from D. Wilkinson's Method (Wilkinson, 1999). Briefly, embryos stored in 75% EtOH at –20˚C, were rehydrated in stepwise fashion to PBST. Then, the embryos were treated with proteinase K, fixed in a 0.25% gluteraldehyde/4% PFA solution, and pre-hybridized at 60°C for 1 hour. The samples were transferred into hybridization mix, containing either *Ngn3* coding region (539 bp), *Sox9* full-length transcript (2305bp, Clone Image ID 5320371 Open Biosystems). The in situ hybridization steps were carried out using a Biolane HTI automated incubation liquid handler (Holle & Huttner). Development of color reaction was done using BM Purple (Roche). Images were taken using a Lumar dissecting microscope (Zeiss) and a DP-70 camera (Olympus).

CHAPTER 2

Immunofluorescence of pancreatic sections

Paraplast sections were deparafinized in xylene twice for 5 min each and then re-hydrated through a serial of alcohol washes. Then sections were washed 3X 1X PBS and 1X in Ag retrieval Buffer (Buffer B Electron Microscopy Sciences). Ag retrieval was performed in the 2100 Retrivier overnight. Sections were then washed several times with 1X PBS and block with CAS-Blocking (INVITROGEN) for several hours at room temperature. Sections were incubated in primary antibody overnight at 4C. Then, sections were washed and incubated with fluorophore-conjugated secondary antibodies for 2hr. Sections were imaged on a LSM150 Confocal microscopy. The concentrations of primary antibodies used were as follows: rabbit anti-APKC (1:500 Santa Cruz); goat anti β-catenin (1:50 Santa Cruz); mouse anti-E-cadherin (1:200 INVITROGEN); guinea pig anti-Glucagon (1:600 kindly provided by Raymond MacDonald); mouse anti-GM130 (1:500 BD Biosciences); rabbit anti-laminin (1:200 SIGMA); rabbit anti-Par3 (1:500 Invitrogen); goat anti-vimentin (1:50 Santa Cruz) and mouse or rabbit anti-ZO1 (1:50 INVITROGEN). Secondary used were 1:500 alexa 555/ alexa 488/ alexa 633 anti-mouse, goat, or rabbit (INVITROGEN) and FITC anti-guinea pig (VECTOR LABS)

Whole-mount immunofluorescence of pancreatic guts

Pancreatic guts were transferred to 50% methanol for 1hr. After, they were re-hydrated with 1X PBS and permeabilized with 1XPBS AND 1% Triton X100 for 1hr. Then guts were block with CAS-Blocking Reagent (INVITROGEN) for several hours and incubated with primary antibody overnight at 4C. After, guts were rinse several times with 1X PBS and incubate with fluorophore conjugated secondary antibody for a couple of hours. Guts were washed with 1X PBS and dehydrated to 100% methanol. BABB was used for visualization and pictures were taken by using either in LMS150 confocal microscope or in the NeoLumar stereomicroscope (Zeiss).

Detection of apoptosis

ZO-1 antibody staining was performed in our E10.5-E11.5 pancreatic sections as described above, with the exception that we used Buffer A (pH6.0 Electron Microscopy Sciences) for antigen retrieval. After, we carried out the TACS TdT-Fluorescein In situ Apoptosis Detection Kit (R&D Systems) following the manufacter's protocol. The positive control was a TACS-Nuclease-treated slide and the negative control was an unlabeled slide. E11.5 sections were also stained with active caspase (3) (1:50 Millipore) following immunofluorescence protocol describe above with the exception of Buffer A (Electron Microscopy Sciences) for antigen retrieval.

CHAPTER 3

RNA isolation, cDNA synthesis and RT-PCR

Individually dissected pancreata from different developmental stages (n $\geq$4 for each stage) were collected either in RNAlater (Ambion) or flash-frozen in liquid nitrogen for RNA extraction. RNA extraction was performed using an RNeasy Micro Kit (QIAGEN). RNA was converted into cDNA utilizing M-MLV RT (Promega), oligos (IDT DNA) and by following instructions from Promega. cDNA concentration was quantified/normalized by gel band intensity and RT-PCR was carried out on a 2720 Thermal Cycler (Applied Biosystems). The annealing temperature used was 57 °C. Normalization of cDNA amounts was carried out by first analyzing *actin* and *Pdx1* mRNA levels. The following primers were used to identify amount of *Ngn3* transcript present at each stage: *Ngn3*: 5'-AGTCGGGAGAACTAGGATGG-3', 5'-TGGAACTGAGCACTTCGTGG-3' yields 113bp product size (32 cycles), *Pdx1*: 5' GAAATCCACCAAAGCTCACG-3', 5' CCCGCTACTACGTTTCTTATCTTCC-3'yields a 271bp product size (35 cycles), and *Actin*: 5'-GACGGCCAGGTCATCACTAT-3', 5'- AGGGAGACCAAAGCCTTCAT-3' yields a 995bp product size (28 cycles).

Immunofluorescence

For immunofluorescence, sections were de-waxed in xylene; rehydrated via an ethanol series; washed several times in 1xPBS; treated with Antigen Unmasking Solution (Vector Labs); quenched for endogenous peroxidases with 3% H_2O_2; blocked for 1hr at room temperature (RT) with 1% Blocking Reagent (TSA kit); and incubated with 1:4000

mouse anti-NGN3 -AB2013 (Beta Cell Biology Consortium, kindly provided by Dr. Raymond MacDonald) diluted in blocking solution overnight at RT. Signal was detected the following day by incubating the slides with mouse secondary antibody (TSA kit) and DAPI (1:1000). Slides were mounted with ProLong Gold Antifade Reagent (Invitrogen). Images were acquired on a LSM510META (Zeiss) confocal microscope.

NGN3 protein quantification

The entire pancreas from several embryos (n $\geq$3 for each developmental stage) were sectioned (10mm) and processed for NGN3 immunofluorescence. NGN3 positive cells were counted on every section using an Axiovert 200M inverted fluorescence microscope (Zeiss). At each stage, the overall cell number per pancreas were added and averaged. Means and standard deviations were calculated and graphed using Microsoft Excel. Mean differences were tested for statistical significance by using the Student-T test.

Immunohistochemistry

E13.5 pancreatic sections were de-waxed with xylene; rehydrated using decreasing concentrations of ethanol; washed several times in PBS; treated with Antigen Unmasking Solution (Vector Labs); quenched for endogenous peroxidases with 3% H_2O_2 for 45 min; blocked for 1hr at RT with 10% NDS (Sigma); and incubated with 1:3000 mouse anti-NGN3 -AB2013 (Beta cell biology Consortium kindly provided by Raymond MacDonald) diluted in 5% NDS blocking solution overnight at room temperature. Slides were then washed with 1X PBS and incubated with 1:200 Biotin anti-mouse antibody for

1hr and then treated with ABC solution (vectastain system from vector labs) for 15 min at room temperature. Signal was detected utilizing DAB substrate (Vector labs). Images were acquired on an Axiovert 200M inverted fluorescence microscope (Zeiss).

CHAPTER 4

GFP visualization in pancreas from embryos, pups, and adults

Rgs8::eGFP and Rgs16::eGFP BAC transgenic mice were generated by the GENSAT Project (Gong et al., 2003; Morales and Hatten, 2006). Pancreata were collected from Rgs8::eGFP and Rgs16::eGFP embryos (E8.5 through E16.5) and from postnatal stages P0 (birth) to P28. Pups were weaned at P16 for time course studies of Rgs16::eGFP expression post weaning. Tissues were dissected and transferred into ice-cold 1xPBS buffer. GFP visualization was accomplished by removing the embryonic gut tube and isolating the midgut, including the pancreas, stomach and spleen. Tissue fragments were equilibrated in 40% glycerol for viewing. The pancreas was visualized using a Zeiss NeoLumar fluorescent microscope and photographed using an Olympus DP70 camera. Ngn3::eGFP embryos were generated by mating Ngn3::eGFP heterozygous males (generously provided by Klaus Kaestner) with CD1 females. Embryos were dissected at different developmental stages, and pancreata dissected and visualized as described above. Pancreata from adult pregnant females and *ob/ob*;Rgs16::eGFP transgenic mice were treated similarly to embryos, as described above.

Section immunofluorescence

E15.5 dorsal pancreata were dissected from Rgs16::eGFP pregnant females and were fixed overnight in 4% PFA in 1xPBS at 4°C. The next day the tissues were washed several times with 1x PBS, equilibrated in 30% sucrose overnight and embedded in OCT medium (Tissue-Tek). 10µm cryosections of complete pancreata were mounted on SuperfrostPlus slides (Fisher) and immunofluorescence was carried out using: 1:500 chicken antibody specific to GFP (AVES LABS); 1:300 guinea-pig anti-Insulin (DakoCy); 1:1000 Rabbit anti-Glucagon (LINCO); 1:300 Rat anti-CD31 (BD Pharmingen); 1:200 Rabbit anti-Synaptophysin (DakoCy); 1:200 DBA (5µg/µl) (Vector Labs); 1:600 Rabbit anti-Pdx1 and 1:4000 Mouse anti-Ngn3 (Beta Cell Biology Consortium, kindly provided by Dr. Raymond MacDonald). TRITC secondary antibodies were from Jackson ImmunoResearch Laboratories and anti-chicken alexa 488 was from Invitrogen. Slides were counterstained with DAPI and mounted with ProLong Gold Antifade Reagent (Invitrogen). Images were acquired on a LSM510 META Zeiss confocal microscope. Histology and immunofluorescence for PANIC-ATTAC samples were done as previously described (Wang et al., 2008). Briefly, pancreas was fixed in 10% buffered formalin overnight. 5 µm paraffin sections were incubated with guinea pig anti-swine insulin (DAKO, 1:500) and with rabbit anti-GFP (Invitrogen, 1:100). The secondary antibodies used were donkey anti-guinea pig IgG-FITC (Jackson Immunoresearch, 1:250) and donkey anti-rabbit IgG-Cy3 labeled (Jackson Immunoresearch, 1:500). Images were taken on a Leica TCS SP5 confocal microscope (Leica).

Whole mount immunofluorescence

Pancreata were fixed for 1hr in 4%PFA in PBS, washed and dehydrated to 70% ethanol. Embryos were then washed in 50% methanol for 1hr and rinsed twice in 1x PBS. The tissue was permeabilized for 1hr in 1%TritonX100-1X PBS. Block in Cas-Block (Zymed) and immunofluorescence was carried out using: 1:250 chicken antibody specific to GFP (AVES LABS); 1:200 guinea-pig anti-Insulin (DakoCy); Rabbit anti-Glucagon (LINCO); 1:200 Rat anti-CD31 (BD Pharmingen); 1:200 Rabbit anti-Synaptophysin (DakoCy); 1:200 DBA (5µg/µl) (Vector Labs); and 1:1000 Rabbit anti-LYVE. TRITC secondary antibodies were from Jackson ImmunoResearch Laboratories and anti-chicken alexa 488 was from Invitrogen. Tissues were dehydrated, cleared with BABB and visualized using Zeiss NeoLumar fluorescent microscope and photographed using an Olympus DP70 camera or LSM510 META Zeiss confocal microscope.

ob/ob;Rgs8::eGFP and ob/ob;Rgs16::eGFP mice

ob/+ breeders obtained from Jackson Labs. Double heterozygous Rgs16::eGFP;*ob/+* mice were intercrossed to obtain *ob/ob* (36-65g), *ob/ob*;Rgs16::eGFP, and *ob/+;*Rgs16::eGFP mice. Animals were fed ad libitum a standard rodent chow diet (Teklad). Blood was acquired via tail clipping and glucose levels were measured by glucometer (AscensiaElite).

PANIC-ATTAC;Rgs16::eGFP transgenic mice

PANIC-ATTAC transgenic mice were generated as previously described (Wang et al., 2008). Briefly, the rat insulin promoter was used to drive the expression of an

FKBPcaspase 8 fusion protein. A PCR generated fragment containing FKBP caspase 8 and 3' untranslated region was cloned into pCR4TA (Invitrogen) and then subcloned into the promoter vector. The linearized DNA was injected into FVB embryos. Homozygous PANIC-ATTAC animals were crossed to Rgs16::eGFP transgenic mice. All progeny were hemizygous for the PANIC-ATTAC transgene. Animals of about 12 weeks were grouped into hemizygous PANIC ATTAC;Rgs16::GFP transgenic mice (n = 2), hemizygous PANIC-ATTAC;Rgs16::eGFP negative mice (n = 4) and FVB control mice (n = 3). Dimerizer *AP20187* was administered to animals according to the manufacturer recommendations (Ariad Pharmaceuticals). For hemizygous PANIC-ATTAC mice, dimerizer of 0.2 µg/g body weight was injected twice a day at 12 pm and 6 pm every other day for a total of 8 injections. Fed glucose levels were monitored using glucometer and strips (Abbott Diabetes Care). After 8 days treatment, hemizygous PANIC-ATTAC animals showed either moderate (glucose < 300 mg/dL) or severe (glucose > 300 mg/dL) hyperglycemia. Animals were sacrificed two more weeks later and pancreas was processed for immunofluorescence staining.

CHAPTER 5

Mice

The *EphB2* ^{lacZ} , the *ephrinB2* ^{laZ} and the *EphB3* $^{-/-}$ mice has previously been described (Dravis et al., 2004; Henkemeyer et al., 1996; Orioli et al., 1996). The *EphB2* and *EphB3* were maintained on a CD1 background while the *ephrin-B2*^{LacZ} was maintained on mixed 129/CD1 background. The *EphB3* ^{LacZ} mice was obtained by

crossing the BAC-Tg-*EphB3* $^{rtTA/+}$ to TRE-LacZ/+ mice. The BAC-Tg-*EphB3* $^{rtTA/+}$ was created by targeting the second generation reverse tetracycline transactivator, rtTA-2sM2 into the ORF of BAC-*EphB3* (Christropher Dravis and Mark Henkemeyer, unpublished data) and the TRE-Lacz has previously been described in (Ludwig et al., 2004)

Embryo isolation

Embryos were isolated from pregnant *EphB2*$^{LacZ/LacZ}$/*EphB3*$^{-/-}$; *EphB2*$^{LacZ/LacZ}$; *EphB3*$^{-/-}$; or females. The following primers were used to genotype *EphB2*$^{LacZ/LacZ}$ mutant embryos: 5'-CAC AAG TCA TTT TTG CCA CTC TAG-3', 5'-TAA AAC GAC GGG ATC ATC GCG AGC C-3', and 5'-AGC CAT GGT ACC TTG AGG CAT TTG-3' yields 450bp for wildtype and 400bp product size for mutant (35 cycles). For *EphB3*$^{-/-}$ we used the following primers: 5'-GCT CCC GAT TCG CAG CGC ATC G -3', 5'-CCA GCA ACG CCG TGT GAC CTG TG -3', and 5'-ACC AGG GAG CTG GTC TAG GTG GG-3' the wildtype band yields 800bp while the mutant band yields a 550bp (35 cycles). Littermates or CD1 staged matched embryos were used as controls in our studies.

Whole mount in situ hybridization

Probes: *ephrinB1* full-length (~800 bp); *ephrinB2* full-length transcript (900bp); *ephrinB3* cytodomain (~200bp); *EphB1* (4626bp, **BC057301**); *EphB2* exon3 (600bp); *EphB3* exon 3 (600bp); *EphB4* (4270bp, **BE573518**); *EphB6* (3355bp, **BI691963**). The anti-sense DIG-RNA probe for in situs was made by using T3 polymerase for *ephrinB1*, *ephrinB1* and *EphB1* and T7 for the rest of the plasmids. The reagents were mixed in the

following order at room temperature: linearized plasmid (1µg), DIG-RNA labeling mix (Roche) 2.0µl, 10 x transcription buffer (Roche) 2.0µl, Placental ribonuclease inhibitor (Promega) 1.5µl, T3/T7 RNA polymerase (Roche) 1.0µl, Double distilled RNase free water to a final volume of 20µl. The mixture was incubated at 37°C for 2 hours. Add 2µl RQ1 DNase I (Promega), incubate at 37°C for 15 min. The probes were then purified with Micro Bio-spin columns (Bio-RAD). Dilute 10 times to 1 µg/ml as a working solution, keep at –20°C. Whole mount in situ hybridization was carried out as described above.

In situ hybridization in sections

Embryonic sections were de-waxed with xylene; rehydrated using decreasing concentrations of ethanol; washed several times in PBS; and treated with 15 µg/ml proteinase K for 10 min at RT. After, they were rinsed with PBS, re-fixed with 4% PFA for 5min, rinse again with PBS and incubate at 65ºC in hybridization buffer (50% formamide, 5X SSC pH4.5, 50µg/ml yeast tRNA, 1% SDS, 50µg/ml heparin) at RT for 1h. Slides were then transferred to a humidified chamber (humidified with 50% formamide/5 × SSC) for probe hybridization (probe at 1 µg/ml). 100 µl of probe was added per slide, slide was covered with glass coverslip and was incubated at 68 °C overnight. Slides were washed post-hybridization in 5× SSC at 72 °C long enough to allow coverslips to separate. Then slides were rinsed 2× 30 min in 0.2xSSC at 72 °C and 1× 5min in 0.2xSSC at RT, then they were washed in MBST buffer (100 mM Maleic acid, 150 mM NaCl, pH 7.5, 0.1% Tween20) at RT for 5min. Slides were then incubated

in blocking solution (2% blocking reagent (Roche) and 5% heat-inactivated sheep serum in MBST) for 1 h at RT and later incubated overnight at 4°C with anti-Dig alkaline phosphatase conjugated antibody (Roche) in blocking solution (1:4000). After, slides were washed for 3 × 30 min in MBST and treated in NTMT (100 mM NaCl, 100 mM Tris, pH 9.5, 50 mM $MgCl_2$, 0.1% Tween20) for 3 × 5 min. Color reaction was carried out using BM purple as described above. For microscopic examination, slides were sealed and coverslipped using Permount (Fisher).

Immunofluorescence

For immunofluorescence, sections were de-waxed with Xylene; rehydrated using decreasing concentrations of ethanol; washed several times in PBS; submitted to antigen retrieval in the 2100 Retriever, blocked for 2 hr in CAS-Block (Invitrogen) at RT and then incubated with primary antibody diluted in blocking solution overnight at 4°C. (Specific dilutions used can be found in chapter text). Slides were then washed in 1x PBS and signal was detected by incubating the slides at RT for 1hr with fluorophore-conjugated antibodies (Jackson ImmunoResearch). Slides were mounted using ProLong Gold with DAPI (Invitrogen). Images were acquired on a LSM510 META confocal microscope.

Table 1. List of Antibodies used in this study

Antigen	Species	Source	Dilution	Type
Amylase	Rabbit	Sigma, A8273	1:1000	Paraffin
APKC	Rabbit	Santa Cruz,sc-216	1:500	Paraffin
β-Catenin	Goat	Santa Cruz,sc1496-R	1:50-1:100	Paraffin
β-Galoctasidase	Rabbit	Cappel, 55976	1:1000	Paraffin
E-cadherin	Mouse	Invitrogen, 33-4000	1:200	Paraffin
E-cadherin	Rat	Sigma, U3254	1:1000	Frozen
Glucagon	Rabbit	Linco,4030-01F	1:300	Paraffin
Insulin	Guinea Pig	DakoCy, A0564	1:300	Paraffin
Laminin	Rabbit	Sigma, L9393	1:1000 or 1:300	Frozen- Paraffin
Muc1	Hamnster Armenian	Thermo Scientific, HM-1630	1:500	Paraffin
Ngn3	Mouse	BCBC, 2013	1:4000	Paraffin
Pdx-1	Rabbit	Gift from Raymond MacDonald	1:600	Paraffin
PECAM	Rat	BD Pharmingen, 550274	1:300	Frozen
Sox9	Rabbit	Gift from Michael Wegner	1:300	Paraffin
Synaphtophysin	Rabbit	DakoCy, A0010	1:300	Paraffin
ZO-1	Mouse	Invitrogen, 33-9100	1:50	Paraffin
ZO-1	Rabbit	Zymed, 40-2200	1:50	Paraffin

Antibodies wre used at the stated dilution on paraffin or frozen pancreatic sections

Glucose tolerance test

Mice were fast for 16hrs by removing the food of their cage but leaving access to drinking water. The next day, mice were weighted and blood was collected from the tail (glucose baseline levels). Animals were then injected with 2g/Kg of body weight of glucose solution (20% D-glucose). Blood was collected from tail every 30 min into a Microvette CB300 K2E (Sarstedt). Glucose was measured by using the autokit Glucose (Wako) and SpectraMax (molecular Devices)

Bibliography

Affolter, M., Bellusci, S., Itoh, N., Shilo, B., Thiery, J. P. and Werb, Z. (2003). Tube or not tube: remodeling epithelial tissues by branching morphogenesis. *Dev Cell* **4**, 11-8.

Ahlgren, U., Jonsson, J., Jonsson, L., Simu, K. and Edlund, H. (1998). beta-cell-specific inactivation of the mouse Ipf1/Pdx1 gene results in loss of the beta-cell phenotype and maturity onset diabetes. *Genes Dev* **12**, 1763-8.

Ahlgren, U., Pfaff, S. L., Jessell, T. M., Edlund, T. and Edlund, H. (1997). Independent requirement for ISL1 in formation of pancreatic mesenchyme and islet cells. *Nature* **385**, 257-60.

Altick, A. L., Dravis, C., Bowdler, T., Henkemeyer, M. and Mastick, G. S. (2005). EphB receptor tyrosine kinases control morphological development of the ventral midbrain. *Mech Dev* **122**, 501-12.

Apelqvist, A., Li, H., Sommer, L., Beatus, P., Anderson, D. J., Honjo, T., Hrabe de Angelis, M., Lendahl, U. and Edlund, H. (1999). Notch signalling controls pancreatic cell differentiation. *Nature* **400**, 877-81.

Artner, I., Blanchi, B., Raum, J. C., Guo, M., Kaneko, T., Cordes, S., Sieweke, M. and Stein, R. (2007). MafB is required for islet beta cell maturation. *Proc Natl Acad Sci U S A* **104**, 3853-8.

Attali, M., Stetsyuk, V., Basmaciogullari, A., Aiello, V., Zanta-Boussif, M. A., Duvillie, B. and Scharfmann, R. (2007). Control of beta-cell differentiation by the pancreatic mesenchyme. *Diabetes* **56**, 1248-58.

Batlle, E., Henderson, J. T., Beghtel, H., van den Born, M. M., Sancho, E., Huls, G., Meeldijk, J., Robertson, J., van de Wetering, M., Pawson, T. et al. (2002). Beta-catenin and TCF mediate cell positioning in the intestinal epithelium by controlling the expression of EphB/ephrinB. *Cell* **111**, 251-63.

Beaupain, D. and Dieterlen-Lievre, F. (1974). [An immunocytological study of differentiation of the endocrine pancreas of the chick embryo. II. Glucagon]. *Gen Comp Endocrinol* **23**, 421-31.

Berman, D. M., Wilkie, T. M. and Gilman, A. G. (1996). GAIP and RGS4 are GTPase-activating proteins for the Gi subfamily of G protein alpha subunits. *Cell* **86**, 445-52.

Bhushan, A., Itoh, N., Kato, S., Thiery, J. P., Czernichow, P., Bellusci, S. and Scharfmann, R. (2001). Fgf10 is essential for maintaining the proliferative capacity of epithelial progenitor cells during early pancreatic organogenesis. *Development* **128**, 5109-17.

Bonal, C. and Herrera, P. L. (2008). Genes controlling pancreas ontogeny. *Int J Dev Biol* **52**, 823-35.

Bonner-Weir, S., Inada, A., Yatoh, S., Li, W. C., Aye, T., Toschi, E. and Sharma, A. (2008). Transdifferentiation of pancreatic ductal cells to endocrine beta-cells. *Biochem Soc Trans* **36**, 353-6.

Bonner-Weir, S., Toschi, E., Inada, A., Reitz, P., Fonseca, S. Y., Aye, T. and Sharma, A. (2004). The pancreatic ductal epithelium serves as a potential pool of progenitor cells. *Pediatr Diabetes* **5 Suppl 2**, 16-22.

Bryant, D. M. and Mostov, K. E. (2008). From cells to organs: building polarized tissue. *Nat Rev Mol Cell Biol* **9**, 887-901.

Burlison, J. S., Long, Q., Fujitani, Y., Wright, C. V. and Magnuson, M. A. (2008). Pdx-1 and Ptf1a concurrently determine fate specification of pancreatic multipotent progenitor cells. *Dev Biol* **316**, 74-86.

Cheng, H. J., Nakamoto, M., Bergemann, A. D. and Flanagan, J. G. (1995). Complementary gradients in expression and binding of ELF-1 and Mek4 in development of the topographic retinotectal projection map. *Cell* **82**, 371-81.

Chu, Z. L., Jones, R. M., He, H., Carroll, C., Gutierrez, V., Lucman, A., Moloney, M., Gao, H., Mondala, H., Bagnol, D. et al. (2007). A role for beta-cell-expressed G protein-coupled receptor 119 in glycemic control by enhancing glucose-dependent insulin release. *Endocrinology* **148**, 2601-9.

Chua, S., Jr., Liu, S. M., Li, Q., Yang, L., Thassanapaff, V. T. and Fisher, P. (2002). Differential beta cell responses to hyperglycaemia and insulin resistance in two novel congenic strains of diabetes (FVB- Lepr (db)) and obese (DBA- Lep (ob)) mice. *Diabetologia* **45**, 976-90.

Cleaver, O., Melton, D.A. (2004). Development of the Endocrine Pancreas.

Cleaver, O. and R. J. MacDonald (2009). Developmental Molecular Biology of the Pancreas. New York, Springer.

Collombat, P., Hecksher-Sorensen, J., Serup, P. and Mansouri, A. (2006). Specifying pancreatic endocrine cell fates. *Mech Dev* **123**, 501-12.

Costantini, F. (2006). Renal branching morphogenesis: concepts, questions, and recent advances. *Differentiation* **74**, 402-21.

Cowan, C. A. and Henkemeyer, M. (2002). Ephrins in reverse, park and drive. *Trends Cell Biol* **12**, 339-46.

Cowan, C. A., Yokoyama, N., Saxena, A., Chumley, M. J., Silvany, R. E., Baker, L. A., Srivastava, D. and Henkemeyer, M. (2004). Ephrin-B2 reverse signaling is required for axon pathfinding and cardiac valve formation but not early vascular development. *Dev Biol* **271**, 263-71.

Cutler, L. S. and Mooradian, B. A. (1987). Lumen formation during development of the rat submandibular gland. *J Dent Res* **66**, 1559-62.

D'Amour, K. A., Agulnick, A. D., Eliazer, S., Kelly, O. G., Kroon, E. and Baetge, E. E. (2005). Efficient differentiation of human embryonic stem cells to definitive endoderm. *Nat Biotechnol* **23**, 1534-41.

D'Amour, K. A., Bang, A. G., Eliazer, S., Kelly, O. G., Agulnick, A. D., Smart, N. G., Moorman, M. A., Kroon, E., Carpenter, M. K. and Baetge, E. E. (2006). Production of pancreatic hormone-expressing endocrine cells from human embryonic stem cells. *Nat Biotechnol* **24**, 1392-401.

Deutsch, G., Jung, J., Zheng, M., Lora, J. and Zaret, K. S. (2001). A bipotential precursor population for pancreas and liver within the embryonic endoderm. *Development* **128**, 871-81.

Dohlman, H. G., Song, J., Ma, D., Courchesne, W. E. and Thorner, J. (1996). Sst2, a negative regulator of pheromone signaling in the yeast Saccharomyces cerevisiae: expression, localization, and genetic interaction and physical association with Gpa1 (the G-protein alpha subunit). *Mol Cell Biol* **16**, 5194-209.

Dor, Y., Brown, J., Martinez, O. I. and Melton, D. A. (2004). Adult pancreatic beta-cells are formed by self-duplication rather than stem-cell differentiation. *Nature* **429**, 41-6.

Dravis, C., Yokoyama, N., Chumley, M. J., Cowan, C. A., Silvany, R. E., Shay, J., Baker, L. A. and Henkemeyer, M. (2004). Bidirectional signaling mediated by ephrin-B2 and EphB2 controls urorectal development. *Dev Biol* **271**, 272-90.

Drescher, U., Kremoser, C., Handwerker, C., Loschinger, J., Noda, M. and Bonhoeffer, F. (1995). In vitro guidance of retinal ganglion cell axons by RAGS, a 25 kDa tectal protein related to ligands for Eph receptor tyrosine kinases. *Cell* **82**, 359-70.

Duvillie, B., Attali, M., Bounacer, A., Ravassard, P., Basmaciogullari, A. and Scharfmann, R. (2006). The mesenchyme controls the timing of pancreatic beta-cell differentiation. *Diabetes* **55**, 582-9.

Edlund, H. (2002). Pancreatic organogenesis--developmental mechanisms and implications for therapy. *Nat Rev Genet* **3**, 524-32.

Egea, J. and Klein, R. (2007). Bidirectional Eph-ephrin signaling during axon guidance. *Trends Cell Biol* **17**, 230-8.

Elghazi, L., Cras-Meneur, C., Czernichow, P. and Scharfmann, R. (2002). Role for FGFR2IIIb-mediated signals in controlling pancreatic endocrine progenitor cell proliferation. *Proc Natl Acad Sci U S A* **99**, 3884-9.

Esni, F., Johansson, B. R., Radice, G. L. and Semb, H. (2001). Dorsal pancreas agenesis in N-cadherin- deficient mice. *Dev Biol* **238**, 202-12.

Frise, E., Knoblich, J. A., Younger-Shepherd, S., Jan, L. Y. and Jan, Y. N. (1996). The Drosophila Numb protein inhibits signaling of the Notch receptor during cell-cell interaction in sensory organ lineage. *Proc Natl Acad Sci U S A* **93**, 11925-32.

Frisen, J., Holmberg, J. and Barbacid, M. (1999). Ephrins and their Eph receptors: multitalented directors of embryonic development. *EMBO J* **18**, 5159-65.

Frisen, J., Yates, P. A., McLaughlin, T., Friedman, G. C., O'Leary, D. D. and Barbacid, M. (1998). Ephrin-A5 (AL-1/RAGS) is essential for proper retinal axon guidance and topographic mapping in the mammalian visual system. *Neuron* **20**, 235-43.

Fujitani, Y., Fujitani, S., Boyer, D. F., Gannon, M., Kawaguchi, Y., Ray, M., Shiota, M., Stein, R. W., Magnuson, M. A. and Wright, C. V. (2006). Targeted deletion of a cis-regulatory region reveals differential gene dosage requirements for Pdx1 in foregut organ differentiation and pancreas formation. *Genes Dev* **20**, 253-66.

Gale, N. W., Holland, S. J., Valenzuela, D. M., Flenniken, A., Pan, L., Ryan, T. E., Henkemeyer, M., Strebhardt, K., Hirai, H., Wilkinson, D. G. et al. (1996). Eph receptors and ligands comprise two major specificity subclasses and are reciprocally compartmentalized during embryogenesis. *Neuron* **17**, 9-19.

Gale, N. W. and Yancopoulos, G. D. (1999). Growth factors acting via endothelial cell-specific receptor tyrosine kinases: VEGFs, angiopoietins, and ephrins in vascular development. *Genes Dev* **13**, 1055-66.

Gittes, G. K. and Rutter, W. J. (1992). Onset of cell-specific gene expression in the developing mouse pancreas. *Proc Natl Acad Sci U S A* **89**, 1128-32.

Golosow, N. and Grobstein, C. (1962). Epitheliomesenchymal interaction in pancreatic morphogenesis. *Dev Biol* **4**, 242-55.

Gong, S., Zheng, C., Doughty, M. L., Losos, K., Didkovsky, N., Schambra, U. B., Nowak, N. J., Joyner, A., Leblanc, G., Hatten, M. E. et al. (2003). A gene expression atlas of the central nervous system based on bacterial artificial chromosomes. *Nature* **425**, 917-25.

Gradwohl, G., Dierich, A., LeMeur, M. and Guillemot, F. (2000). neurogenin3 is required for the development of the four endocrine cell lineages of the pancreas. *Proc Natl Acad Sci U S A* **97**, 1607-11.

Grapin-Botton, A., Majithia, A. R. and Melton, D. A. (2001). Key events of pancreas formation are triggered in gut endoderm by ectopic expression of pancreatic regulatory genes. *Genes Dev* **15**, 444-54.

Gu, G., Dubauskaite, J. and Melton, D. A. (2002). Direct evidence for the pancreatic lineage: NGN3+ cells are islet progenitors and are distinct from duct progenitors. *Development* **129**, 2447-57.

Gu, G., Wells, J. M., Dombkowski, D., Preffer, F., Aronow, B. and Melton, D. A. (2004). Global expression analysis of gene regulatory pathways during endocrine pancreatic development. *Development* **131**, 165-79.

Gupta, R. K., Gao, N., Gorski, R. K., White, P., Hardy, O. T., Rafiq, K., Brestelli, J. E., Chen, G., Stoeckert, C. J., Jr. and Kaestner, K. H. (2007). Expansion of adult beta-cell mass in response to increased metabolic demand is dependent on HNF-4alpha. *Genes Dev* **21**, 756-69.

Guz, Y., Montminy, M. R., Stein, R., Leonard, J., Gamer, L. W., Wright, C. V. and Teitelman, G. (1995). Expression of murine STF-1, a putative insulin gene transcription factor, in beta cells of pancreas, duodenal epithelium and pancreatic exocrine and endocrine progenitors during ontogeny. *Development* **121**, 11-8.

Hale, M. A., Kagami, H., Shi, L., Holland, A. M., Elsasser, H. P., Hammer, R. E. and MacDonald, R. J. (2005). The homeodomain protein PDX1 is required at mid-pancreatic development for the formation of the exocrine pancreas. *Dev Biol* **286**, 225-37.

Harada, N., Tamai, Y., Ishikawa, T., Sauer, B., Takaku, K., Oshima, M. and Taketo, M. M. (1999). Intestinal polyposis in mice with a dominant stable mutation of the beta-catenin gene. *EMBO J* **18**, 5931-42.

Hebrok, M., Kim, S. K. and Melton, D. A. (1998). Notochord repression of endodermal Sonic hedgehog permits pancreas development. *Genes Dev* **12**, 1705-13.

Hecksher-Sorensen, J., Watson, R. P., Lettice, L. A., Serup, P., Eley, L., De Angelis, C., Ahlgren, U. and Hill, R. E. (2004). The splanchnic mesodermal plate directs spleen and pancreatic laterality, and is regulated by Bapx1/Nkx3.2. *Development* **131**, 4665-75.

Henkemeyer, M., Orioli, D., Henderson, J. T., Saxton, T. M., Roder, J., Pawson, T. and Klein, R. (1996). Nuk controls pathfinding of commissural axons in the mammalian central nervous system. *Cell* **86**, 35-46.

Henseleit, K. D., Nelson, S. B., Kuhlbrodt, K., Hennings, J. C., Ericson, J. and Sander, M. (2005). NKX6 transcription factor activity is required for alpha- and beta-cell development in the pancreas. *Development* **132**, 3139-49.

Herrera, P. L. (2000). Adult insulin- and glucagon-producing cells differentiate from two independent cell lineages. *Development* **127**, 2317-22.

Hieda, Y., Iwai, K., Morita, T. and Nakanishi, Y. (1996). Mouse embryonic submandibular gland epithelium loses its tissue integrity during early branching morphogenesis. *Dev Dyn* **207**, 395-403.

Himanen, J. P., Henkemeyer, M. and Nikolov, D. B. (1998). Crystal structure of the ligand-binding domain of the receptor tyrosine kinase EphB2. *Nature* **396**, 486-91.

Hindges, R., McLaughlin, T., Genoud, N., Henkemeyer, M. and O'Leary, D. D. (2002). EphB forward signaling controls directional branch extension and arborization required for dorsal-ventral retinotopic mapping. *Neuron* **35**, 475-87.

Hogan, B. L. and Kolodziej, P. A. (2002). Organogenesis: molecular mechanisms of tubulogenesis. *Nat Rev Genet* **3**, 513-23.

Hogg, N. A., Harrison, C. J. and Tickle, C. (1983). Lumen formation in the developing mouse mammary gland. *J Embryol Exp Morphol* **73**, 39-57.

Holmberg, J. and Frisen, J. (2002). Ephrins are not only unattractive. *Trends Neurosci* **25**, 239-43.

Holmberg, J., Genander, M., Halford, M. M., Anneren, C., Sondell, M., Chumley, M. J., Silvany, R. E., Henkemeyer, M. and Frisen, J. (2006). EphB receptors coordinate migration and proliferation in the intestinal stem cell niche. *Cell* **125**, 1151-63.

Horne-Badovinac, S., Lin, D., Waldron, S., Schwarz, M., Mbamalu, G., Pawson, T., Jan, Y., Stainier, D. Y. and Abdelilah-Seyfried, S. (2001). Positional cloning of heart and soul reveals multiple roles for PKC lambda in zebrafish organogenesis. *Curr Biol* **11**, 1492-502.

Huang, H. P., Liu, M., El-Hodiri, H. M., Chu, K., Jamrich, M. and Tsai, M. J. (2000). Regulation of the pancreatic islet-specific gene BETA2 (neuroD) by neurogenin 3. *Mol Cell Biol* **20**, 3292-307.

Huang, J., Pashkov, V., Kurrasch, D. M., Yu, K., Gold, S. J. and Wilkie, T. M. (2006). Feeding and fasting controls liver expression of a regulator of G protein signaling (Rgs16) in periportal hepatocytes. *Comp Hepatol* **5**, 8.

Humphreys, R. C., Krajewska, M., Krnacik, S., Jaeger, R., Weiher, H., Krajewski, S., Reed, J. C. and Rosen, J. M. (1996). Apoptosis in the terminal endbud of the murine mammary gland: a mechanism of ductal morphogenesis. *Development* **122**, 4013-22.

Inada, A., Nienaber, C. and Bonner-Weir, S. (2006). Endogenous beta-galactosidase expression in murine pancreatic islets. *Diabetologia* **49**, 1120-2.

Jaskoll, T. and Melnick, M. (1999). Submandibular gland morphogenesis: stage-specific expression of TGF-alpha/EGF, IGF, TGF-beta, TNF, and IL-6 signal transduction in normal embryonic mice and the phenotypic effects of TGF-beta2, TGF-beta3, and EGF-r null mutations. *Anat Rec* **256**, 252-68.

Jensen, J. (2004). Gene regulatory factors in pancreatic development. *Dev Dyn* **229**, 176-200.

Johansson, K. A., Dursun, U., Jordan, N., Gu, G., Beermann, F., Gradwohl, G. and Grapin-Botton, A. (2007). Temporal control of neurogenin3 activity in pancreas progenitors reveals competence windows for the generation of different endocrine cell types. *Dev Cell* **12**, 457-65.

Jonsson, J., Carlsson, L., Edlund, T. and Edlund, H. (1994). Insulin-promoter-factor 1 is required for pancreas development in mice. *Nature* **371**, 606-9.

Jorgensen, M. C., Ahnfelt-Ronne, J., Hald, J., Madsen, O. D., Serup, P. and Hecksher-Sorensen, J. (2007). An illustrated review of early pancreas development in the mouse. *Endocr Rev* **28**, 685-705.

Karnik, S. K., Chen, H., McLean, G. W., Heit, J. J., Gu, X., Zhang, A. Y., Fontaine, M., Yen, M. H. and Kim, S. K. (2007). Menin controls growth of pancreatic beta-cells in pregnant mice and promotes gestational diabetes mellitus. *Science* **318**, 806-9.

Kaufman, M. H. (1992). Atlas of Mouse Development. San Diego, CA USA: Elsevier Academic Press.

Keller, M. P., Choi, Y., Wang, P., Davis, D. B., Rabaglia, M. E., Oler, A. T., Stapleton, D. S., Argmann, C., Schueler, K. L., Edwards, S. et al. (2008). A gene expression network model of type 2 diabetes links cell cycle regulation in islets with diabetes susceptibility. *Genome Res* **18**, 706-16.

Kim, M., Datta, A., Brakeman, P., Yu, W. and Mostov, K. E. (2007). Polarity proteins PAR6 and aPKC regulate cell death through GSK-3beta in 3D epithelial morphogenesis. *J Cell Sci* **120**, 2309-17.

Kim, S. K., Hebrok, M. and Melton, D. A. (1997a). Notochord to endoderm signaling is required for pancreas development. *Development* **124**, 4243-52.

Kim, S. K., Hebrok, M. and Melton, D. A. (1997b). Pancreas development in the chick embryo. *Cold Spring Harb Symp Quant Biol* **62**, 377-83.

Kim, S. K. and MacDonald, R. J. (2002). Signaling and transcriptional control of pancreatic organogenesis. *Curr Opin Genet Dev* **12**, 540-7.

Kim, S. K. and Melton, D. A. (1998). Pancreas development is promoted by cyclopamine, a hedgehog signaling inhibitor. *Proc Natl Acad Sci U S A* **95**, 13036-41.

Kodama, S., Toyonaga, T., Kondo, T., Matsumoto, K., Tsuruzoe, K., Kawashima, J., Goto, H., Kume, K., Kume, S., Sakakida, M. et al. (2005). Enhanced expression of PDX-1 and Ngn3 by exendin-4 during beta cell regeneration in STZ-treated mice. *Biochem Biophys Res Commun* **327**, 1170-8.

Konstantinova, I. and Lammert, E. (2004). Microvascular development: learning from pancreatic islets. *Bioessays* **26**, 1069-75.

Konstantinova, I., Nikolova, G., Ohara-Imaizumi, M., Meda, P., Kucera, T., Zarbalis, K., Wurst, W., Nagamatsu, S. and Lammert, E. (2007). EphA-Ephrin-A-mediated beta cell communication regulates insulin secretion from pancreatic islets. *Cell* **129**, 359-70.

Kroon, E., Martinson, L. A., Kadoya, K., Bang, A. G., Kelly, O. G., Eliazer, S., Young, H., Richardson, M., Smart, N. G., Cunningham, J. et al. (2008). Pancreatic endoderm derived from human embryonic stem cells generates glucose-responsive insulin-secreting cells in vivo. *Nat Biotechnol* **26**, 443-52.

Kullander, K. and Klein, R. (2002). Mechanisms and functions of Eph and ephrin signalling. *Nat Rev Mol Cell Biol* **3**, 475-86.

Kumar, M., Jordan, N., Melton, D. and Grapin-Botton, A. (2003). Signals from lateral plate mesoderm instruct endoderm toward a pancreatic fate. *Dev Biol* **259**, 109-22.

Lammert, E., Cleaver, O. and Melton, D. (2001). Induction of pancreatic differentiation by signals from blood vessels. *Science* **294**, 564-7.

Lammert, E., Cleaver, O. and Melton, D. (2003). Role of endothelial cells in early pancreas and liver development. *Mech Dev* **120**, 59-64.

Lee, C. S., De Leon, D. D., Kaestner, K. H. and Stoffers, D. A. (2006). Regeneration of pancreatic islets after partial pancreatectomy in mice does not involve the reactivation of neurogenin-3. *Diabetes* **55**, 269-72.

Lee, C. S., Perreault, N., Brestelli, J. E. and Kaestner, K. H. (2002). Neurogenin 3 is essential for the proper specification of gastric enteroendocrine cells and the maintenance of gastric epithelial cell identity. *Genes Dev* **16**, 1488-97.

Lee, H. S., Nishanian, T. G., Mood, K., Bong, Y. S. and Daar, I. O. (2008). EphrinB1 controls cell-cell junctions through the Par polarity complex. *Nat Cell Biol* **10**, 979-86.

Lee, J. C., Smith, S. B., Watada, H., Lin, J., Scheel, D., Wang, J., Mirmira, R. G. and German, M. S. (2001). Regulation of the pancreatic pro-endocrine gene neurogenin3. *Diabetes* **50**, 928-36.

Li, H., Arber, S., Jessell, T. M. and Edlund, H. (1999). Selective agenesis of the dorsal pancreas in mice lacking homeobox gene Hlxb9. *Nat Genet* **23**, 67-70.

Li, H. and Edlund, H. (2001). Persistent expression of Hlxb9 in the pancreatic epithelium impairs pancreatic development. *Dev Biol* **240**, 247-53.

Lioubinski, O., Muller, M., Wegner, M. and Sander, M. (2003). Expression of Sox transcription factors in the developing mouse pancreas. *Dev Dyn* **227**, 402-8.

Ludwig, A., Schlierf, B., Schardt, A., Nave, K. A. and Wegner, M. (2004). Sox10-rtTA mouse line for tetracycline-inducible expression of transgenes in neural crest cells and oligodendrocytes. *Genesis* **40**, 171-5.

Mailleux, A. A., Overholtzer, M. and Brugge, J. S. (2008). Lumen formation during mammary epithelial morphogenesis: insights from in vitro and in vivo models. *Cell Cycle* **7**, 57-62.

Mailleux, A. A., Overholtzer, M., Schmelzle, T., Bouillet, P., Strasser, A. and Brugge, J. S. (2007). BIM regulates apoptosis during mammary ductal morphogenesis, and its absence reveals alternative cell death mechanisms. *Dev Cell* **12**, 221-34.

Metzger, R. J., Klein, O. D., Martin, G. R. and Krasnow, M. A. (2008). The branching programme of mouse lung development. *Nature* **453**, 745-50.

Morales, D. and Hatten, M. E. (2006). Molecular markers of neuronal progenitors in the embryonic cerebellar anlage. *J Neurosci* **26**, 12226-36.

Murai, K. K. and Pasquale, E. B. (2003). 'Eph'ective signaling: forward, reverse and crosstalk. *J Cell Sci* **116**, 2823-32.

Murtaugh, L. C. (2007). Pancreas and beta-cell development: from the actual to the possible. *Development* **134**, 427-38.

Nanba, D., Hieda, Y. and Nakanishi, Y. (2000). Remodeling of desmosomal and hemidesmosomal adhesion systems during early morphogenesis of mouse pelage hair follicles. *J Invest Dermatol* **114**, 171-7.

Nanba, D., Nakanishi, Y. and Hieda, Y. (2001). Changes in adhesive properties of epithelial cells during early morphogenesis of the mammary gland. *Dev Growth Differ* **43**, 535-44.

Nikolova, G., Jabs, N., Konstantinova, I., Domogatskaya, A., Tryggvason, K., Sorokin, L., Fassler, R., Gu, G., Gerber, H. P., Ferrara, N. et al. (2006). The vascular basement membrane: a niche for insulin gene expression and Beta cell proliferation. *Dev Cell* **10**, 397-405.

Nir, T., Melton, D. A. and Dor, Y. (2007). Recovery from diabetes in mice by beta cell regeneration. *J Clin Invest* **117**, 2553-61.

Nishimura, W., Kondo, T., Salameh, T., El Khattabi, I., Dodge, R., Bonner-Weir, S. and Sharma, A. (2006). A switch from MafB to MafA expression accompanies differentiation to pancreatic beta-cells. *Dev Biol* **293**, 526-39.

Nolan, C. J., Leahy, J. L., Delghingaro-Augusto, V., Moibi, J., Soni, K., Peyot, M. L., Fortier, M., Guay, C., Lamontagne, J., Barbeau, A. et al. (2006). Beta cell compensation for insulin resistance in Zucker fatty rats: increased lipolysis and fatty acid signalling. *Diabetologia* **49**, 2120-30.

Offield, M. F., Jetton, T. L., Labosky, P. A., Ray, M., Stein, R. W., Magnuson, M. A., Hogan, B. L. and Wright, C. V. (1996). PDX-1 is required for pancreatic outgrowth and differentiation of the rostral duodenum. *Development* **122**, 983-95.

Ohlsson, H., Karlsson, K. and Edlund, T. (1993). IPF1, a homeodomain-containing transactivator of the insulin gene. *EMBO J* **12**, 4251-9.

Oliver-Krasinski, J. M. and Stoffers, D. A. (2008). On the origin of the beta cell. *Genes Dev* **22**, 1998-2021.

Orioli, D., Henkemeyer, M., Lemke, G., Klein, R. and Pawson, T. (1996). Sek4 and Nuk receptors cooperate in guidance of commissural axons and in palate formation. *EMBO J* **15**, 6035-49.

Park, S., Frisen, J. and Barbacid, M. (1997). Aberrant axonal projections in mice lacking EphA8 (Eek) tyrosine protein kinase receptors. *EMBO J* **16**, 3106-14.

Pasquale, E. B. (2005). Eph receptor signalling casts a wide net on cell behaviour. *Nat Rev Mol Cell Biol* **6**, 462-75.

Patel, V. N., Rebustini, I. T. and Hoffman, M. P. (2006). Salivary gland branching morphogenesis. *Differentiation* **74**, 349-64.

Pictet, R. L., Clark, W. R., Williams, R. H. and Rutter, W. J. (1972). An ultrastructural analysis of the developing embryonic pancreas. *Dev Biol* **29**, 436-67.

Prentki, M. and Nolan, C. J. (2006). Islet beta cell failure in type 2 diabetes. *J Clin Invest* **116**, 1802-12.

Puri, S. and Hebrok, M. (2007). Dynamics of embryonic pancreas development using real-time imaging. *Dev Biol* **306**, 82-93.

Risley, M., Garrod, D., Henkemeyer, M. and McLean, W. (2009). EphB2 and EphB3 forward signalling are required for palate development. *Mech Dev* **126**, 230-9.

Ross, E. M. and Wilkie, T. M. (2000). GTPase-activating proteins for heterotrimeric G proteins: regulators of G protein signaling (RGS) and RGS-like proteins. *Annu Rev Biochem* **69**, 795-827.

Rukstalis, J. M. and Habener, J. F. (2007). Snail2, a mediator of epithelial-mesenchymal transitions, expressed in progenitor cells of the developing endocrine pancreas. *Gene Expr Patterns* **7**, 471-9.

Sander, M. and German, M. S. (1997). The beta cell transcription factors and development of the pancreas. *J Mol Med* **75**, 327-40.

Sander, M., Sussel, L., Conners, J., Scheel, D., Kalamaras, J., Dela Cruz, F., Schwitzgebel, V., Hayes-Jordan, A. and German, M. (2000). Homeobox gene Nkx6.1 lies downstream of Nkx2.2 in the major pathway of beta-cell formation in the pancreas. *Development* **127**, 5533-40.

Scharfmann, R. (2000). Control of early development of the pancreas in rodents and humans: implications of signals from the mesenchyme. *Diabetologia* **43**, 1083-92.

Schonhoff, S. E., Giel-Moloney, M. and Leiter, A. B. (2004). Neurogenin 3-expressing progenitor cells in the gastrointestinal tract differentiate into both endocrine and non-endocrine cell types. *Dev Biol* **270**, 443-54.

Schwitzgebel, V. M., Scheel, D. W., Conners, J. R., Kalamaras, J., Lee, J. E., Anderson, D. J., Sussel, L., Johnson, J. D. and German, M. S. (2000). Expression of neurogenin3 reveals an islet cell precursor population in the pancreas. *Development* **127**, 3533-42.

Seymour, P. A., Freude, K. K., Dubois, C. L., Shih, H. P., Patel, N. A. and Sander, M. (2008). A dosage-dependent requirement for Sox9 in pancreatic endocrine cell formation. *Dev Biol* **323**, 19-30.

Seymour, P. A., Freude, K. K., Tran, M. N., Mayes, E. E., Jensen, J., Kist, R., Scherer, G. and Sander, M. (2007). SOX9 is required for maintenance of the pancreatic progenitor cell pool. *Proc Natl Acad Sci U S A* **104**, 1865-70.

Sherry, N. A., Chen, W., Kushner, J. A., Glandt, M., Tang, Q., Tsai, S., Santamaria, P., Bluestone, J. A., Brillantes, A. M. and Herold, K. C. (2007). Exendin-4 improves reversal of diabetes in NOD mice treated with anti-CD3 monoclonal antibody by enhancing recovery of beta-cells. *Endocrinology* **148**, 5136-44.

Slack, J. M. (1995). Developmental biology of the pancreas. *Development* **121**, 1569-80.

Sommer, L., Ma, Q. and Anderson, D. J. (1996). neurogenins, a novel family of atonal-related bHLH transcription factors, are putative mammalian neuronal determination genes that reveal progenitor cell heterogeneity in the developing CNS and PNS. *Mol Cell Neurosci* **8**, 221-41.

Spooner, B. S., Walther, B. T. and Rutter, W. J. (1970). The development of the dorsal and ventral mammalian pancreas in vivo and in vitro. *J Cell Biol* **47**, 235-46.

Stanger, B. Z., Tanaka, A. J. and Melton, D. A. (2007). Organ size is limited by the number of embryonic progenitor cells in the pancreas but not the liver. *Nature* **445**, 886-91.

Stefan, Y., Orci, L., Malaisse-Lagae, F., Perrelet, A., Patel, Y. and Unger, R. H. (1982). Quantitation of endocrine cell content in the pancreas of nondiabetic and diabetic humans. *Diabetes* **31**, 694-700.

Sussel, L., Kalamaras, J., Hartigan-O'Connor, D. J., Meneses, J. J., Pedersen, R. A., Rubenstein, J. L. and German, M. S. (1998). Mice lacking the homeodomain transcription factor Nkx2.2 have diabetes due to arrested differentiation of pancreatic beta cells. *Development* **125**, 2213-21.

Swift, M. R. and Weinstein, B. M. (2009). Arterial-venous specification during development. *Circ Res* **104**, 576-88.

Teta, M., Rankin, M. M., Long, S. Y., Stein, G. M. and Kushner, J. A. (2007). Growth and regeneration of adult beta cells does not involve specialized progenitors. *Dev Cell* **12**, 817-26.

Tourrel, C., Bailbe, D., Meile, M. J., Kergoat, M. and Portha, B. (2001). Glucagon-like peptide-1 and exendin-4 stimulate beta-cell neogenesis in streptozotocin-treated newborn rats resulting in persistently improved glucose homeostasis at adult age. *Diabetes* **50**, 1562-70.

Van Assche, F. A., Aerts, L. and De Prins, F. (1978). A morphological study of the endocrine pancreas in human pregnancy. *Br J Obstet Gynaecol* **85**, 818-20.

van Eyll, J. M., Passante, L., Pierreux, C. E., Lemaigre, F. P., Vanderhaeghen, P. and Rousseau, G. G. (2006). Eph receptors and their ephrin ligands are expressed in developing mouse pancreas. *Gene Expr Patterns* **6**, 353-9.

Villasenor, A., Chong, D. C. and Cleaver, O. (2008). Biphasic Ngn3 expression in the developing pancreas. *Dev Dyn* **237**, 3270-9.

von Herrath, M. and Homann, D. (2004). Islet regeneration needed for overcoming autoimmune destruction - considerations on the pathogenesis of type 1 diabetes. *Pediatr Diabetes* **5 Suppl 2**, 23-8.

Wang, S., Jensen, J. N., Seymour, P. A., Hsu, W., Dor, Y., Sander, M., Magnuson, M. A., Serup, P. and Gu, G. (2009). Sustained Neurog3 expression in hormone-expressing islet cells is required for endocrine maturation and function. *Proc Natl Acad Sci U S A*.

Wang, X., Chu, L. T., He, J., Emelyanov, A., Korzh, V. and Gong, Z. (2001). A novel zebrafish bHLH gene, neurogenin3, is expressed in the hypothalamus. *Gene* **275**, 47-55.

Wang, Z. V., Mu, J., Schraw, T. D., Gautron, L., Elmquist, J. K., Zhang, B. B., Brownlee, M. and Scherer, P. E. (2008). PANIC-ATTAC: a mouse model for inducible and reversible beta-cell ablation. *Diabetes* **57**, 2137-48.

Warburton, D., Bellusci, S., De Langhe, S., Del Moral, P. M., Fleury, V., Mailleux, A., Tefft, D., Unbekandt, M., Wang, K. and Shi, W. (2005). Molecular mechanisms of early lung specification and branching morphogenesis. *Pediatr Res* **57**, 26R-37R.

Wells, J. M. and Melton, D. A. (1999). Vertebrate endoderm development. *Annu Rev Cell Dev Biol* **15**, 393-410.

White, P., May, C. L., Lamounier, R. N., Brestelli, J. E. and Kaestner, K. H. (2008). Defining pancreatic endocrine precursors and their descendants. *Diabetes* **57**, 654-68.

Wiebe, P. O., Kormish, J. D., Roper, V. T., Fujitani, Y., Alston, N. I., Zaret, K. S.,

Wright, C. V., Stein, R. W. and Gannon, M. (2007). Ptf1a binds to and activates area III, a highly conserved region of the Pdx1 promoter that mediates early pancreas-wide Pdx1 expression. *Mol Cell Biol* **27**, 4093-104.

Wilkinson, D. G. (1999). In situ hybidization: A practical approach. Oxford, New York, USA: Oxford University Press.

Wilkinson, D. G. (2001). Multiple roles of EPH receptors and ephrins in neural development. *Nat Rev Neurosci* **2**, 155-64.

Wilson, M. E., Scheel, D. and German, M. S. (2003). Gene expression cascades in pancreatic development. *Mech Dev* **120**, 65-80.

Xu, G., Stoffers, D. A., Habener, J. F. and Bonner-Weir, S. (1999). Exendin-4 stimulates both beta-cell replication and neogenesis, resulting in increased beta-cell mass and improved glucose tolerance in diabetic rats. *Diabetes* **48**, 2270-6.

Xu, X., D'Hoker, J., Stange, G., Bonne, S., De Leu, N., Xiao, X., Van de Casteele, M., Mellitzer, G., Ling, Z., Pipeleers, D. et al. (2008). Beta cells can be generated from endogenous progenitors in injured adult mouse pancreas. *Cell* **132**, 197-207.

Ye, F., Duvillie, B. and Scharfmann, R. (2005). Fibroblast growth factors 7 and 10 are expressed in the human embryonic pancreatic mesenchyme and promote the proliferation of embryonic pancreatic epithelial cells. *Diabetologia* **48**, 277-81.

Yoshida, T., Tokunaga, A., Nakao, K. and Okano, H. (2003). Distinct expression patterns of splicing isoforms of mNumb in the endocrine lineage of developing pancreas. *Differentiation* **71**, 486-95.

Yucel, S., Dravis, C., Garcia, N., Henkemeyer, M. and Baker, L. A. (2007). Hypospadias and anorectal malformations mediated by Eph/ephrin signaling. *J Pediatr Urol* **3**, 354-363.

Zaret, K. S. (2008). Genetic programming of liver and pancreas progenitors: lessons for stem-cell differentiation. *Nat Rev Genet* **9**, 329-40.

Zaret, K. S. and Grompe, M. (2008). Generation and regeneration of cells of the liver and pancreas. *Science* **322**, 1490-4.

Zegers, M. M., O'Brien, L. E., Yu, W., Datta, A. and Mostov, K. E. (2003). Epithelial polarity and tubulogenesis in vitro. *Trends Cell Biol* **13**, 169-76.

Zhou, Q., Law, A. C., Rajagopal, J., Anderson, W. J., Gray, P. A. and Melton, D. A. (2007). A multipotent progenitor domain guides pancreatic organogenesis. *Dev Cell* **13**, 103-14.